DEVELOPMENT OF HIGH THROUGHPUT, MAMMALIAN CELL-BASED METABOLIC RATE ASSAYS FOR SCREENING COMPOUNDS

By

Yuansheng Yang

Dissertation

Submitted to the Faculty of the

Graduate School of Vanderbilt University

in partial fulfillment of the requirements

for the degree of

DOCTOR OF PHILOSOPHY

in

Chemical Engineering

May, 2005

Nashville, Tennessee

Approved:

Professor R. Robert Balcarcel

Professor G. Kane Jennings

Professor Robert D. Tanner

Professor John A. Roth

Professor Owen Patrick McGuinness

ACKNOWLEDGEMENTS

First and foremost, I thank my advisor, Dr. R. Robert Balcarcel, for his guidance, teaching, support, and friendship. I truly appreciate all the time and efforts he devoted to my research, personal growth, and career development during my study at Vanderbilt University. His work spirit of being a curious and original researcher, critical evaluator to research results, and open-minded learner will impact my career for the rest of my life. As his first Ph.D. student to graduate, I wish him all the best in his life and future research.

I thank all members in our research group, Sean M. Hartig, Lindsey M. Clark, Benjamin Roy, and Tiffany D. Rau, for their help during my research. I especially thank Sean for proofreading of my publications, thesis, and improving my English skills, and the happiness he added to my life at Vanderbilt University.

I thank my outstanding doctoral committee members chaired by Dr. Balcarcel — Dr. G. Kane Jennings, Dr. Robert D. Tanner, Dr. John A. Roth, and Dr. Owen Patrick McGuinness. They were kind enough to provide excellent advice and suggestions for my research.

I also want to thank the faculty and staff from the Vanderbilt University Chemical Engineering Department.

In addition, I gratefully acknowledge financial support from the Defense Advanced Research Projects Agency (N66001-01-C-8064).

I sincerely thank my parents, my brother, and my sister for their unconditional love and support from the time when I was born. I could not have been possible to finish any work without your support and encouragement.

Finally, I sincerely appreciate my wife, Xuesong Yang, for all of her support and tolerance of my absence over the years. I want you to know that I love you and that I could not have done this without your support.

TABLE OF CONTENTS

LIST OF TABLES

LIST OF FIGURES

CHAPTER I

INTRODUCTION

Introduction to toxicity testing with mammalian cell cultures

Chemical toxicity has been a public concern due to adverse effects on human health and environment. All chemicals, no matter for pharmaceutical or industrial purposes, need to go through extensive toxicity testing before they are released for public use as required by regulatory agencies.[1] In many cases, development and application of a product has to be discontinued due to its toxic effects, which makes this knowledge of significant economic value.[2,3] Toxicity testing usually involves a large number of animal experiments.[2,4] However, there is much pressure to reduce the use of animals due to practical, economic, and ethical reasons.[5,6] This is especially true for processes which involve large numbers of compounds, particularly in drug discovery and development; millions of compounds are screened at the beginning and early toxicity information is required for confirmation of the most appropriate candidates for further development.[7-9] In short, there is a increasing need for development of cost effective, high throughput *in vitro* methods as animal substitutes.[6]

Cultured cells, which keep the complexity of life in a very simplified system, provide an attractive alternative to whole animals for toxicity testing. The use of cell culture for measuring chemical toxicity has attracted much attention since the 1970s.[10] The many efforts devoted to this field over the past years are demonstrated by new research centers and organizations as well as publications.[11-13] Many cell-based toxicity

testing methods have been developed and their applications are becoming increasingly acceptable due to their practical and economical convenience while providing information relevant to *in vivo*.[14,15]

In contrast to animal testing, toxicity tests using cultured cells for many variables and replicates are cheaper, and the ethical, economical, and technical questions of animal experimentation are avoided.[16] Scientifically, the simplified, well controlled experimental system reduces the variability and bioavailability problems of animal experiments. Moreover, the better controlled experimental conditions offer the ability to obtain more refined mechanistic information on toxicity at the cellular level, which may be lost or masked in the intact organisms.[12] Furthermore, the availability of cell lines from different origins allows "elementary analysis" of a complicated toxicity event. Integration of the cellular events, organ specific events, and kinetic events may generate a sensible toxicity profile more efficiently than using animal-based approaches.[2,4,12,14,17]

However, there are many limitations for toxicity testing with cell cultures. Certain effects occurring *in vitro* for a certain cell type may not represent the toxic effects caused by the chemical in the intact organism. First, the processes regarding absorption, distribution, metabolism and excretion (ADME) are omitted, which not only affect the final concentrations reaching the target *in vivo*, but also sometimes change the chemical behavior.[2,4,14,17] Second, many cultured cell behaviors and their counterparts *in vivo* are different. The specific cell interaction characteristics of the tissue histology are lost, and as the cells are propagated in the synthetic medium, many differentiated functions may be lost or changed.[16] Third, in some cases, toxic effects *in vivo* are due to a tissue response (e.g. an inflammatory reaction, fibrosis) or a systemic response (e.g. pyrexia, vascular

dilation), which can not be monitored at the cellular level.[1,17] Considering these limitations, it is recognized that application of cell culture for obtaining mechanism-derived information is more promising than toxicity quantification.[14]

Current methods of toxicity testing with cell cultures are mainly used in the early stage of any toxicological approach with the exception of very specialized tests. Three types of testing can be identified.[3,12,14,18,19] The most common type of testing is screening as preliminary steps in a complex strategy, mainly for priority setting and determination of active concentration ranges to narrow the scope for subsequent investigations. Secondly, there are many tests used for determining the mechanism of action of chemicals to complement to the animal tests. Thirdly, a few tests are also used as animal alternatives for make a definitive toxicological assessment.

Up to now, most *in vitro* methods have been focused on acute toxic effects (<24 hr). This is mainly due to the challenge of maintaining cell-specific functions in long-term cell culture.[14] As a result of the multitude of biological structures and processes that can be impaired by different types of chemicals, there are a tremendous number of toxic effects and many different ways to test toxicity at the cellular level, or cytotoxicity. Biochemical, physiological, and molecular events all can provide measures of toxicity or valuable mechanistic information. Many endpoint assays have been developed based on membrane damage, mitochondrial dysfunction, changes in metabolism, morphology, and cell replication.[11,14] They are widely used because they are cheap, easily quantified, and reproducible. However, all of these assays oversimplify the events that they measure, providing a binary outcome for multiple step, kinetic processes. The obtained information is limited and not mechanistically indicative. There is a growing need to supplement them

with more subtle yet revealing tests for molecular events and precise metabolic regulation.[1]

Many technologies have been developed for analysis of cellular components, such as genomics (DNA micro-assay) and proteomics (2D-Gel-Mass Spectrometry), which now enable simultaneous measurements of thousands of gene expression and protein levels. Their uses for toxicity testing provide the opportunity to define the molecular events that precede and accompany toxicity at unprecedented levels of detail. Expectations are high for their potential in toxicology, which has stimulated the emergence of a new research area, toxicogenomics.[20] Their applications have been identified in at least two areas of toxicity testing: mechanistic investigations and predictive toxicology.[20-25] For mechanism studies, valuable clues could be provided by examining changes in gene expression for further investigation of targeted molecules. In contrast, the basis of the second approach is more empirical. In this approach, databases containing expression patterns are constructed from compounds with known toxicity, with which to predict toxicity of unknown chemicals. Some preliminary studies have applied genomics and proteomics in studies of mechanisms and discrimination of classes of toxicants.[26,27]

However, many challenges remain to realize their potential in toxicology[14,25]. First, the technologies are still not mature and further improvements with respect to speed, cost, and sensitivity are needed for screening purposes. Second, both techniques are very labor intensive and expensive, rendering them accessible only to few research groups. Third, cellular components themselves do not allow functions to be inferred without considering dynamic metabolic status. Moreover, in some cases, xenobiotics may

not affect gene regulation and expression directly, and significant toxicological effects may be completely unrelated to gene switching. Thus, metabolic status should be included to augment and complement the information collected by genomics and proteomics.[14,23,25]

Introduction to cellular metabolism and of metabolic flux analysis

Metabolism is the overall process through which living systems acquire and use free energy to carry out their functions.[28] Cellular metabolism is generally expressed as sequenced biochemical reactions in the form of a metabolic network. The pioneering research has constructed a complex metabolic network map. Generally, only inclusion of feasible and observable biochemical reaction steps in a network is valuable for specific metabolic studies. In many ways, it is preferable to simplify the network by lumping a series of linear reactions as one pathway whose overall flux can be experimentally determined.[29,30] Inside the network, any sequence of biochemical reaction steps connecting a specified set of input and output metabolites is called a metabolic pathway, and the rate at which material is processed through a metabolic pathway is defined as the metabolic flux.

The metabolic fluxes define the minimum information needed to describe cellular metabolism.[29] In a cellular system, the metabolic behavior, as indicated by the fluxes, is the culmination of regulatory processes at multiple levels, including metabolite substrates and intermediates, expression of enzymes and regulatory proteins, and the transcription of genes into mRNA based on the sequence information of DNA components (Figure 1).[31] Residing at the median of a biological paradigm, metabolic fluxes provide a link

between genetics and cell physiology. Quantitative determination of metabolic fluxes and flux analysis can help connect effects of genetic and/or environmental modifications to cell physiology.[32]

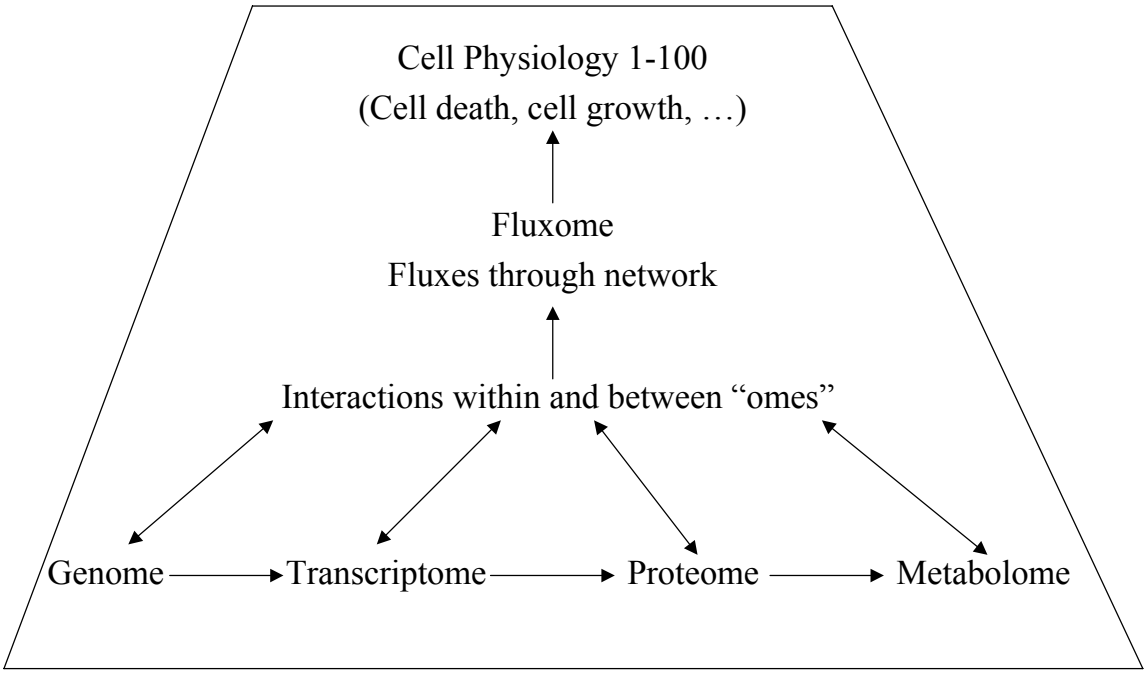

Figure 1.1. Schematic overview of the connection between compositional and functional units in metabolic systems.

The metabolic fluxes generally can be estimated using metabolite balancing and isotopic tracer methods. The former approach applies mass balances around the network of intracellular metabolites to calculate metabolic fluxes throughout the network under the assumption of steady state or quasi-steady-state.[30,33] Inputs for this analysis are the uptake and secretion rates of extracellular metabolites. The latter approach is based on the notion that activities of metabolic pathways can be determined by providing substrates enriched in carbon isotopes (typically ^{13}C or ^{14}C) and analyzing the distribution of the

isotopes in metabolic intermediate.[34-37] Isotopic tracers incorporated into metabolites can be detected using nuclear magnetic resonance (NMR) spectroscopy or mass spectroscopy. Although the isotopic methods are powerful to quantify more detailed metabolic pathways even for complex metabolic networks, the high cost of equipment, the cumbersome operation, and the difficulty of data interpretation limit their applications. In general, metabolite balancing is the easiest method for obtaining fluxes for a given metabolic network.[33] With a list of flux estimates for a metabolic network under various conditions, changes in fluxes and flux distribution around branch points can provide insights into how cells regulate metabolism under various conditions.

Traditional methods have often measured metabolic rates of biological systems in large volumes of cultivation systems (such as flasks and reactors) operated in continuous, batch, or fed-batch mode.[32] They have often been used for conducting metabolic studies in bioprocess and bioengineering research to improved cellular properties.[29,37,38] Measuring metabolic rates in large-scale systems is preferable because the obtained information is more relevant to industry. However, these approaches are time consuming, expensive, labor- and instrument intensive and not suitable for screening purposes.[32] Continuous bioreactor cultures allow for precise determination of metabolic rates under well-defined environmental conditions.[30] However, running a continuous bioreactor system to obtain data for just one steady state following inoculation of the bioreactor takes about 10-30 days, depending on the dilution rate. Operating a small, readily, commercially available bioreactor (working volume at 1.0 liter) in continuous mode at a dilution rate of 1.0 L/day costs approximately $ 40/day just for the raw materials and without accounting the cost from the large amount of testing agents. Moreover, the time

and high cost required per experiment results in fewer replicates to check reproducibility. Even using relatively time efficient and cost effective batch experiments, data acquisition for one experimental point can take days.

Motivation and objectives of the dissertation research

Functional characterization of diseased metabolic states is necessary for a holistic toxicity profile. At the start of this thesis, established approaches for conducting studies of metabolism were not suitable for screening toxicants and drugs due to obstacles such as high cost, labor, lengthy time consumption, low reproducibility and throughput. Easily performed, inexpensive, and high throughput methods for measuring cellular metabolic rates of mammalian cells were identified as a urgent needed to meet this deficit. Development of such methods for metabolic studies is also required in other areas, such as screening mutant collections in functional genomics, identification of pathways for genetic modification in metabolic engineering, and screening cell lines and media for preliminary optimization to ensure better cellular properties in bioprocess development.[31,39]

The overall aim of my research was to develop and apply high throughput metabolic rate assays for characterizing effects of compounds on cellular metabolism. To combat the high cost and low throughput of conventional methods for measuring metabolic rates in large scaled bioreactors or flasks, the assays that I developed would be performed in 24- or 96-well plates, which allow for multi-parallel, 100-500 μL cell cultures to simultaneously test many chemicals with adequate replication. Average metabolic rates would be measured in batch mode for a short period during which

changes in metabolite concentrations are sufficient to detect a difference, but not so much as to affect cell physiology and metabolic states. To handle the large amount of samples produced from the well plate systems, certain metabolites would be measured using dye-based or enzymatic methods, which allow multiplexed detection using high throughput fluorescence or spectrophotometric microplate readers.

Overview of the thesis

By recognizing that one assay cannot satisfy all purposes, a series of assays were developed which can be used alone or in a sequence depending on the information needed. In chapter II, a 90-min, 24-well plate acidification rate assay based on spectrophotometric detection of phenol red was developed for screening global metabolic effects of chemicals. The assay is simple, inexpensive and suitable for rapid measurement of short time, global metabolic effects. In chapter III, a 24-well plate CO_2 production rate assay was developed for the determination of CO_2 production rate of mammalian cells. The viability and cell growth were measured as comparison to validate its application for toxicity testing. It is found that metabolic change corresponds to growth inhibition and there is a sublethal concentration range for a chemical where changes in metabolism occur but without causing cell death. Inspired by the finding that metabolic change occurs at sublethal concentrations, and motivated that dose selection remains a challenge in toxicity testing, in chapter IV, a 96-well plate assay which combines resazurin reduction with lactate production and glucose consumption rate assays was designed to assess effects of compounds on both culture viability and metabolism during 6 or 24 hr exposure. The assay was used to bound sublethal, metabolic active concentration ranges

for a chemical to serve as a cost-effective and time-saving step for subsequent investigations with more expensive, lengthy, and/or detailed methods. The previous three assays paved the way for a more detailed investigation of effects of compound on cellular metabolism. In chapter V, based on the three developed assays, a 24-well plate assay was synthesized for simultaneous measurements of glucose, lactate and CO_2/pH. The assay, in conjunction with a carbon material balance model and statistical analysis, was used to characterize the changes in metabolic state of mammalian cells exposed to four model metabolic agents. In contrast to traditional methods which mainly focused on the late, irreversible cell death events, the metabolic responses at sublethal levels were investigated. In the last chapter, VI, the major conclusions of this study are summarized and potential applications of the developed assays are discussed.

References

1. Freshney, R.I. (2000). Cytotoxicity, pp. 329-330. *In* Culture of Animal Cells, A Manual of Basic Techniques. John Wiley & Sons, New York.

2. Blaauboer, B.J. (2002). The applicability of in vitro-derived data in hazard identification and characterisation of chemicals. *Environ Toxicol Pharmacol* **11**, 213-225.

3. Fry, J. and E. George. (2001). In vitro toxicology in the light of new technologies. *ATLA-Altern Lab Anim* **29**, 745-748.

4. Blaauboer, B.J. (2001). Toxicodynamic modelling and the interpretation of in vitro toxicity data. *Toxicol Lett* **120**, 111-123.

5. (2000). Approaches to High Throughput Toxicity Screening. Taylor & Francis, London.

6. Atterwill, C.K. and M.G. Wing. (2002). In vitro preclinical lead optimisation technologies (PLOTs) in pharmaceutical development. *Toxicol Lett* **127**, 143-151.

7. Johnson, D.E.W., G. H. I. (2001). Assessing the Potential Toxicity of New Pharmaceuticals. *Current Topics in Medicinal Chemistry* **1**, 233-245.

8. Verkman, A.S. (2004). Drug discovery in academia. *American Journal of Physiology-Cell Physiology* **286**, C465-C474.

9. Yu, H.S. and A. Adedoyin. (2003). ADME-Tox in drug discovery: integration of experimental and computational technologies. *Drug Discov Today* **8**, 852-861.

10. Paganuzzi Stammati, A., V. Silano and F. Zucco. (1981). Toxicology investigations with cell culture systems. *Toxicology* **20**, 91-153.

11. Cao CJ, M.R., Menking DE, Valdes JJ, Cortes VI, Eldefrawi ME, Eldefrawi AT. (1997). Validation of the cytosensor for in vitro cytotoxicity studies. *Toxicol Vitro* **11**, 285-293.

12. Zucco, F. and A.L. Vignoli. (1998). In vitro toxicology in Europe 1986-1997 - Final report to the European Commission DGXI Financial Contribution no. B4-3040/96/424/DEB/E2. *Toxicol Vitro* **12**, 739-+.

13. Clemedson, C. (2001). Bjorn Ekwall, 1940-2000 - A pioneer in the field of in vitro toxicology - Obituary. *Toxicol Vitro* **15**, 263-264.

14. Eisenbrand, G., B. Pool-Zobel, V. Baker, M. Balls, B.J. Blaauboer, A. Boobis, A. Carere, S. Kevekordes, J.C. Lhuguenot, R. Pieters and J. Kleiner. (2002). Methods of in vitro toxicology. *Food Chem Toxicol* **40**, 193-236.

15. Zucco, F., I. De Angelis, E. Testai and A. Stammati. (2004). Toxicology investigations with cell culture systems: 20 years after. *Toxicol Vitro* **18**, 153-163.

16. Freshney, R.I. (2000). Introduction, pp. 4-5. *In* Culture of animal cells, a manual of basic techniques. A John Wiley & Sons, New York, USA.

17. Clemedson, C., M. Nordin-Andersson, H.F. Bjerregaard, J. Clausen, A. Forsby, H. Gustafsson, U. Hansson, B. Isomaa, C. Jorgensen, A. Kolman, N. Kotova, G. Krause, U. Kristen, K. Kurppa, L. Romert and E. Scheers. (2002). Development of an in vitro test battery for the estimation of acute human systemic toxicity: An outline of the EDIT project. *ATLA-Altern Lab Anim* **30**, 313-321.

18. Liebsch, M. and H. Spielmann. (2002). Currently available in vitro methods used in the regulatory toxicology. *Toxicol Lett* **127**, 127-134.

19. Fry, J.R. (2000). Cytotoxicity and mechanistic studies in high throughput toxicity screening, pp. 31-42. *In* Approaches to High Throughput Toxicity Screening. Taylor & Francis, London, UK.

20. Waters, M., G. Boorman, P. Bushel, M. Cunningham, R. Irwin, A. Merrick, K. Olden, R. Paules, J. Selkirk, S. Stasiewicz, B. Weis, B. Van Houten, N. Walker

and R. Tennant. (2003). Systems toxicology and the Chemical Effects in Biological Systems (CEBS) knowledge base. *Environ Health Perspect* **111**, 811-824.

21. Guillouzo, A. (2001). Applications of biotechnology to pharmacology and toxicology. *Cell Mol Biol* **47**, 1301-1308.

22. Goodsaid, F.M. (2003). Genomic biomarkers of toxicity. *Current Opinion in Drug Discovery & Development* **6**, 41-49.

23. Hellmold, H., C.B. Nilsson, I. Schuppe-Koistinen, K. Kenne and L. Warngard. (2002). Identification of end points relevant to detection of potentially adverse drug reactions. *Toxicol Lett* **127**, 239-243.

24. Lord, P.G. (2004). Progress in applying genomics in drug development. *Toxicol Lett* **149**, 371-375.

25. Orphanides, G. (2003). Toxicogenomics: challenges and opportunities. *Toxicol Lett* **140**, 145-148.

26. Amin, R.P., H.K. Hamadeh, P.R. Bushel, L. Bennett, C.A. Afshari and R.S. Paules. (2002). Genomic interrogation of mechanism(s) underlying cellular responses to toxicants. *Toxicology* **181**, 555-563.

27. Hong, Y., U.R. Muller and F. Lai. (2003). Discriminating two classes of toxicants through expression analysis of HepG2 cells with DNA arrays. *Toxicol Vitro* **17**, 85-92.

28. Voet, D., J.G. Voet and C.W. Pratt**.** (1999). Fundamentals of Biochemistry. John Wiley & Sons, New York.

29. Stephanopoulos G. (1999). Metabolic fluxes and metabolic engineering. *Metab Eng* **1**, 1-11.

30. Stephanopoulos G., A.A.A., Nielsen Jens. (1998). Metabolic Engineering: Principles and Methodologies. 22.

31. Sauer, U. (2004). High-throughput phenomics: experimental methods for mapping fluxomes. *Current Opinion in Biotechnology* **15**, 58-63.

32. Balcarcel, R.R. and L.M. Clark. (2003). Metabolic screening of mammalian cell cultures using well- plates. *Biotechnol Prog* **19**, 98-108.

33. Varma, A. and B.O. Palsson. (1994). Metabolic Flux Balancing - Basic Concepts, Scientific and Practical Use. *Bio-Technology* **12**, 994-998.

34. Schmidt, K., A. Marx, A.A. de Graaf, W. Wiechert, H. Sahm, J. Nielsen and J. Villadsen. (1998). C-13 tracer experiments and metabolite balancing for

metabolic flux analysis: Comparing two approaches. *Biotechnol Bioeng* **58**, 254-257.

35. Schmidt, K. and N.L. C. (1999). Quantification of Intracellular Metabolic Fluxes from Fractional Enrichment and13C-13C Coupling Constraints on the Isotopomer Distribution in Labeled Biomass Components. *Metab Eng* **1**, 166-179.

36. Wiechert, W. (2001). C-13 metabolic flux analysis. *Metab Eng* **3**, 195-206.

37. Lee, K., F. Berthiaume, G.N. Stephanopoulos and M.L. Yarmush. (1999). Metabolic flux analysis: A powerful tool for monitoring tissue function. *Tissue Eng* **5**, 347-368.

38. Shimizu, K. (2000). An overview on metabolic systems engineering approach and its future perspectives for efficient microbial fermentation. *J Chin Inst Chem Eng* **31**, 429-442.

39. Kumar, S., C. Wittmann and E. Heinzle. (2004). Minibioreactors. *Biotechnology Letters* **26**, 1-10.

CHAPTER II

SPECTROPHOTOMETRIC ACIDIFICATION RATE ASSAY FOR PRELIMINARY SCREENING OF METABOLIC ACTIVITY

Abstract

A 90-minute assay using 24-well plates was developed for screening global metabolic effects of chemicals by measuring extracellular acidification rate of mammalian cells. During a 90-minute test, the pH of each well of a 24-well plate is monitored by measuring the absorbance of phenol red using a spectrophotometric plate reader. The acidification rate is then calculated from the change in pH divided by the time interval and cell density. The assay was verified by testing the effects of five well-characterized chemicals on fibroblast cell cultures. As expected, the responses of the fibroblasts were dependent on the dose and type of chemicals. They also corresponded with their established mechanisms of action and well with measured lactate production rates. The set up is simple, inexpensive and amenable to be automated. The method is easy to perform and rapid. Uses include screening compounds for gross metabolic effects in mammalian cell lines, determining preliminary metabolic dose-response curves for guiding further research, and designing and optimizing media for *in vitro* systems utilizing cell cultures.

Introduction

Recent advances in organic chemistry (combinatorial chemistry) have led to the development of large chemical libraries, which not only drive the rapid development of

pharmaceutical and other industries, but also further increase the burden of toxicity testing which mainly rely on animal experiments.[1,2] There is an increasing need for rapid, high throughput, and cost-effective *in vitro* toxicity testing methods as animal alternatives.[3] In recent years, mammalian cell-based, high-throughput toxicity screening has played an important role in drug development and toxicological safety testing, especially at early stages.[4-6] In general, the purpose of one toxicity screen would not necessarily be to predict the extent and nature of all possible effects, but rather to provide information for narrowing the scope of subsequent investigations that could be more information containing but also expensive and time-consuming, thereby enhancing the overall efficiency and decreasing the overall cost for a entire toxicological testing process.[1,3,7]

Quite a few high-throughput assays have been developed for *in vitro* drug and toxicity screening. Many of them are biochemical assays for specific enzyme activities related to basic cellular functions, which can be measured based on change in light absorption, fluorescence or luminescence intensity. The assays are amenable for miniaturization and automation. The commonly used commercial assays include ATP-based luminescence assay,[8-10] Alamar blue assay,[7,11,12] LDH leakage,[13,14] and MTT.[15-17] However, these assays require the addition of assay reagents at the end of exposure and additional incubation times in order to generate a signal. These extra steps may distort the effects of the chemicals and provide obstacles for adaptation for high- or ultrahigh-throughput screening automation.[9,18]

Screening cell lines for effects of chemicals on metabolism can provide another alternate, non-specific test, as all compounds can cause global changes in cell

metabolism. The changes in consumed nutrients or excreted metabolites all can be used as indicators for changes in metabolism. In this vein, measuring uridine uptake has been reported for toxicity testing.[19] However, this assay is relatively expensive and labor intensive, and requires the handling and disposal of radioisotopic waste. The well plate-based BD oxygen biosensor system developed by BD Science Company has been reported for monitoring oxygen consumption rate. However, the assay is limited to the use of suspended cell line and its low sensitivity requires the use of high density of cells.[18] Measuring medium acidification rate provides another alternative for monitoring changes in metabolism. The rationale of using acidification rate as a general index of metabolism is based on the fact that the extracellular pH is a strong function of lactate and CO_2 production from the cells.[20,21] In contrast to measurement of other metabolites, the advantage of using pH is that it is sensitive to both glycolytic metabolism and respiration.[22] Moreover, measuring acidification rate has also been found to be more sensitive than other cytotoxicity assay methods such as MTT.[23] Monitoring medium acidification rate has been reported using a 4- or 8-channel Molecular Devices Cytosensor. Its applications have been identified in different steps of drug development as a functional assay or generally as a cytotoxicity assay.[20,21,24-26] However, this method is not well suited for multiple parallel measurements and is not applicable for high throughput screening.[26]

In this work, I present a 24-well plate assay for mammalian cell culture acidification rate that characterizes the metabolic effects of chemicals such as 2,4-dinitrophenol (DNP), antimycin A (AA), rotenone, sodium fluoride, and sodium oxamate. Our results demonstrate the feasibility of performing the acidification rate

assay in a multi-replicate format and of screening chemicals for their impact on overall metabolic activity. The assay is relatively simple, fast (90 minutes), fairly inexpensive, multi-replicate, and is also amenable to automation. It can be used in screening sensitivity of cell lines to classes of agents, to better define the concentration ranges where agents cause measurable metabolic effects on cell lines, as well as in formulating and optimizing media for cell culture studies.

Materials and methods

Cell culture and media

Mouse fibroblast cells (ATCC CRL10225) used in this study were grown in "maintenance medium" consisting of DMEM (Mediatech, Herndon, VA, USA) supplemented with 10% FBS (Sigma, St. Louis, MO, USA), 10 U/mL penicillin-10 μg/mL streptomycin (Sigma), and 4 mM L-glutamine (Mediatech). The cells were maintained in 75 cm^2 T-flasks (Corning, NY, USA) in an incubator (Model 3100 series, Forma Scientific, Marietta, OH, USA) controlled at 37 °C, 95% humidity, and 10% CO_2. Every 4-6 days, cultures were trypsinized using a 0.25% solution of trypsin (Mediatech), counted by microscopy (Model BX60, Olympus, USA) using trypan blue (Mediatech) with a hemacytometer (Double Neubauer Counting Chamber Set, VWR International, Suwanee, GA, USA), and subcultured at an initial cell density of 2×10^5 cells/mL in maintenance medium.

Medium for the 90-min 24-well plate acidification assay (test medium) is based on a low-buffered bicarbonate-free RPMI 1640 medium containing 1 mM phosphate (Molecular Devices), which is supplemented with 10 mg/L insulin, 5 mg/L holo-

transferrin, and 10 U/mL penicillin–10 μg/mL streptomycin (Sigma Chemical Co.). Sodium bicarbonate is not added since loss of CO_2 converted from it negatively interferes with the monitoring of pH. Moreover, the test medium is modified to contain 25 mg/L phenol red for clearer signals of phenol red absorbance. Furthermore, the initial pH is adjusted to a value of 7.7 to make the pH of the medium more sensitive to acidification since this higher pH is further from the buffer pK_a of phosphate at 7.21.[27]

Medium for 6-hr 24-well plate glucose and lactate rate assays consisted of RPMI 1640 (Sigma Chemical Co.) supplemented with 2g/L sodium bicarbonate, 4.0 mM D-glucose, 10 mg/L insulin, 5 mg/L holo-transferrin, and 10U/ml penicillin-10 μg/mL streptomycin, as reported but without 2-aminoethanol and 2-mercaptoethanol. [28]

Chemicals

DNP, antimycin A, rotenone, sodium fluoride, and sodium oxamate were purchased from Sigma Chemical Co. Concentrated stock solutions of DNP, antimycin A, and rotenone were made in ethanol, while concentrated sodium fluoride and sodium oxamate were made in sterilized water. Prior to a screen, 5.0-mL volumes of test media with 4 concentrations of a chemical plus a control without containing chemicals were prepared by further dilution of a concentrated stock into test medium. The pH was adjusted to the equal value of 7.7 with hydrochloride and/or sodium hydroxide. Test media of different concentrations of a chemical were still administered the same total amount of solvent. The maximum concentration of solvent used (from the stock solution) was less than 2% vol/vol.

Monitoring pH during the acidification rate assay

In preparation of a screen, the fibroblast cells are harvested from a 75-cm^2 T-flask at 80-90% fluency, centrifuged at 200 g for 10 min (model 5677, Forma Scientific), and resuspended in maintenance medium at a density of $1.5x10^6$ cells/mL. High cell density is used for clearer signal of acidification rate. 600 μL of this cell culture is placed into each well of a 24-well plate (BD Falcon), with the exception of 4 wells that are reserved for cell-free medium. The plate is incubated at 37°C, 95% humidity, and 10% CO_2 for 10 hours to allow cell attachment. Next, maintenance medium is removed, all wells are washed twice with PBS, and 600 μL of test media with 4 different concentrations of an agent plus control is added to each well of a 24-well plate, each column corresponding to one concentration. The cell-free wells were also added with test medium without containing chemicals. The plate is thereafter placed on the FL600 (Bio-Tek Instruments, Winooski, VT) for monitoring and temperature control at 37°C during the 90-min acidification rate assay. The absorbance at 560 nm of each well is measured to estimate pH every 15 min for 90 minutes. Twenty-five locations were scanned to obtain the average for each well. At the end of the monitoring period, culture viability is determined in one well of each column (of each concentration) by trypan blue exclusion method (Double Neubauer Counting Chamber Set, VWR International, Suwanee, GA).

pH calibration

Phenol red (phenolsulphonephthalein, $C_{19}H_{15}O_5S$) is a weak acid, which is generally contained in medium as a pH indicator in cell culture. It is the color change during its dissociation that is used for pH estimation (Equation 2-1).

$$HInd \longleftrightarrow H^+ + Ind^- \tag{2-1}$$

It is red at pH 7.4 and becomes orange at 7.0, yellow at pH 6.5, lemon yellow below pH 6.5, more pink at pH 7.6, and purple at pH 7.8.

The qualitative assessment of color is highly subjective, but quantitative pH monitoring can be achieved by measuring absorbance at 560 nm. To set up a calibration line for pH monitoring, twelve standard solutions are prepared which vary pH from 3.54 to 10.01. The standard solutions are test media whose pH's are adjusted using acid chloride or sodium hydroxide. 600 μL of these standard solutions are added to each well of a 24-well plate, each column corresponding to one pH value. The well plate is then placed on the FL600 plate reader which temperature is maintained constant at 37°C. After incubation inside the plate reader for 15 minutes until the temperature of the standard solutions reaches 37°C, the absorbance at 560 nm of each well is measured. The calibration curve as depicted in figure 2.1 shows the relation between pH values and the absorbance values, which can be described by a linear equation based on the Henderson-Hasselbalch equation as done previously:[29,30]

$$pH = B1 + B2 \cdot \log\left(\frac{O.D. - A_{\min}}{A_{\max} - O.D.}\right) \qquad (2\text{-}2)$$

A_{min} and A_{max} were determined from absorbance reading at low and high pH (3.54 and 10.01) to be 0.2335 and 1.0142, respectively. Six absorbance measurements made for medium at pH values between 6 and 8 were used to fit the equation parameters B1 and B2 by linear regression in Microsoft Excel. Values that we determined for B1 and B2, namely 7.70 and 1.04, agree well with the Henderson-Hasselbalch equation that states B1 is equivalent to the pKa of the indicator, which is 7.9 for phenol red,[27] and B2 is close to unity.

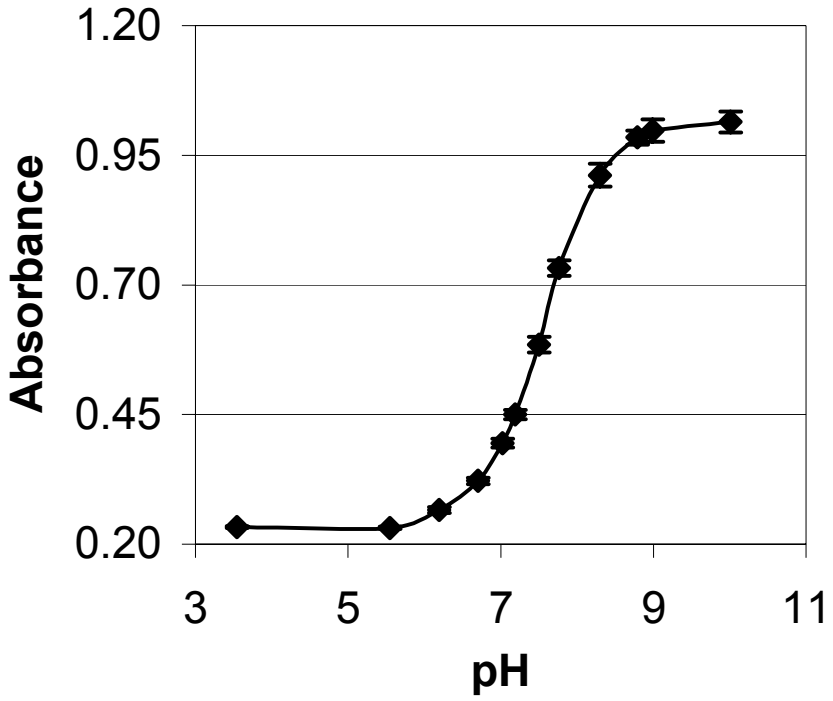

Figure 2.1. Measured absorbance of phenol red at 562 nm at different pH values in the 24-well plate filled with 600 μL of test medium without cells. At every point, mean values and standard deviations for four measurements are shown.

Calculation of acidification, glucose, and lactate metabolic rates

The pH of each well is determined from absorbance readings using the calibration line that is established for test medium. Additionally, for wells that contain cells, the absorbance readings are adjusted by subtracting the absorbance due to the presence of cells. This absorbance due to cells is determined for each well at time zero as the difference between the OD of wells with cells and the OD of wells without cells at time zero, when the pH of all the wells are the same.

The acidification rate for each well of this pH monitoring experiment is calculated as the total change in proton concentration at 90 minutes minus the change associated

with the wells without cells, divided by the cell density of the seed culture and time interval of 90 minutes. Average rates for control and test cultures were taken as the average and standard deviation from 4 wells.

$$q_{acidification} = \frac{\Delta[H^+] - \Delta[H^+]_{cell-free}}{n_v \cdot \Delta t} \tag{2-3}$$

Glucose consumption and lactate production rates were determined during separate experiments using another 24-well plate method. After cell attachment, maintenance medium is removed, and 400 μL of test medium for the glucose and lactate rates assays is added to each well. Next, the well plate is incubated for six hours at 37 °C, 95% humidity, and 10% CO_2. Finally, culture viability is determined in one well of each column by removing and counting the cells stained with trypan blue on a hemocytometer. Samples for initial and final concentrations of glucose and lactate are removed before and after six hours incubation period. Triplicate measurements of glucose and lactate concentrations for each well of a 24-well plate at initial and final time points are conducted in a separate 96-well plate using enzymatic assays.[28] More details about the recipes and procedures of both assays are described in Chapter IV.

Calculation of glucose and lactate rates is similar as for acidification rate. Rates for each well of the experiment were calculated as the change in concentration divided by the cell density of the seed culture and the time interval of 6 hours (Equation 2-4). Average rates for control and test cultures were taken as the average and standard deviation from 4 wells.

$$q_{glc\ or\ lac} = \frac{\left|C_{final} - C_{initial}\right|}{n_v \cdot \Delta t} \tag{2-4}$$

Statistical significance of differences in measured rates between test and control cultures were compared using a Dunnett's test in software JMPIN™.

Results

Monitoring extracellular pH

Monitoring of pH in 24-well plates was demonstrated for the exposure of fibroblasts to five chemicals: DNP, antimycin A, sodium fluoride, rotenone, and oxamate. Figure 2.2 shows the dynamic pH profiles during 90 minutes for cell-free wells, control cultures, and test cultures containing chemicals given four different concentrations. The concentrations used were based loosely about those reported for other cell lines in recent literature [31-33], and in some cases with some foreknowledge from glucose and lactate rate assays.[28] The pH for cell-free wells dropped by approximately 0.3 pH unit in the first 30-45 minutes of the assay, but then remained fairly stable. This change in cell-free cultures is due primarily to a change in plate temperature from about ambient (25-30°C) during preparation of the plate up to the set point temperature of the plate reader (37°C). Even though the cell free cultures exhibit changes in pH, the data demonstrate that the cell-containing cultures exhibit notably greater changes that can be clearly distinguished from the cell-free curve. Among the wells containing cells, the changes in pH are also quite clearly distinguished between many of the concentrations tested. Whether a test well (one with a certain concentration of a chemical) changes to a similar, greater, or lesser degree as compared to control wells (wells with cells but no chemical) depends on the chemical and the dose. Among the chemicals shown, pH changes in the presence of fluoride and oxamate were smaller than that of the control, in a monotonic fashion over the

concentration ranges tested. The opposite was true for cultures given rotenone: the pH changes were larger with increasing dose. Non-monotonic trends were evident for other chemicals. Cultures with DNP exhibited increased changes in pH for all four concentrations tested; yet the maximum increase occurred for intermediate doses of 0.10-0.20 mM. Cultures with Antimycin A had changes in pH that were greater than those of the control for lower doses tested (0.005-0.010 mM), yet smaller than the control at higher doses (0.04-0.1 mM). These changes in pH occurred in the absence of significant changes in cell number and without observable cell death, as was confirmed by trypan blue cell counts immediately following the 90-minute test interval.

Determination and validation of acidification rate

Calculated acidification rates more clearly demonstrate the impact of each of the four chemicals on overall metabolism (Figure 2.3). Cultures with DNP and rotenone exhibited increased acidification rates while cultures with fluoride and oxamate exhibited decreased acidification. Cultures with AA had increased acidification rates at lower concentrations while decreased rates at higher doses. These calculated acidification rates correspond well with lactate production and glucose uptake rates (also shown in Figure 2.3) that were obtained in 6-hour experiments that were conducted separately from the acidification assay. As would be expected, a high level of correlation was found between acidification rates and lactate production rates (Figure 2.4). Culture viability and cell number was also assessed at the end of the 6-hour experiments. With the exception of cultures exposed to 0.04 and 0.10 mM antimycin A, all cultures retained high viability and cell numbers that were unchanged during the 6-hour incubation period. Even though

they did not exhibit such traits at 90 minutes, the two cultures given higher doses of AA had very low viabilities and significant cell detachment at the end of 6 hours.

(A)

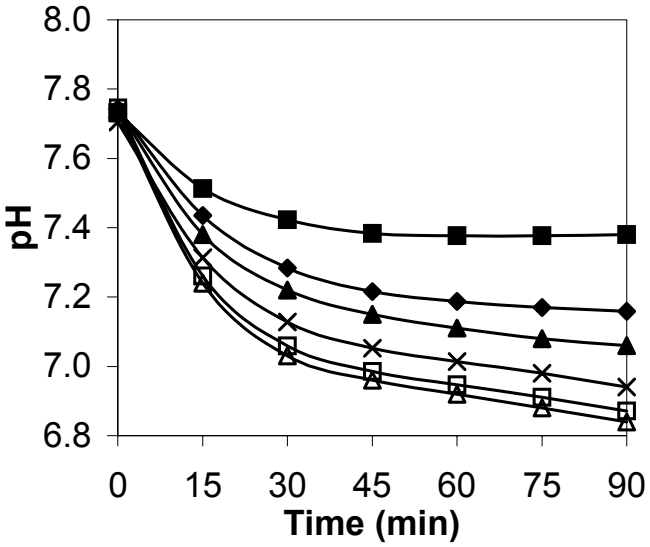

(B)

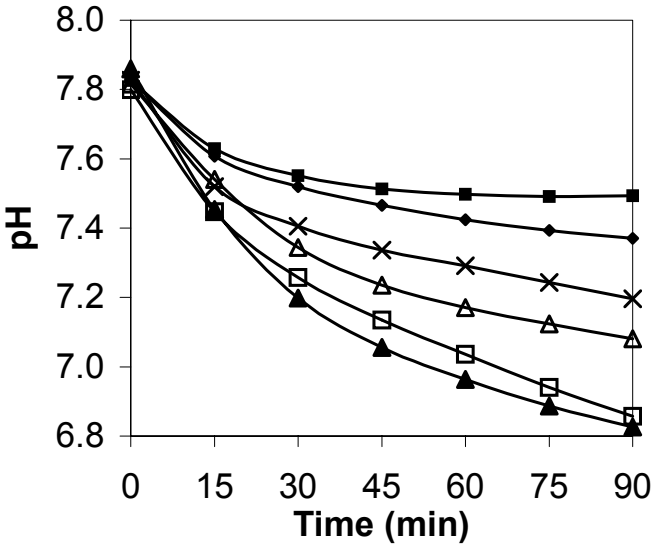

(C)

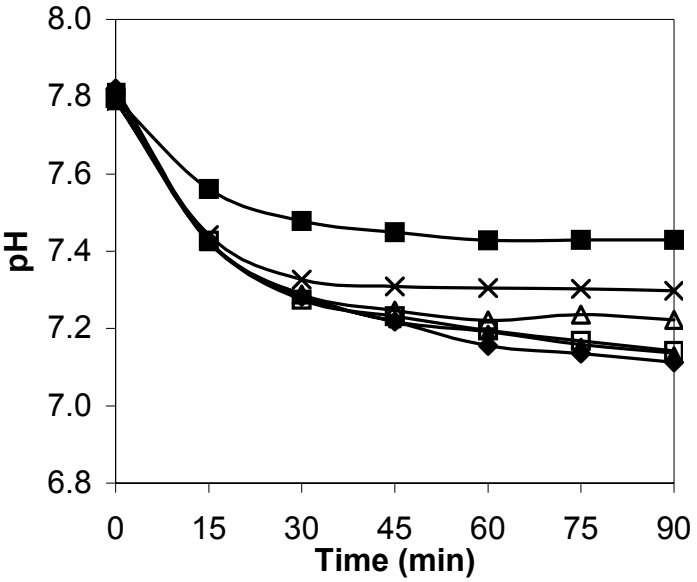
8.0
7.8
7.6
7.4
7.2
7.0
6.8
pH
0
15
30
45
60
75
90
Time (min)

(D)

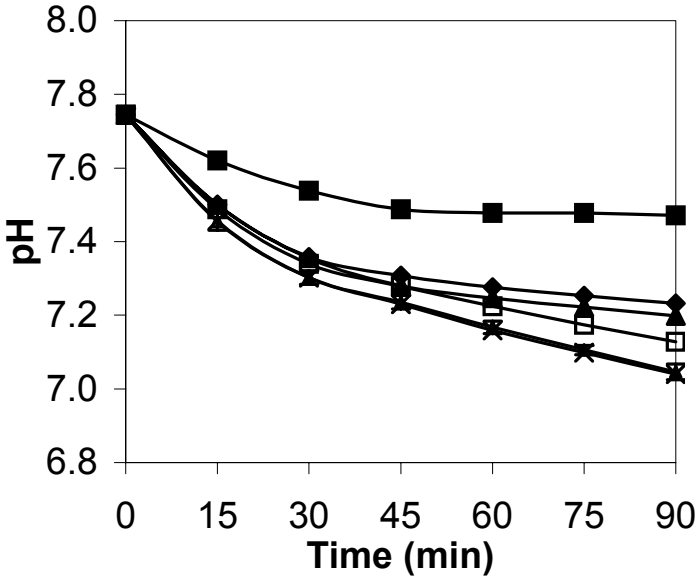
8.0
7.8
7.6
7.4
7.2
7.0
6.8
pH
0
15
30
45
60
75
90
Time (min)

(E)

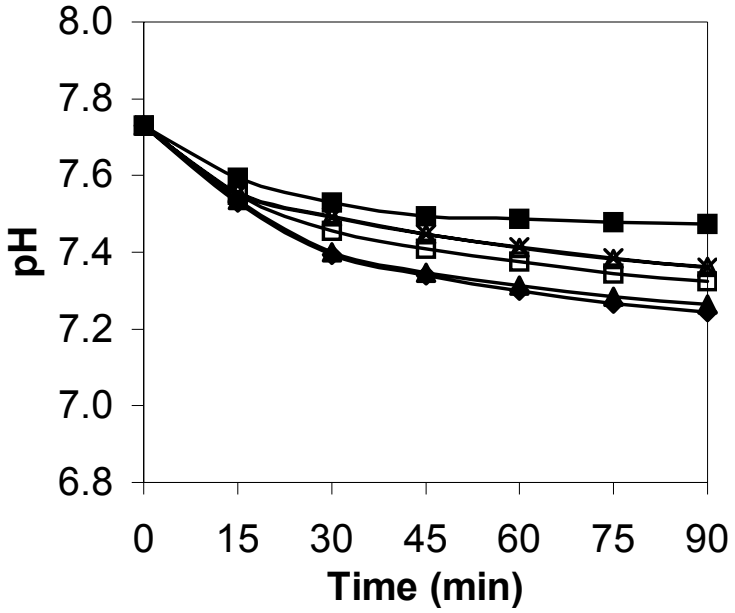

Fig 2.2. Monitoring pH of fibroblast cultures exposed to five chemicals. (A) DNP: test medium without cells (■), test medium with cells ("control") (♦), and test media containing DNP at 0.05 (▲), 0.10 (□), 0.20 (Δ), and 0.40 (×) mM; (B) AA: test medium without cells (■), test medium with cells ("control") (♦), and test media containing AA at 0.005 (▲), 0.010 (□), 0.040 (Δ) and 0.100 (×) mM; (C) Fluoride: test medium without cells (■), test medium with cells ("control") (♦), and test media with fluoride at 0.5 (▲), 1.0 (□), 2.0 (Δ), and 4.0 (×) mM; (D) Rotenone: test medium without cells (■), test medium with cells ("control") (♦), and test media containing rotenone at 0.015 (▲), 0.030 (□), 0.060 (Δ) and 0.090 (×) mM; and (E) Oxamate: test medium without cells (■), test medium with cells ("control") (♦), and test media with oxamate at 1.0 (▲), 2.0 (□), 4.0 (Δ), and 8.0 (×) mM. pH values reported are the mean and standard deviation of measurements from four separate wells. Viabilities of all cultures were greater than or equal to 90% at the end of the 90-minute interval.

(A)

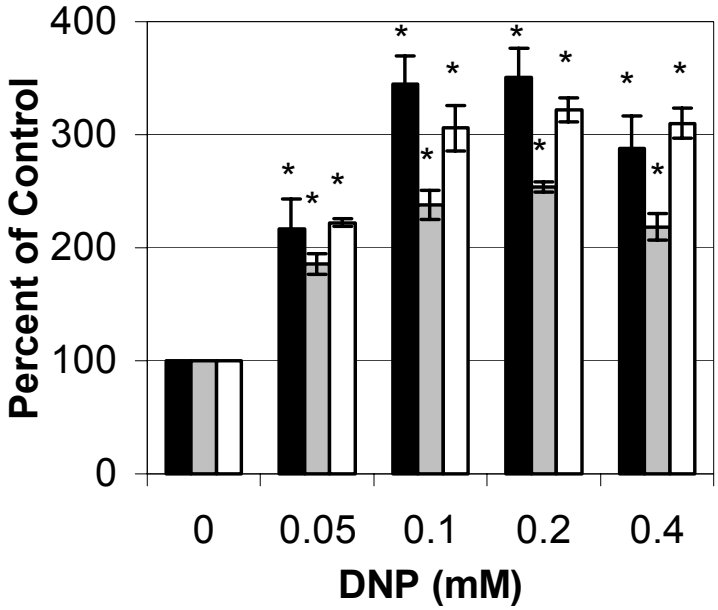
400
300
200
100
0
Percent of Control
0
0.05
0.1
0.2
0.4
DNP (mM)

(B)

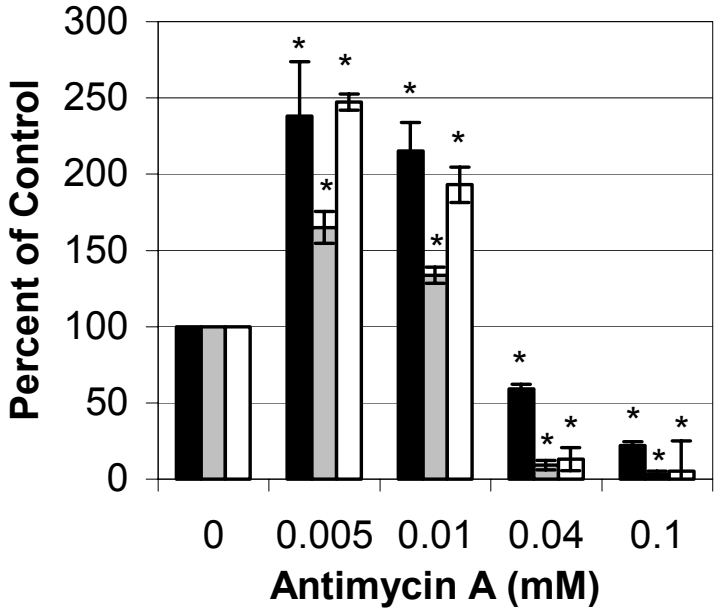
300
250
200
150
100
50
0
Percent of Control
0
0.005
0.01
0.04
0.1
Antimycin A (mM)

(C)

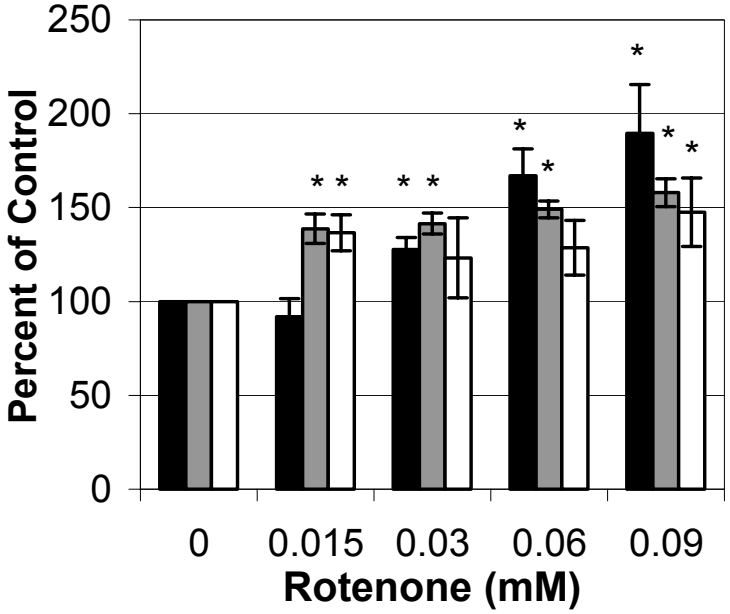
250
200
150
100
50
0
Percent of Control
0
0.015
0.03
0.06
0.09
Rotenone (mM)

(D)

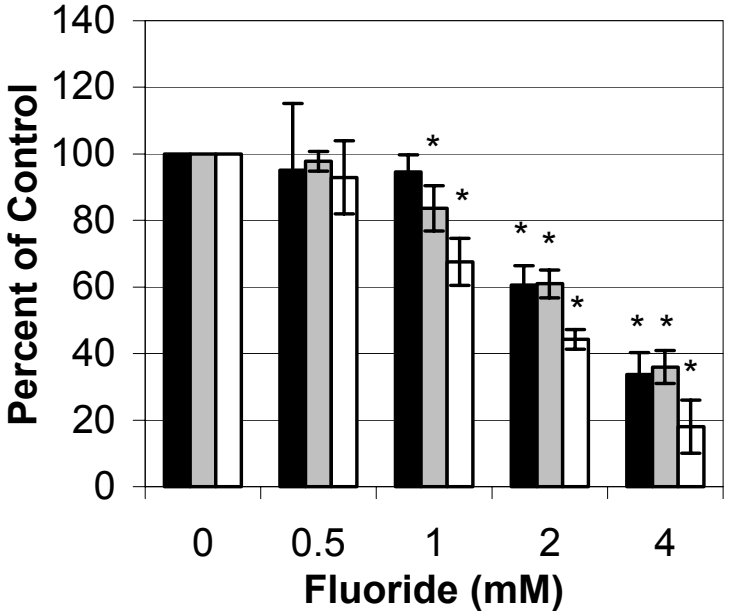
140
120
100
80
60
40
20
0
Percent of Control
0
0.5
1
2
4
Fluoride (mM)

(E)

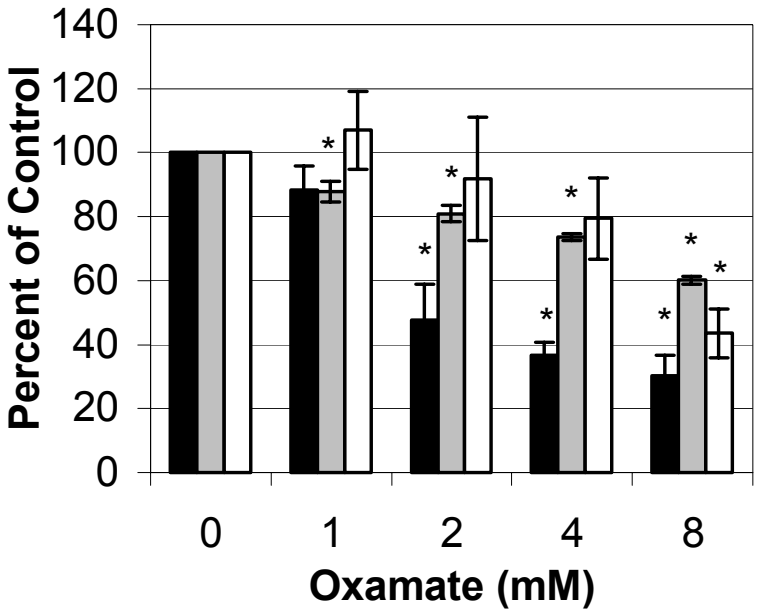

Fig 2.3. Relative acidification (black bars), lactate production (gray bars), and glucose uptake (clear bars) rates for fibroblast cultures exposed to different concentrations of (A) DNP, (B) AA, (C) fluoride, (D) Rotenone, and (E) Oxamate. Acidification rates were measured over 90 minutes. Lactate production and glucose uptake rates were measured over 6 hours. Viabilities of all cultures were greater than or equal to 90% at the end of the 90-minute interval and 6-hour interval, with the exception of cultures exposed to 0.04 and 0.10 mM of AA for 6 hours. Each bar is the average of four wells, and error bars reflect the standard deviation of the normalized values. Asterisks denote that differences in test cultures compared to controls are statistically significant with $p<0.05$.

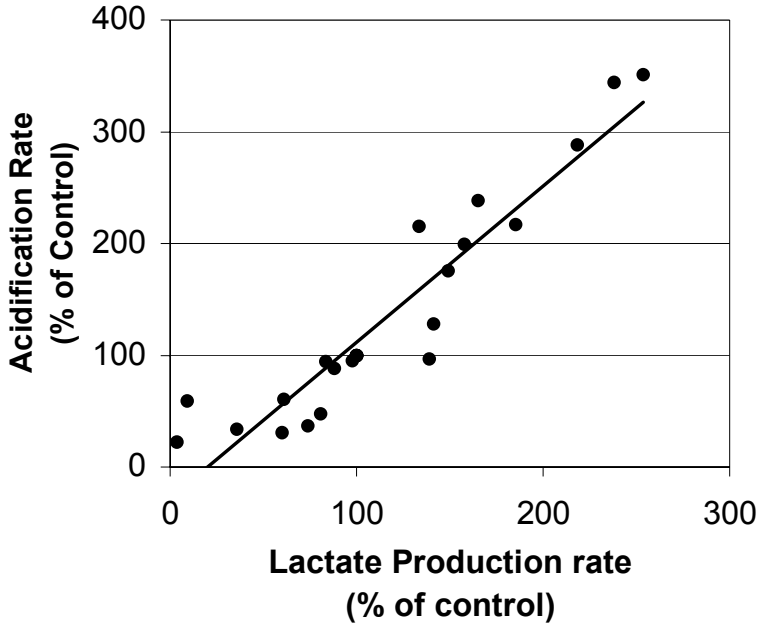

Fig 2.4. Correlation of medium acidification rate with lactate production rate of fibroblast cells exposed to DNP, AA, rotenone, or fluoride. Data from cultures exhibiting high viability during both assays: DNP at 0, 0.05, 0.10, 0.20, and 0.40 mM; AA at 0, 0.005, and 0.010 mM; fluoride at 0.0, 0.5, 1.0, 2.0, and 4.0 mM; and rotenone at 0, 0.015, 0.030, 0.060, and 0.090 mM; and oxamate at 0, 1.0, 2.0, 4.0 and 8.0 mM. The correlation coefficient is 0.88 for 23 points (5 points coincide at 100%-100%).

Discussion

The creation of this 24-well plate assay for acidification rate of mammalian cells was accomplished through several key modifications. First, the interference of temperature on pH measurement was minimized by using a plate reader which can maintain a constant temperature during monitoring. Moreover, the effect of change in temperature at the start of a pH monitoring experiment was accounted for by including the monitoring of wells that only contain medium. Second, a higher phenol red concentration and bicarbonate-free media resulted in clearer signals of phenol red absorbance and a lesser influence that would result from CO_2 evolution. Low buffer

capacity of the medium increased its sensitivity to minor changes in acidification rate. Moreover, a higher initial pH of 7.7 (rather than 7.4) for test medium at the start of the experiment provided a wider measurement space before reaching the shoulder of the buffer near a pH of 6.9-7.2. Third, variations of acidification rates due to differences in cell number and spatial distribution were decreased by scanning each well at 25 locations. As demonstrated in figures 2.2 and 2.3, the assay provides a quite precise measure of changes in extracellular pH's and acidification rates.

Five chemicals with well-characterized metabolic effects were used to demonstrate the acidification rate assay. Some of the chemicals' most distinct interactions with intracellular metabolic pathways were shown in figure 2.5. DNP is an uncoupling agent that acts as a proton ionophore to dissipate the proton gradient across the mitochondrial membrane.[31,34-37] Rotenone and antimycin A inhibit oxidative phosphorylation by inhibiting complex I and III respectively, where antimycin A has been reported to cause excess lactate production.[33,38] Sodium fluoride is known to inhibit glycolysis by interfering with the enzyme enolase.[32,39] Sodium oxamate has been reported to inhibit glucose consumption and lactate production by acting on lactate dehydrogenase.[40] Uncoupling ATP production from oxidative phosphorylation and blocking oxidative phosphorylation pathway are expected to result in low efficiency of energy production. Reduced energy production might be compensated through increased glycolysis and increased production of lactate.[36,38,41] Conversely, inhibition of glycolysis is expected to result in decreased glucose and lactate metabolic rates. Indeed, the observed changes in metabolism witnessed in our acidification results for DNP, AA, rotenone, oxamate, and fluoride correspond well with that expected from their established

mechanisms of action. DNP, rotenone and AA caused increases in acidification, and oxamate and fluoride caused decreases. While higher concentrations of AA deviated from our expectations, this might be due to the initiation of cell death that is not visible until 6-hours.

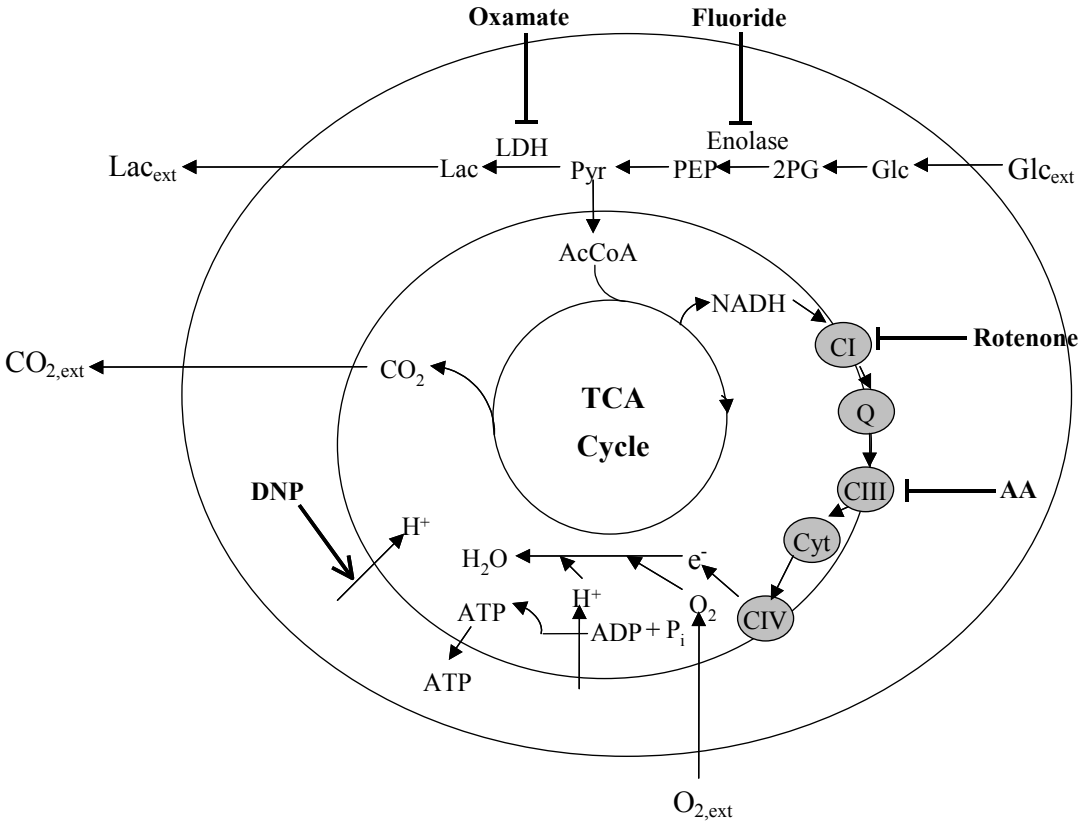

Fig 2.5. Interaction sites for DNP, AA, fluoride, rotenone, and oxamate on metabolic pathways. DNP uncouples ATP production from mitochondrial respiration. Antimycin A and rotenone inhibit complex III and I respectively in the electron transport chain. Fluoride inhibits the enzyme enolase in glycolysis. Oxamate inhibits lactate dehydrogenase. Abbreviations: AcCoA = Acetyl-CoA; ADP = adenosine diphosphate; ATP = adenosine triphosphate; AA = antimycin A; Cyt = Cytochrome C; CI = Complex I; CIII = Complex III; CIV = Complex IV; DNP = 2,4-dinitrophenol; Glc = Glucose; Lac = lactate; NADH = Nicotinamide Adenine Dinucleotide; PEP = Phosphoenolpyruvate; 2PG = 2-phosphoglycerate; Pyr = Pyruvate; TCA cycle = tricarboxylic acid cycle; Q = coenzyme Q.

While this method provides relatively fast quantitative data regarding the effects of chemicals on gross metabolic function of cells, it is really intended as a way to screen cells, media, and/or compounds for metabolic activity. Elucidation of the meaning behind acidification rate changes during a 90-min screen of an *in vitro* cell culture in a "test medium" will require further analysis. Ascertaining a working concentration range in regard to metabolic activity could constitute a resource-saving first step in the analysis of a vast variety of compounds, ranging from environmental pollutants to novel compounds of potential therapeutic value. Results from metabolic screens such as these should help in the design of subsequent experiments that employ more sophisticated tools to better document the effect of a compound. Thus far, this assay for metabolic activity has been successful in quickly identifying working ranges, which were otherwise unavailable for cell culture systems of cell lines, media, and compounds that were new and not necessarily documented in regard to metabolic activity. When correlated with traditional clinical or toxicological endpoints, a high-throughput metabolic screen might also be able to provide high content information regarding the efficacy or toxicology of test compounds.

In contrast to other commonly used cytotoxicity assays which generally require reagent addition and additional incubation time, acidification rate assay by measuring absorbance of phenol red, which is a regular component of the medium, avoids the interference of assay reagent on cells and is more amenable to be adapted to HTS. Moreover, avoiding reagent addition and additional incubation time also saves time which allow for rapid screening. However, the inherent characteristic of the assay limits its application for long term evaluation of toxicity due to two reasons: first, buffer

capacity of the medium will disguise the chemical impact when pH of the medium is within the action range of a buffer; second, the very low pH due to acid production over a long time period will perturb cells and distort the impact of the compound. Thus, some degree of caution should be given for application of this assay.

References

1. Fry, J.R. (2000). Cytotoxicity and mechanistic studies in high throughput toxicity screening, pp. 31-42. *In* Approaches to High Throughput Toxicity Screening. Taylor & Francis, London, UK.

2. Blaauboer, B.J. (2001). Toxicodynamic modelling and the interpretation of in vitro toxicity data. *Toxicol Lett* **120**, 111-123.

3. Atterwill, C.K. and M.G. Wing. (2002). In vitro preclinical lead optimisation technologies (PLOTs) in pharmaceutical development. *Toxicol Lett* **127**, 143-151.

4. Eisenbrand, G., B. Pool-Zobel, V. Baker, M. Balls, B.J. Blaauboer, A. Boobis, A. Carere, S. Kevekordes, J.C. Lhuguenot, R. Pieters and J. Kleiner. (2002). Methods of in vitro toxicology. *Food Chem Toxicol* **40**, 193-236.

5. Zucco, F. and A.L. Vignoli. (1998). In vitro toxicology in Europe 1986-1997 - Final report to the European Commission DGXI Financial Contribution no. B4-3040/96/424/DEB/E2. *Toxicol Vitro* **12**, 739-+.

6. Zucco, F., I. De Angelis, E. Testai and A. Stammati. (2004). Toxicology investigations with cell culture systems: 20 years after. *Toxicol Vitro* **18**, 153-163.

7. Evans, S.M., A. Casartelli, E. Herreros, D.T. Minnick, C. Day, E. George and C. Westmoreland. (2001). Development of a high throughput in vitro toxicity screen predictive of high acute in vivo toxic potential. *Toxicol Vitro* **15**, 579-584.

8. Cree, I.A. and P.E. Andreotti. (1997). Measurement of cytotoxicity by ATP-based luminescence assay in primary cell cultures and cell lines. *Toxicol Vitro* **11**, 553-556.

9. Slater, K. (2001). Cytotoxicity tests for high-throughput drug discovery. *Current Opinion in Biotechnology* **12**, 70-74.

10. Bradbury, D.A., T.D. Simmons, K.J. Slater and S.P.M. Crouch. (2000). Measurement of the ADP : ATP ratio in human leukaemic cell lines can be used

as an indicator of cell viability, necrosis and apoptosis. *J Immunol Methods* **240**, 79-92.

11. O'Brien, J., I. Wilson, T. Orton and F. Pognan. (2000). Investigation of the Alamar Blue (resazurin) fluorescent dye for the assessment of mammalian cell cytotoxicity. *Eur J Biochem* **267**, 5421-5426.

12. Slaughter, M.R., P.J. Bugelski and P.J. O'Brien. (1999). Evaluation of Alamar Blue reduction for the in vitro assay of hepatocyte toxicity. *Toxicol Vitro* **13**, 567-569.

13. Jauregui, H.O., N.T. Hayner, J.L. Driscoll, R. Williamsholland, M.H. Lipsky and P.M. Galletti. (1981). Trypan Blue-Dye Uptake and Lactate-Dehydrogenase in Adult-Rat Hepatocytes - Freshly Isolated Cells, Cell-Suspensions, and Primary Monolayer-Cultures. *In Vitro-Journal of the Tissue Culture Association* **17**, 1100-1110.

14. Trohalaki, S., R.J. Zellmer, R. Pachter, S.M. Hussain and J.M. Frazier. (2002). Risk assessment of high-energy chemicals by in vitro toxicity screening and quantitative structure-activity relationships. *Toxicol Sci* **68**, 498-507.

15. Chiba, K., K. Kawakami and K. Tohyama. (1998). Simultaneous evaluation of cell viability by neutral red, MTT and crystal violet staining assays of the same cells. *Toxicol Vitro* **12**, 251-258.

16. Green, L.M., J.L. Reade and C.F. Ware. (1984). Rapid Colormetric Assay for Cell Viability - Application to the Quantitation of Cyto-Toxic and Growth Inhibitory Lymphokines. *J Immunol Methods* **70**, 257-268.

17. Putnam, K.P., D.W. Bombick and D.J. Doolittle. (2002). Evaluation of eight in vitro assays for assessing the cytotoxicity of cigarette smoke condensate. *Toxicol Vitro* **16**, 599-607.

18. Wodnicka, M., R.D. Guarino, J.J. Hemperly, M.R. Timmins, D. Stitt and J.B. Pitner. (2000). Novel fluorescent technology platform for high throughput cytotoxicity and proliferation assays. *J Biomol Screen* **5**, 141-152.

19. Valentin, I., M. Philippe, J.C. Lhuguenot and M.C. Chagnon. (2001). Uridine uptake inhibition as a cytotoxicity test for a human hepatoma cell line (HepG2 cells): comparison with the neutral red assay. *Toxicology* **158**, 127-139.

20. Cao CJ, M.R., Menking DE, Valdes JJ, Cortes VI, Eldefrawi ME, Eldefrawi AT. (1997). Validation of the cytosensor for in vitro cytotoxicity studies. *Toxicol Vitro* **11**, 285-293.

21. Hafner, F. (2000). Cytosensor((R)) Microphysiometer: technology and recent applications. *Biosens Bioelectron* **15**, 149-158.

22. Bousse, L. (1996). Whole cell biosensors. *Sens Actuator B-Chem* **34**, 270-275.

23. Cooke, D. and R. O'Kennedy. (1999). Comparison of the tetrazolium salt assay for succinate dehydrogenase with the cytosensor microphysiometer in the assessment of compound toxicities. *Anal Biochem* **274**, 188-194.

24. Cao CJ, E.M., Eldefrawi AT, Burnett JW, Mioduszewski RJ, Menking DE, Valdes JJ. (1998). Toxicity of sea nettle toxin to human hepatocytes and the protective effects of phosphorylating and alkylating agents. *TOXICON* **36**, 269-281.

25. Cao CJ, M.R., Menking DE, Valdes JJ, Katz EJ, Eldefrawi ME, Eldefrawi AT. (1999). Cytotoxicity of organophosphate anticholinesterases. *IN VITRO CELLULAR & DEVELOPMENTAL BIOLOGY-ANIMAL* **35**, 493-500.

26. Wille, K., L.A. Paige and A.J. Higgins. (2003). Application of the Cytosensor (TM) microphysiometer to drug discovery. *Receptors & Channels* **9**, 125-131.

27. CRC press, c., OH. (2000/01). *In* CRC handbook of chemistry and physics. CRC Press, Cleveland, OH.

28. Balcarcel, R.R. and L.M. Clark. (2003). Metabolic screening of mammalian cell cultures using well- plates. *Biotechnol Prog* **19**, 98-108.

29. Girard, P., M. Jordan, M. Tsao and F.M. Wurm. (2001). Small-scale bioreactor system for process development and optimization. *Biochem Eng J* **7**, 117-119.

30. John, G.T. and E. Heinzle. (2001). Quantitative screening method for hydrolases in microplates using ph indicators: Determination of kinetic parameters by dynamic pH monitoring. *Biotechnol Bioeng* **72**, 620-627.

31. Linsinger, G., S. Wilhelm, H. Wagner and G. Hacker. (1999). Uncouplers of oxidative phosphorylation can enhance a Fas death signal. *Mol Cell Biol* **19**, 3299-3311.

32. Niknahad, H., S. Khan, C. Sood and P.J. Obrien. (1994). Prevention of Cyanide-Induced Cytotoxicity by Nutrients in Isolated Rat Hepatocytes. *Toxicol Appl Pharmacol* **128**, 271-279.

33. Zhang, J.G., M.A. Tirmenstein, F.A. Nicholls-Grzemski and M.W. Fariss. (2001). Mitochondrial electron transport inhibitors cause lipid peroxidation-dependent and -independent cell death: Protective role of antioxidants. *Arch Biochem Biophys* **393**, 87-96.

34. Sibille, B., C. Filippi, M.A. Piquet, P. Leclercq, E. Fontaine, X. Ronot, M. Rigoulet and X. Leverve. (2001). The mitochondrial consequences of uncoupling intact cells depend on the nature of the exogenous substrate. *Biochem J* **355**, 231-235.

35. Sibille, B., X. Ronot, C. Filippi, V. Nogueira, C. Keriel and X. Leverve. (1998). 2,4 dinitrophenol-uncoupling effect on Delta Psi in living hepatocytes depends on reducing-equivalent supply. *Cytometry* **32**, 102-108.

36. Khayat, Z.A., T. Tsakiridis, A. Ueyama, R. Somwar, Y. Ebina and A. Klip. (1998). Rapid stimulation of glucose transport by mitochondrial uncoupling depends in part on cytosolic Ca2+ and cPKC. *American Journal of Physiology-Cell Physiology* **44**, C1487-C1497.

37. Leverve, X., B. Sibille, A. Devin, M.A. Piquet, P. Espie and M. Rigoulet. (1998). Oxidative phosphorylation in intact hepatocytes: Quantitative characterization of the mechanisms of change in efficiency and cellular consequences. *Molecular and Cellular Biochemistry* **184**, 53-65.

38. Tiefenthaler, M., A. Amberger, N. Bacher, B.L. Hartmann, R. Margreiter, R. Kofler and G. Konwalinka. (2001). Increased lactate production follows loss of mitochondrial membrane potential during apoptosis of human leukaemia cells. *Br J Haematol* **114**, 574-580.

39. Kerai, M.D.J. and J.A. Timbrell. (1997). Effect of fructose on the biochemical toxicity of hydrazine in isolated rat hepatocytes. *Toxicology* **120**, 221-230.

40. Sanfeliu, A., C. Paredes, J.J. Cairo and F. Godia. (1997). Identification of key patterns in the metabolism of hybridoma cells in culture. *Enzyme Microb Technol* **21**, 421-428.

41. Pilatus, U., E. Aboagye, D. Artemov, N. Mori, E. Ackerstaff and Z.M. Bhujwalla. (2001). Real-time measurements of cellular oxygen consumption, pH, and energy metabolism using nuclear magnetic resonance spectroscopy. *Magnetic Resonance in Medicine* **45**, 749-755.

CHAPTER III

DETERMINATION OF CARBON DIOXIDE PRODUCTION RATES FOR MAMMALIAN CELLS IN A SEALED 24-WELL PLATE

Abstract

This work describes a high throughput method for quantitative determination of carbon dioxide production rates of mammalian cells in 24-well plate format. Gas-liquid mass transfer of CO_2 produced by the cells is simulated in a sealed system with variable pH, which guides the design of custom-made, reusable, optically clear plugs to seal the wells of a 24-well plate. These plugs prevent the loss of CO_2 produced by the mammalian cells cultured in bicarbonate-free medium. Measurements of pH, total liquid phase CO_2, and viable cell density are used to estimate the average CO_2 production rate during a 6-hour incubation period. The method is demonstrated using fibroblast cells treated with four chemicals that are known to act on mitochondria: 2,4-dinitrophenol, antimycin A, rotenone, and cyanide. Significant changes in CO_2 production were observed for given concentrations of the chemicals within 6-h and without a decline in culture viability. Similar concentrations of chemicals corresponded with growth inhibition over longer times but not with cell death. An assay based on metabolic change corresponding to growth inhibition that is more sensitive than traditional measure of cell death is a feasible complement to existing methods in drug discovery and toxicity testing.

Introduction

Research in metabolic engineering, cell culture process, and drug discovery all involve studies of cellular responses to culture environment, biochemical molecules, and drugs. Rates of metabolic reactions are the bases for many cellular physiological functions, including growth, death, and generation of energy. Studies of the metabolic status of cells often involve parameters such as glucose, lactate, pH, CO_2 and oxygen, changes in which are relevant to major metabolic pathways such as glycolysis, the TCA cycle, and oxidative phosphorylation. CO_2 is a major product of mammalian cell metabolism and is produced in many biochemical reactions, chiefly the pentose phosphate pathway and the citric acid cycle. Thus, measurement of CO_2 produced by mammalian cells can provide a complementary measure of changes in central carbon metabolism and mitochondrial function.

A lot attention has focused on the determination and control of CO_2 in mammalian cell culture process due to its impact on growth rate, product production rate and quality, intracellular pH, and apoptosis.[1-6] Historically, CO_2 production rate of mammalian cells could not be easily monitored because of the solution/dissolution of carbon dioxide in the culture medium and small amount of CO_2 produced compared to microbial cultures.[4] In addition, the use of $NaHCO_3$ buffer for most animal cell culture process further complicates the measurement of CO_2 production rate because a substantial CO_2 converted from them may mask the contribution of CO_2 that produced by cells.[4,7] Currently, quantitative determination of CO_2 production rates is feasible only in bioreactors equipped with mass spectrometers or gas analyzers for gas phase mole

fraction determinations and CO_2 probes and/or blood gas analyzers for total liquid phase CO_2.[4-10] None of them has been in a format readily amenable for high-throughput usage.

In this work, I made novel sealing plugs for a 24-well plate system and a corresponding method that allows for measurement of CO_2 production rates of mammalian cell cultures. The method is demonstrated using fibroblast cells treated with four chemicals that are known to act on mitochondria: 2,4-dinitrophenol, antimycin A, rotenone, and cyanide.[11-14] Presumably, perturbation of mitochondrial function and the indirect effect on the rate of oxidation of metabolic substrates would be manifested in changes in CO_2 production. The method presented in this paper provides a faster, cheaper, multi-replicate, and comparably quantitative way to determine CO_2 production rates of mammalian cells. It is applicable to suspension as well as adherent cell lines and is useful for screening volatile compounds too. It will be of use in various fields such as cell culture engineering, metabolic engineering, toxicology, and drug discovery and drug development.

Materials and methods

Modeling gas-liquid mass transfer of CO_2 produced by cells

To guide the design for measurement of CO_2 production rate, a model was set up to describe the mass transfer of CO_2 within liquid and gas phase in open and sealed batch culture system. In a sealed system, the carbon dioxide produced by cells will exist in the liquid phase as dissolved CO_2 in equilibrium with bicarbonate and carbonate or in the gas phase as gaseous CO_2. It should be noted that only CO_2 could be exchanged with the gas phase.

$$cell \xrightarrow{q_{CO_2}} CO_2 + H_2O \longleftrightarrow H_2CO_3 \longleftrightarrow HCO_3^- + H^- \longleftrightarrow 2H^+ + CO_3^{2-} \quad (3\text{-}1)$$

At a temperature of 37 °C and a pH value of approximately 7 under regular cell culture conditions, less than 0.5% of the dissolved CO_2 is presented as H_2CO_3 and almost none as CO_3^{2-}.[6] Thus, both species are neglected and the equilibrium reaction can be simplified as:

$$cell \xrightarrow{q_{CO_2}} CO_2 + H_2O \longleftrightarrow HCO_3^- + H^+ \quad (3\text{-}2)$$

At known pH, CO_2 and HCO_3^- are in equilibrium according to:

$$C_{CO_2} = \frac{C_A}{1 + \frac{K_{CO_2}}{10^{-pH}}} \quad (3\text{-}3)$$

where C_{CO_2} is the dissolved CO_2 concentration, C_A is the sum of liquid concentration of C_{CO_2} and $C_{HCO_3^-}$, and K_{CO_2} is the dissociate equilibrium constant.

Due to the high mass transfer coefficient of CO_2 in the gas phase, the concentration of CO_2 in the gas phase is in relatively rapid equilibrium with the CO_2 concentration in the gas liquid interphase ($C^*_{CO_2}$) according to Henry's law:

$$Py = HC^*_{CO_2} \quad (3\text{-}4)$$

The CO_2 transfer between liquid and gas phases can be described by two mass balance equations.[7] In liquid phase, the C_A balance for a batch culture becomes:

$$V_l \frac{dC_A}{dt} = n_v q_{CO_2} V_l + kla(C^*_{CO_2} - C_{CO_2})V_l \quad (3\text{-}5)$$

For gas phase, the mass balance can be described as:

$$\frac{PV_g}{RT}\frac{d(y)}{dt} = -kla\,(C^*_{CO_2} - C_{CO_2})V_l \quad (3\text{-}6)$$

For a system with variable pH, CO_2 transfer also depends on the pH and buffer capacity of the liquid phase. Both CO_2 and lactate produced by cells contribute the acid production for change in pH of liquid phase as shown in equation 3-1 and 3-7.

$$cell \xrightarrow{q_{lac}} Lactate \longrightarrow Lac^- + H^+ \tag{3-7}$$

In the liquid phase containing buffer, the buffer will quench a portion of the protons.

$$B^- + H^+ \xleftrightarrow{K_a^{buffer}} HB \tag{3-8}$$

Since the change in concentration of protons consumed by or produced from each species is equal to its dissociated basic species, the differential change of proton concentration in liquid can be expressed as:

$$dC_{H^+} = dC_{Lac^-} + dC_{HCO_3^-} + dC_{B^-} \tag{3-9}$$

From the dissociated reaction equilibrium, the concentration of dissociated basic species is dependent on total concentration of buffer and pH:

$$C_{B^-} = \frac{K_B C_{tot-B}}{C_{H^+} + K_B} \tag{3-10}$$

where total buffer concentration (C_{tot-B}) is the sum of concentration of HB and its dissociated basic species B^-. Derivative yields equation:

$$dC_{B^-} = \frac{K_B}{C_{H^+} + K_B} dC_{tot-B} - \frac{C_{tot-B} K_B}{(C_{H^+} + K_B)^2} dC_{H^+} \tag{3-11}$$

Total concentration of buffer is constant, thus

$$dC_{B^-} = -\frac{K_B C_{tot-B}}{(C_{H^+} + K_B)^2} dC_{H^+} \tag{3-12}$$

Lactate and CO_2, however, are functions of time:

$$dC_{tot-lac} = n_v q_{lac} dt \tag{3-13}$$

and

$$dC_{tot-CO_2} = n_v q_{CO_2} dt \tag{3-14}$$

where $C_{tot-lac}$ and C_{tot-CO_2} are total lactate and CO_2 concentrations, q_{lac} and q_{CO_2} are the lactate production rate and CO_2 production rate, respectively. Substitution of equations 3-13 and 3-14 into 3-11 to get $dC_{HCO_3^-}$ and dC_{lac^-}, and then substitution of 3-12 into 3-10 to finally yields equation 3-15, after rearrangement.

$$(1 + \sum_{i=1}^{3} \frac{K_i C_{tot-i}}{(C_{H^+} + K_i)^2}) \frac{dC_{H^+}}{dt} = \frac{K_{CO_2}}{C_{H^+} + K_{CO_2}} \frac{dC_{A-CO_2}}{dt} + n_v q_{lac} \tag{3-15}$$

where K_i represents the dissociation constant of bicarbonate, lactate and buffer; C_{tot-i} represents the total concentrations of three species. The medium for CO_2 production rate assay is buffered with Hepes. Other components of the medium, such as phenol red and amino acids, are also buffers. Their buffer capacity is neglected due to either their concentrations are low or their pKa's are out of the range of the pH of the medium under culture condition. A combination of mass balance equations for CO_2 and protons with phase equilibrium equations allows for calculation of dynamic changes of CO_2 in gas and liquid phases and pH in liquid phase. Dissociation constants and the Henry's law constant are from literature.[15,16] The pK_a values used here are 6.138, 3.86, and 7.5 for HCO_3^-, lactate, and Hepes, respectively. Henry's law constant of CO_2 is 4.20×6 $Pa \cdot m^3 \cdot mmol^{-1}$. kla is determined experientially to be 28.2 hr^{-1}. n_v is 1.5×10^6 cells/mL and q_{lac} and q_{CO_2} are estimated to be 3×10^{-10} and 1×10^{-10} mmol/cell/hr, respectively, based on cells growing at regular culture condition. Coupled normal differential equations are solved numerically in Matlab.

Cell culture and media

Mouse fibroblast cells (CRL-10225) were obtained from ATCC (Manassas, VA, USA). During routine maintenance, cells are grown in T-75 cm^2 flasks (VWR International, Inc., Suwanee, GA, USA) placed in an incubator (Forma Scientific, Inc., Marietta, OH, USA) controlled at 37°C, 95% humidity, and 10% CO_2. Maintenance medium consists of DMEM (Mediatech, Herndon, VA, USA) supplemented with 10% fetal bovine serum (Sigma Chemical Co. St. Louis, MO, USA), 10 U/ml penicillin–10 μg/mL streptomycin (Sigma Chemical Co.), and 4 mM L-glutamine (Mediatech). This medium contains 25 mM D-glucose and is buffered with 3700 mg/L of sodium bicarbonate. Medium used during cell attachment prior to the start of a CO_2 production rate ("pretest" medium) consists of bicarbonate-free/glucose-free RPMI 1640 medium containing 2.05 mM glutamine (Sigma Chemical Co.). It is supplemented with 10% fetal bovine serum, 25 mM D-glucose, 10 U/mL penicillin–10 μg/mL streptomycin, and 50 mM Hepes (Sigma Chemical Co.). Medium used during the CO_2 production rate assay ("CPR-test" medium) is the same as pretest media, with the exceptions of substituting10 mg/L insulin and 5 mg/L holo-transferrin for serum, reducing glucose to 5.0 mM, and increasing phenol red to 30.0 mg/L for the spectrophotometric pH measurement (all from Sigma Chemical Co.).

Test chemicals

2,4-dinitrophenol (DNP), antimycin A, rotenone and potassium cyanide were purchased from Sigma Chemical Co. Concentrated stocks of DNP, antimycin A, and rotenone were made in ethanol, whereas a concentrated stock of potassium cyanide was made in sterilized water. Test media for control and 5 different concentrations of a

chemical received the necessary amount of concentrated stock, as well pure solvent so that the final concentration of solvent in every medium was 1% (vol/vol).

Sealing plugs for the 24-well plate CO_2 production rate assay

Determination of CO_2 production rates was accomplished in 24-well plates (BD Biosciences, Benford, MA, USA) sealed with custom-made plugs (Figure 3.1). The plugs were milled from clear polycarbonate plastic rods by the Vanderbilt science machine shop and fitted with Viton® O-rings (McMaster, Atlanta, GA, USA). The O-rings are under slight tension when placed in the groove near the top of the plug, causing their outer diameter match that of the well near its opening. When inserted into a well filled with 0.50 mL of culture, a plug reduces the headspace volume in a well to 1.10 mL. The plugs are inserted by pushing softly until the O-ring is just within the top of the well. Prior to use in an experiment, the plugs are sterilized using 70% isopropyl alcohol (Sigma Chemical Co.).

pH measurement

The pH of each sealed well at the end of a CO_2 production rate test is determined prior to unsealing it by measuring the absorbance of the pH indicator, phenol red, using a method described previously in chapter II.[17] Absorbance readings for pH measurement were performed on an FL 600 plate reader (Bio-Tek Instruments, Winooski, Vermont, USA) with temperature controlled at 37°C. To correct for variations in plug clarity, condensation, and well plate background, an absorbance at A_{720} is taken and subtracted from one at A_{562}. Furthermore, the mean of absorbance of scans at twenty-five distinct locations per well is used to reduce variation of cell coverage. The net absorbance is converted to pH using a calibration line constructed in advance, and the estimated error in

the pH measured using this method is less than 0.03 pH units. For all experiments conducted, the pH of a given well and chemical concentration decreased from 7.3 initially to a minimum of 6.8.

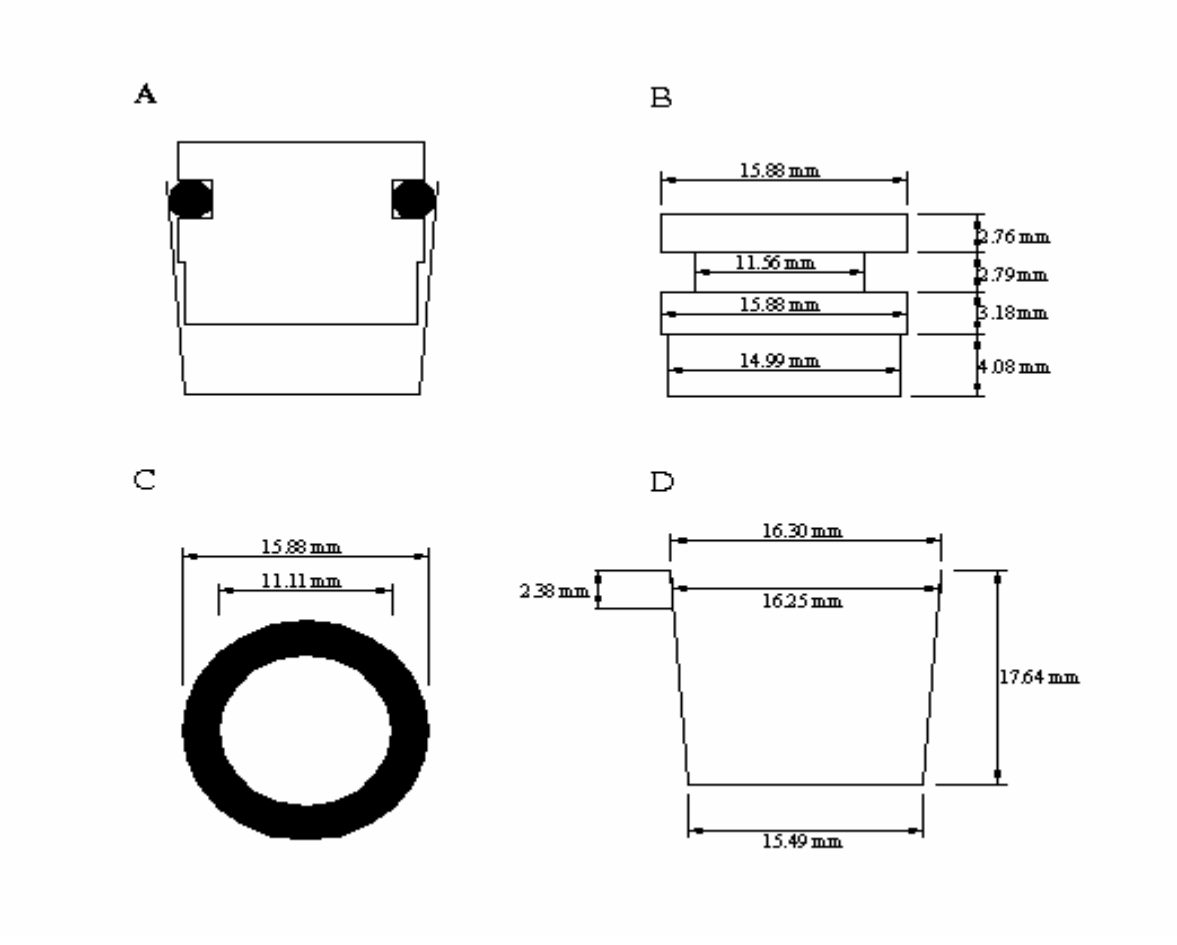

Figure. 3.1. Sealed well-plate system for CO_2 production rate assay. (A) Side view section of well sealed with a plug. (B) Side view of a polycarbonate plug. (C) Top view of Viton O-ring. (D) Side view section of a well dimensions; also shown are the width of O-ring and width of the well at the O-ring's point of contact.

Enzymatic assay for total liquid phase CO_2

The total liquid phase CO_2 (dissolved CO_2 and HCO_3^-) for each well of a 24-well plate is determined by enzymatic assay. The enzymatic assay is based on an original Sigma recipe developed by Forrester.[18] In this assay, phosphoenol pyruvate is converted to malate in two reactions catalyzed by phosphoenol pyruvate carboxylase (Calbiochem-Novabiochem Corp., La Jolla, CA, USA) and malic dehydrogenase (Sigma Chemical Co.).

$$HCO_3^- + Phosphoenolpyruvate \xrightarrow{PEPC} Oxaloacetate + H_2PO_4^- \quad (3\text{-}16)$$

$$Oxaloacetate + NADH \xrightarrow{MDH} Malate + NAD^+ \quad (3\text{-}17)$$

The first reaction requires a stoichiometric proportion of bicarbonate. The second reaction consumes the intermediate oxaloacetate while concomitantly consuming NADH (β-nicotinamide adenine dinucleotide reduced disodium salt hydrate, Sigma Chemical Co.), which is detected by loss of absorbance. We reconstructed the assay to increase its precision for concentrations in the range of 0.0 to 4.0 mM total CO_2 and to optimize absorbance reading from a 96-well plate instead of cuvettes. The new recipes are as follows: the buffer solution is comprised of 100 mM Tris buffer and 10 mM magnesium chloride (Sigma Chemical Co.), at a pH of 8.5; reagent A contains 37.3 mM PEP (Sigma Chemical Co.) and 4.7 mM NADH in buffer solution; and reagent B contains 11200 U/L MDH and 22400 U/L PEPC in buffer solution.

To conduct the assay, an appropriate number of wells of a 96-well plate (VWR International, Inc) are pre-filled with 120 μL of reagent A. Then, triplicate 70 μL volumes of standards (sodium bicarbonate in distilled water, Sigma Chemical Co.) and

test samples are added to each well. Test samples are obtained from the 24-well plate by unplugging each well one at a time. The initial absorbencies of the wells are read at 375 nm using a μ-Quant UV/vis plate reader (Bio-Tek Instruments) at room temperature. Then, 10 μL of reagent B is added to each well, the plate is incubated for 15 minutes at room temperature, and the final absorbencies are determined at 375 nm.

Determination of CO_2 production rates of fibroblast cell cultures treated with chemicals

Fibroblast cells harvested from T-75 cm^2 flasks are centrifuged at 200g for 10 minutes and resuspended in pretest medium at a cell density of $1.5x10^6$ cells/mL. 500 μL of this culture are seeded into wells of three rows of the 24-well plate, where a first row is reserved as cell-free. The well plate is then incubated in an oven (VWR International, Inc.) with ambient levels of CO_2 at 37 °C for 10 hours to allow cell attachment. Next, pretest medium is removed; all wells are washed twice with PBS (phosphate-buffered saline, Mediatech) and 500 μL of test media containing specific chemical concentrations is added to each well of one column, including the cell-free well. Each well of the plate is sealed by manual application of the plugs and incubated in the oven for 6 hours at 37 °C. At the end of the incubation period, absorbencies at 562 nm and 720 nm are read. Finally, each well is opened, immediately sampled in triplicate, and samples added into a 96-well plate prepared with CO_2 assay reagent. After sampling, cell number and viability are determined for one well of each column (of each chemical concentration) by hemocytometer with trypan blue staining.

Calculation of CO_2 production rates

The actual measured quantity in the enzymatic assay is C_A, the sum of dissolved CO_2 (C_{CO_2}) and bicarbonate ($C_{HCO_3^-}$). After pH and C_A are determined for each well, dissolved CO_2 can be calculated using dissociated equilibrium equation 3-3. For gas-liquid systems at equilibrium, as shown in equation 3-4, Henry's law adequately describes the relationship between gas liquid interphase equilibrium ($C^*_{CO_2}$) and y_{CO_2}, the mole fraction in the headspace of a well. With a large mass transfer rate of CO_2 of 28.2 hr^{-1} (experimentally determined), it is reasonable to assume equilibrium between liquid and gas phase CO_2 and to use the bulk concentration in the Henry's law expression. Thus, the fraction of CO_2 (y_{CO_2}) in headspace can be calculated using equation 3-4 based on calculated dissolved CO_2. Finally, total CO_2 (C_{tot}) present in the well can be expressed as the total amount of CO_2 existing in gas plus the liquid phases divided by the culture volume, which is shown in equation 3-18 after rearrangement.

$$C_{tot} = C_A \left(1 + \frac{HV_g}{(1 + \frac{K}{10^{-pH}})V_l RT} \right) \tag{3-18}$$

Values of dissociation constant K and Henry's law constant were same as used in the CO_2 transfer simulation. The value of R used in the calculation is 8.31×10^3 Pa·L/mol/K.

The average CO_2 production rate for each well during the exposure interval is calculated as the difference of endpoint total CO_2 content of wells with cells and cell-free wells, divided by the viable cell density and time interval (Equation 3-19).

$$\bar{q}_{CO_2} = \frac{C_{tot} - C_{tot-cell\ free}}{n_v \cdot \Delta t} \tag{3-19}$$

The viable cell density used is the average of initially seeded viable cell density and final viable cell density determined by the trypan blue count, neglecting growth during 10 hours of attachment.

Additional assays for culture viability

The viabilities of fibroblast cultures exposed to the chemicals were further assessed using separate experiments in unsealed 24-well plates during 6- and 24-h incubations. Here, culture viability was determined using MTT (Sigma Chemical Co.) and resazurin (Sigma Chemical Co; also known as Alamar Blue^{TM}) assays. The resazurin reagent was prepared at a concentration of 0.0105%.[19] The pre-test medium for these viability tests was the same as the pre-test medium used prior to the CO_2 production rate assay. Media during 6-h incubations was the same as the CPR-test media, with the exception of having a standard amount of phenol red (5.3 mg/L) to avoid interference with the MTT and resazurin readings. Medium for 24-h incubations was the same as media for 6-h incubations, with the exception of having 25 mM glucose.

Growth of fibroblast cell cultures treated with chemicals

The effects of chemicals on cell growth were determined in 6-well plate (VWR International, Inc.) experiments. Prior to adding medium with chemicals, the cells were placed into wells at a density of 2×10^5 viable cells/mL and allowed to attach by incubating in maintenance medium for 10 hours in an incubator controlled at 37 °C, 95% humidity, and 10% CO_2. Then, maintenance medium was removed, cells were washed with PBS, and growth-test medium containing a specific concentration of a chemical was added to the cultures. Cell growth was followed for 6 days. Each day and for each concentration tested, one well was sacrificed for a cell count of both adherent and

detached cells using the trypan blue exclusion method. Medium used for these assays consisted of bicarbonate-free and glucose-free RPMI 1640 medium containing 2.05 mM glutamine and supplemented with 25.0 mM D-glucose, 10% fetal bovine serum, 10U/mL penicillin-10 μg/mL streptomycin, and 2000 mg/L of sodium bicarbonate. This formulation differs from CPR-test medium in glucose content and buffering in order to allow for longer-term monitoring of cultures.[7]

Statistical analysis

Statistical significance at the 95% confidence level of differences between test and control cultures was compared using a Dunnett's test in software JMPIN™ (DUXBURY, Pacific Grove, CA, USA).

Results

Simulated dynamic change of CO_2 concentration in the liquid and gas phase

The CO_2 production rate assay is designed under the direction of simulated mass transfer of CO_2 between liquid and gas phase. The mass transfer coefficient of CO_2 used for the model is determined experimentally by simultaneously monitoring CO_2 release and pH change of test medium in open well plate, which initial CO_2 concentration is obtained by equilibrating with 10% CO_2 in the incubator. The simulated dynamic changes of total liquid phase CO_2 concentration and mole percentage of CO_2 in the gas phase are shown in figure 3.2. In open condition, the accumulated CO_2 concentration in the liquid phase is less than 0.10 mM at all times, and the mole percentage of CO_2 released into the air increases up to over 90% at 10 hr incubation. In contrast, in sealed condition, the total liquid phase CO_2 concentration accumulate appreciably in a linear

fashion, up to 0.87 mM and 1.20 mM at 10 hr for headspace at volume of 3 mL and1.0 mL, respectively. The percentage of CO_2 released into the gas phase also increases slightly with the accumulation of CO_2 in the liquid phase, and the percentage is up to 40% and 20% for headspace at volume of 3 mL and1.0 mL. In comparison of the effect of the volume of headspace, more CO_2 is accumulated in the liquid phase with reduced volume of headspace. Since the enzyme assay measures the total liquid phase CO_2 concentration, therefore, the culture system needs to be sealed with a reduced volume of headspace for clearer signal. Moreover, the amount of CO_2 in the gas phase is significant and needs to be taken account for accurate determination of CO_2 production rate.

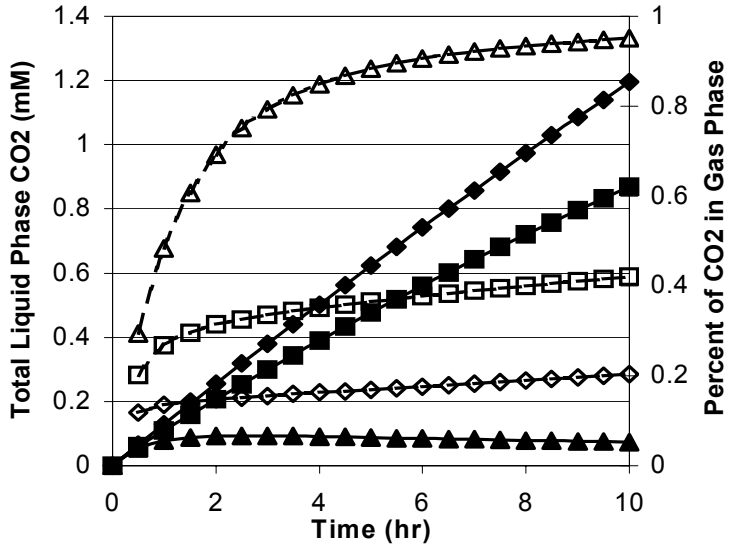

Fig. 3.2. Simulated distribution of CO_2 produced by cells in liquid phase and gas phase in open and sealed conditions. Solid lines and markers represent dynamic changes of total liquid phase CO_2 concentration in open (▲) and sealed conditions with the volume of headspace at 1 mL (♦) and 3 mL (■). Dashed lines corresponds to the percentage of CO_2 produced by cells (mol/mol) released to gas phase in open (△) and sealed conditions with the volume of headspace at 1 mL (◊) and 3 mL (□).

Accumulation of CO_2 in plug-sealed wells

Based on the simulated results, plugs were designed to seal the wells to reduce the volume of headspace at volume of 1.10 mL. To verify the design and optimize the incubation time, the total liquid phase CO_2 concentrations of wells containing 500 μL of fibroblast culture in sealed condition were analyzed at the end of 2-, 4-, 6-, 8- and 10-hr intervals and compared to the results obtained in open condition. As shown in figure 3.3, wells that were left open only reached a total liquid phase CO_2 concentration of 0.08 mM at all times. In contrast, wells that were sealed with the custom-made plugs demonstrated a fairly linear increase in CO_2 accumulation, up to 1.2 mM at 10 hours. The results agreed with those predicted from modeling.

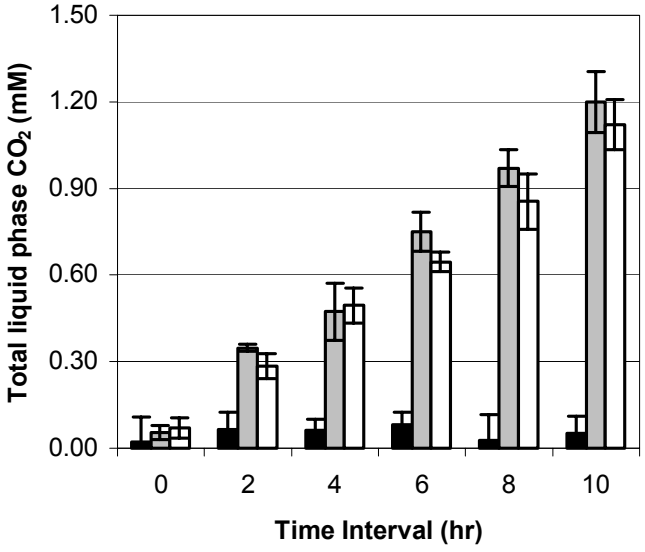

Fig. 3.3. Measurement of total liquid phase CO_2 in open and sealed-well fibroblast cell cultures. Total liquid phase CO_2 measured at the end of a time interval for open wells (black bar), plug-sealed wells (gray bars), and an independent replicate experiment for plug-sealed wells (white bars). Results are the average and standard deviation of measurements from three separate wells.

The well headspace volume of the current design is small enough to allow CO_2 to accumulate appreciably for clear signal. As predicted from modeling, the increase in CO_2 accumulation in the liquid phase can be obtained by further reducing the volume of headspace. However, this is not achievable because bigger size of the plug will contact the medium and interfere with the pH measurement. Moreover, too small headspace might cause oxygen depletion which will perturb metabolic status of cells. To verify that the oxygen is not limited under current design, the metabolic statuses of fibroblast cells cultured in the open and sealed conditions are compared by measuring glucose uptake and lactate production over 10 hr incubation. As shown in figure 3.4, there is no significant difference observed between results obtained in sealed and open condition for both glucose uptake and lactate production.

The loss of CO_2 during opening of plug and sampling of supernatant is also one factor which can affect the accuracy for determination of CO_2 production rate. The procedures of plug opening and supernatant sampling can be accomplished in a less than 10 seconds. The loss of CO_2 in such a short period is verified to be negligible based on the mass transfer experiments (not shown). The concentrations of accumulated CO_2 in the liquid phase over 6 hr are sufficient to detect the difference and the signal-to-noise ratio is acceptable. In a batch system, significant changes in extracellular environment will affect the precision of average metabolic rates. Thus, short incubation period is preferred and 6-hr interval is used for subsequent exposure experiments.

(A)

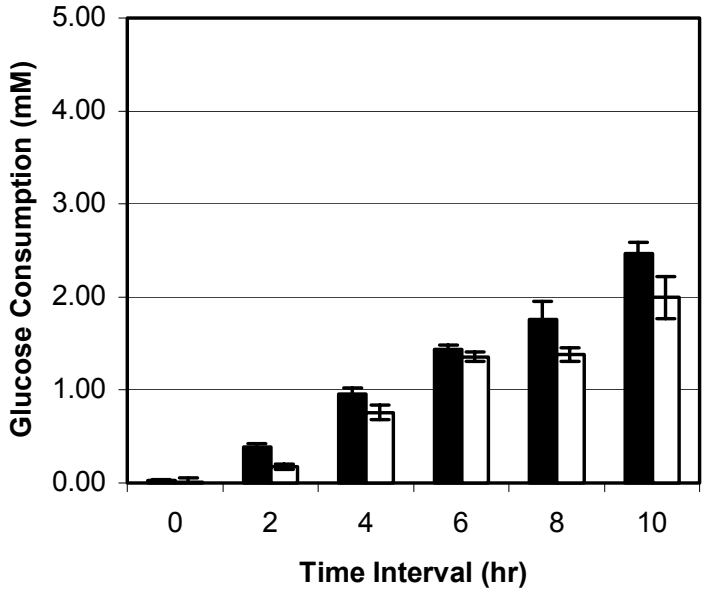

(B)

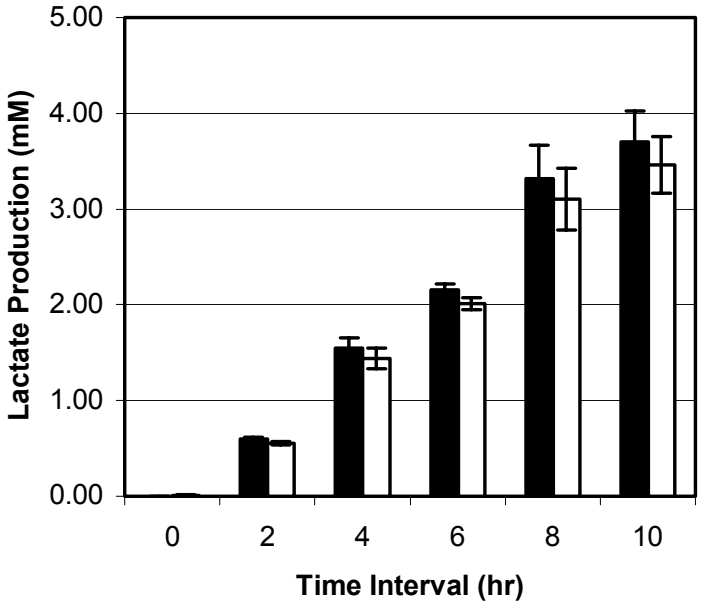

Fig. 3.4. Comparison of well plate fibroblast cell culture glucose uptake and lactate production in open and sealed condition. Figure shows the changes in glucose (A) and lactate (B) concentration at the end of a time interval for open wells (white bar) and plug-sealed wells (black bar). Results are the mean and standard deviation of measurements from three separate wells.

Estimation of headspace CO_2 mole fractions

Since the fraction of total CO_2 to be found in the headspace of a plug-sealed well under culture conditions is about 20%, it needs to be taken account for more accurate determination of CO_2 production rate. To verify the estimation of headspace mole fractions of CO_2 based on measurements for pH and total liquid phase CO_2, we equilibrated test medium in cell-free wells in a temperature-controlled CO_2 incubator set to maintain CO_2 at a particular level, which was confirmed by FYRITE Gas Analyzer (Bacharach, New Kensington, PA, USA). Results are shown in table 3.1 for tests accomplished with incubator gas phase CO_2 settings of 3, 5, 7, and 10%, where incubator settings less than 3% were not achievable with high precision. The calculated values agreed sufficiently well with those set during the incubation, obviating a need to better define the parameters obtained from the literature.

Table 3.1. Comparison of measured and calculated total liquid phase CO_2. Measured total liquid phase CO_2 and measured pH obtained from cell-free test medium in 24-well plates equilibrated in an incubator with fixed percentage of CO_2. The estimated mole fraction is that calculated using equilibrium equations (with dissociation and Henry's law constants from the literature) and the measured quantities. The % Difference is the difference of the estimated and set mole percentages divided by the set mole percentage.

Incubator setting for mole percentage of CO2 (%) in gas phase	**3.0**	**5.0**	**7.0**	**10.0**
Measured pH	6.3±0.01	6.27±0.01	6.20±0.03	6.16±0.03
Measured total liquid phase CO2 (mM)	1.69±0.05	2.68±0.05	3.91±0.03	4.50±0.21
Estimated mole percentage (%)	**2.86**	**4.72**	**7.56**	**9.14**
% Difference	-4.6	-5.6	8.0	8.6

Monitoring CO_2 production rates of fibroblast cell cultures exposed to four chemicals

The developed assay was demonstrated by testing the effects of various concentrations of DNP, antimycin A, rotenone, and potassium cyanide on the average CO_2 production rates of fibroblast cell cultures obtained over 6-h (Figure 3.5). DNP caused increases in CO_2 production up to approximately 50% for all concentrations tested, as low as 0.02 mM. CO_2 production was inhibited by 60-70% for all concentrations of antimycin A and rotenone tested, as low as 0.002 and 0.02 mM, respectively. Cyanide inhibited CO_2 production by 35% to 65% for doses ranging from 0.20 to 1.00 mM.

(A)

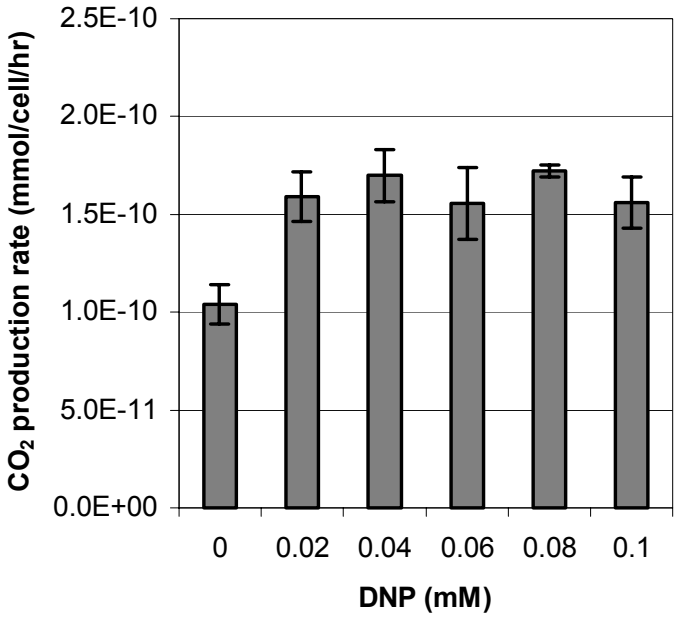

(B)

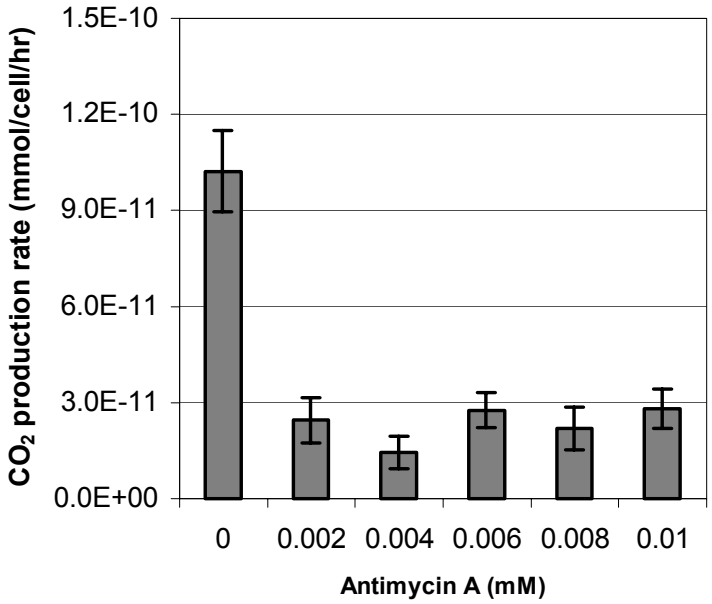
1.5E-10
1.2E-10
9.0E-11
6.0E-11
3.0E-11
0.0E+00
CO2 production rate (mmol/cell/hr)
0
0.002
0.004
0.006
0.008
0.01
Antimycin A (mM)

(C)

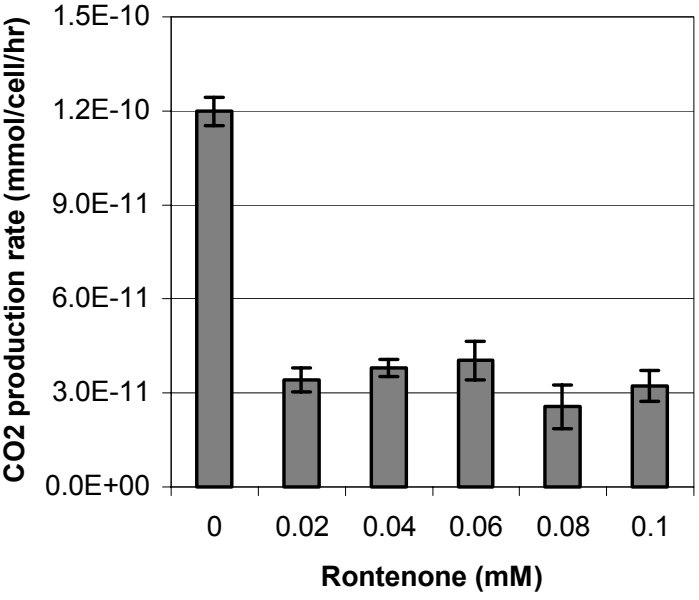
1.5E-10
1.2E-10
9.0E-11
6.0E-11
3.0E-11
0.0E+00
CO2 production rate (mmol/cell/hr)
0
0.02
0.04
0.06
0.08
0.1
Rontenone (mM)

(D)

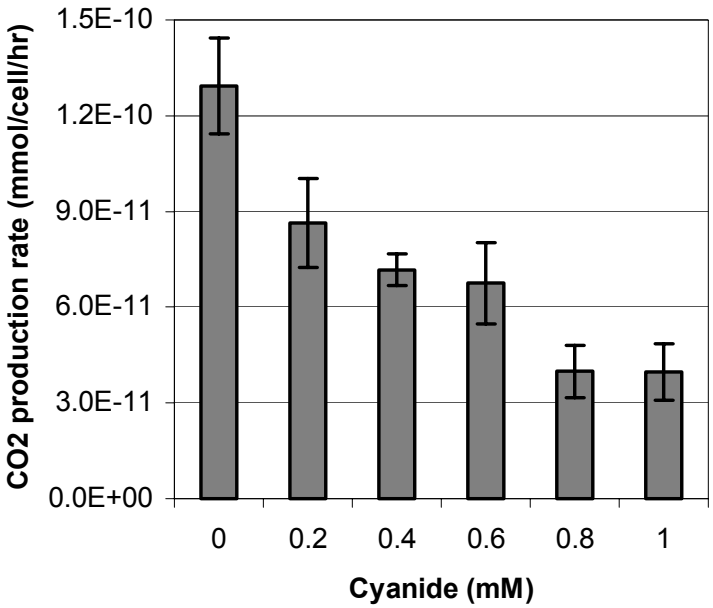

Figure 3.5. Determination of CO_2 production rates for fibroblast cell cultures exposed to four toxic chemicals. Rates are determined at six concentrations for fibroblasts exposed for 6 hr to (A) DNP, (B) antimycin A, (C) rotenone, and (D) cyanide. Experiments were performed independently from each other. Data shown are the average and standard deviations of measurements from three separate wells. Culture cell density and viability were unchanged during the 6-hour exposure period (not shown). DNP, 2,4-dinitrophenol.

Short- and long-term effects of chemicals on growth and death of fibroblast cultures

The fibroblast cultures exposed to these chemicals showed no noticeable changes in cell density or culture viability at the end of the 6-h incubation as determined by cell counts using trypan blue (not shown). The lack of effect on viability of the cultures at 6-h was further confirmed in additional experiments where viability was measured by MTT and resazurin assays (data not shown). Decreases in culture viability at 6-h were observed for two chemicals, antimycin A and cyanide, when we increased their concentrations to 0.06-0.09 mM and 5.0-20.0 mM, respectively, where the range quoted is that taken from both the resazurin and MTT results (Figure 3.6). Maximum achievable concentrations of

DNP and rotenone of 1.0 mM and 0.1 mM, respectively (based on solubility limits of stock solutions and the specification of 1% vol/vol final solvent concentration), were not high enough to cause cell death in 6 hours (not shown).

Decreases in fibroblast culture viability (determined by a resazurin assay, not shown) were not observable during 24-h exposures to the same concentrations of DNP, antimycin A, and rotenone used in the CO_2 production rate assay. We were able, however, to observe growth inhibition of fibroblast cultures over a 6-day period at the minimum concentrations of antimycin A and rotenone tested in the CO_2 production rate assay (0.002 mM and 0.02 mM, respectively) but not for the minimum concentration of DNP (Figure 3.6). The effects of cyanide could not be assessed in these longer-term experiments due to its evolution as HCN.

(A)

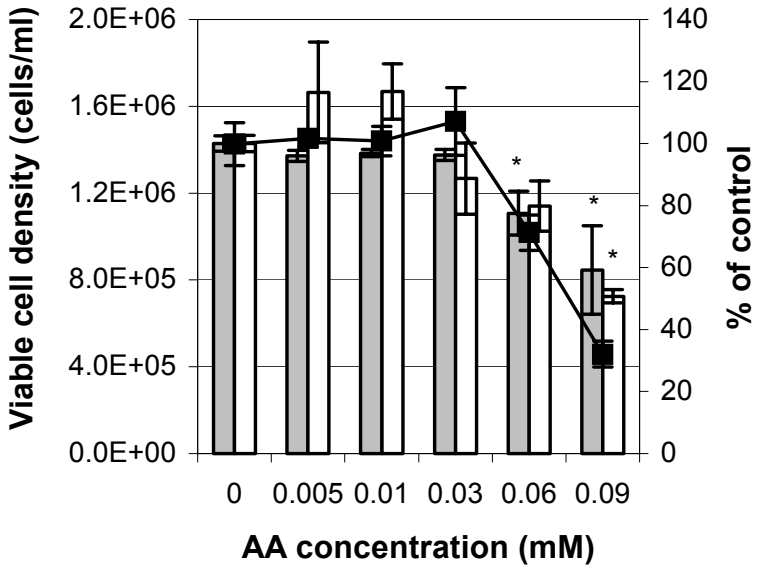

(B)

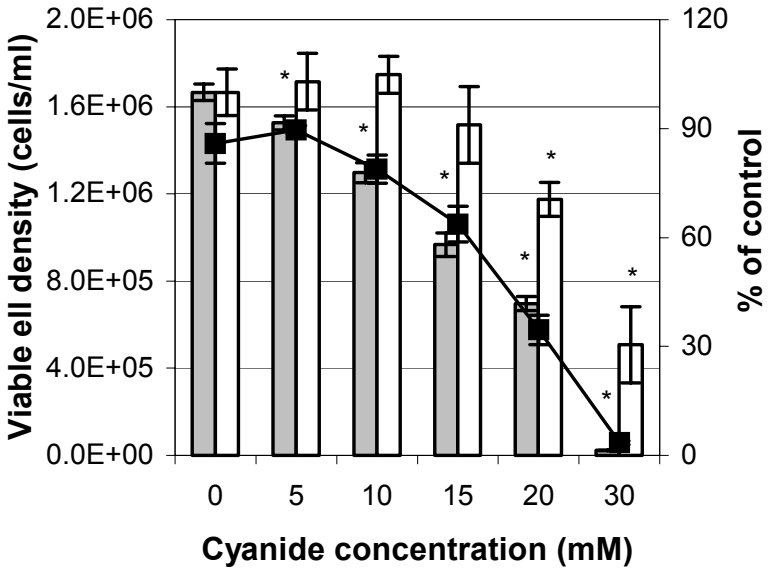

Figure 3.6. Culture viability immediately following a 6-hr exposure. Viable cell density by trypan blue cell counting (solid line), relative fluorescence of resazurin assay (gray bars) and relative absorbance of MTT (white bars) for fibroblast cell cultures exposed to higher concentrations of antimycin A (A) and cyanide (B). Data for cell densities are the averages and standard deviations of duplicate counts from a single well of each concentration. Results for resazurin and MTT assays are the averages and standard deviations of measurements from three separate wells. Significant differences relative to the control culture at a 95% confidence level are denoted by asterisks.

(A)

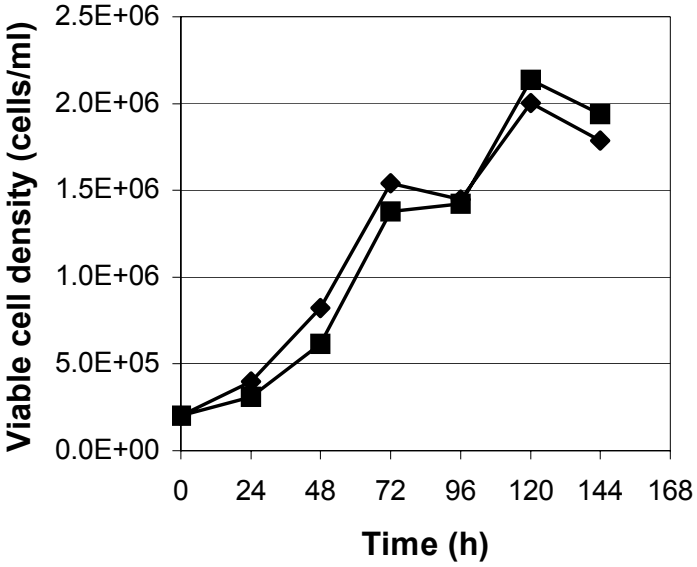
Viable cell density (cells/ml)
2.5E+06
2.0E+06
1.5E+06
1.0E+06
5.0E+05
0.0E+00
0
24
48
72
96
120
144
168
Time (h)

(B)

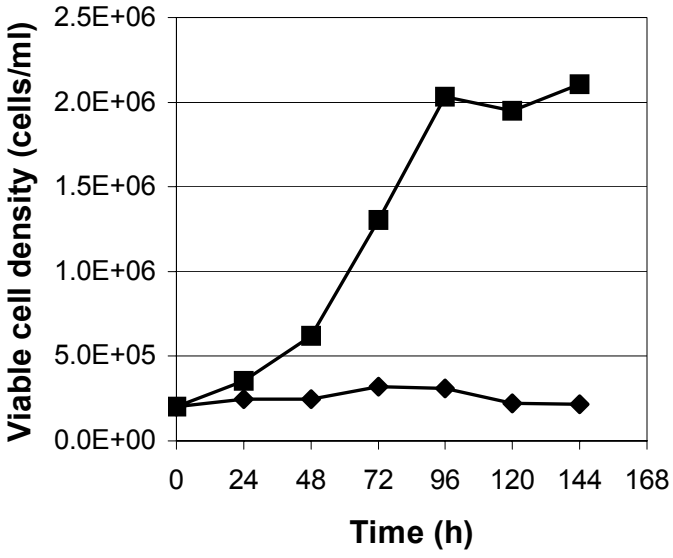
Viable cell density (cells/ml)
2.5E+06
2.0E+06
1.5E+06
1.0E+06
5.0E+05
0.0E+00
0
24
48
72
96
120
144
168
Time (h)

(C)

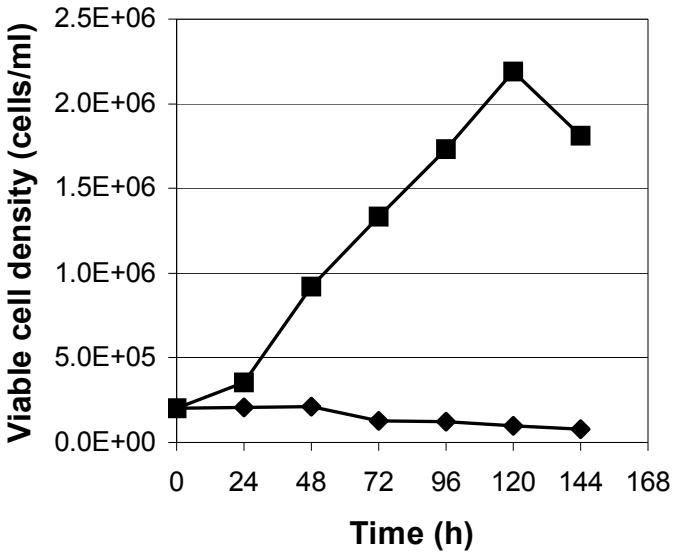

Figure 3.7. Effect of chemicals on cell growth. Cell density of control (■) and treated (♦) cultures. DNP (A) at 0.02 mM, antimycin A (B) at 0.002 mM, and rotenone (C) at 0.02 mM.

Discussion

In this work, we designed a sealed system for faster, cheaper, multi-parallel, and quantitative determination of CO_2 production rate. The design was directed by using a mathematic model for transfer of CO_2 between gas and liquid phases which takes into account pH changes that affect the transfer and CO_2 determination. The method hinges on specialized plugs for individually sealing the wells. Without plugging the wells, the total liquid phase CO_2 concentration does not exceed 0.10 mM. Sealing the well with conventional sealing tapes yields a larger headspace of 3.0 ml, but the measured concentration is still less than 0.1 mM because the tapes can not seal the wells air tightly. The quality of the seal provided by the plug fitted with an O-ring was tested by placing plug-sealed wells into an incubator set with 10% CO_2 for 6 hours and measuring that no

CO_2 was found in the enclosed medium. Additionally, the plugs were made of optically clear material to allow for determination of pH prior to opening a well. The volume of the headspace of well was optimized to be small enough to allow CO_2 to accumulate appreciably, but not so small as to allow oxygen depletion to occur. That oxygen was not limited in plugged wells was indirectly confirmed by measurement of similar glucose consumption and lactate production rates for cultures in sealed wells and open wells over ten hours of incubation.

The CO_2 production rate assay also relies on not exposing the well plate and cell cultures to high levels of CO_2 prior to or during the assay. Clearly, standard levels of bicarbonate-buffer in medium would confound the measurement of the lesser amounts of CO_2 from cellular production. In addition, during development we discovered that the polystyrene well plates can actually reversibly adsorb CO_2 from the CO_2-incubator and media with standard amounts of bicarbonate buffer. Thus, we used Hepes instead of bicarbonate as a buffer and used an oven with ambient levels of CO_2 to maintain culture temperature. Furthermore, we determined the adsorption of CO_2 produced by cells during an incubation period in the sealed wells is negligible (results not shown). Finally, in deciding a concentration for buffering, we chose a higher concentration of Hepes that would minimize changes in pH and allow more carbon dioxide to accumulate in the liquid phase as bicarbonate.[6]

The new system was demonstrated by studying the effects of DNP, antimycin A, rotenone, and cyanide, whose mechanisms are well known [11-14], on fibroblast cell metabolism. The observed changes in CO_2 production rates witnessed in our new system correspond well with the established mechanisms of action. The dissipation of proton

gradient by DNP was expected to yield an increase in CO_2 production, whereas direct blocking of components in the electron chain transport was expected to yield decreases in CO_2 production. The assay results provide quantitative measures for the degree of stimulation or inhibition of CO_2 production by these chemicals.

The sensitivity of the CO_2 production rate assay was comparable to the growth test, where severe growth inhibition at minimum concentrations of antimycin A and rotenone first became visible at 48 hr. While DNP did not have a significant effect on growth at concentrations at its minimum tested, it did inhibit growth substantially at concentrations of 0.04 and higher (not shown). However, in all cases, the test was more sensitive than a cell death screen, as none of the chemicals caused cell death at 6 or 24 hr at the given concentration ranges that were tested in the CO_2 production rate assay. For two chemicals, antimycin A and cyanide, we observed decreased viability at concentrations that were 25-30 times greater than those causing significant metabolic change within 6 hours. In summary, for the given fibroblast cell line and the chemicals tested, we have been able to precisely determine changes in CO_2 production at concentrations which correspond to growth inhibition without cell death. Further work is needed to examine the correlation between metabolic changes and growth inhibition, as well as verify the use of shorter-term metabolic measures to predict longer-term physiological outcomes.

References

1. deZengotita, V.M., L.R. Abston, A.E. Schmelzer, S. Shaw and W.M. Miller. (2002). Selected amino acids protect hybridoma and CHO cells from elevated carbon dioxide and osmolality. *Biotechnol Bioeng* **78**, 741-752.

2. deZengotita, V.M., R. Kimura and W.M. Miller. (1998). Effects of CO2 and osmolality on hybridoma cells: growth, metabolism and monoclonal antibody production. *Cytotechnology* **28**, 213-227.

3. deZengotita, V.M., A.E. Schmelzer and W.M. Miller. (2002). Characterization of hybridoma cell responses to elevated pCO(2) and osmolality: Intracellular pH, cell size, apoptosis, and metabolism. *Biotechnol Bioeng* **77**, 369-380.

4. Frahm, B., H.C. Blank, P. Cornand, W. Oelssner, U. Guth, P. Lane, A. Munack, K. Johannsen and R. Portner. (2002). Determination of dissolved CO2 concentration andCO(2) production rate of mammalian cell suspension culture based on off-gas measurement. *J Biotechnol* **99**, 133-148.

5. Pattison, R.N., J. Swamy, B. Mendenhall, C. Hwang and B.T. Frohlich. (2000). Measurement and control of dissolved carbon dioxide in mammalian cell culture processes using an in situ fiber optic chemical sensor. *Biotechnol Prog* **16**, 769-774.

6. Frick, R. and B. Junker. (1999). Indirect methods for characterization of carbon dioxide levels in fermentation broth. *J Biosci Bioeng* **87**, 344-351.

7. Bonarius, H.P.J., C.D.d. Gooijer, J. Tramper and G. Schmid. (1995). Determination of the respiration quotient in mammalian cell culture in bicarbonate buffered media. *Biotechnol Bioeng* **45**, 542-535.

8. Bonarius, H.P.J., V. Hatzimanikatis, K.P.H. Meesters, C.D. deGooijer, G. Schmid and J. Tramper. (1996). Metabolic flux analysis of hybridoma cells in different culture media using mass balances. *Biotechnol Bioeng* **50**, 299-318.

9. Royce, P.N.C. and N.F. Thornhill. (1991). Estimation of Dissolved Carbon Dioxide Concentrations in Aerobic Fermentations. *AICHE J* **37**, 1680-1686.

10. Ziu, Z.L., W.D. Deckwer and A.P. Zeng. (1999). Estimation of rates of oxygen uptake and carbon dioxide evolution of animal cell culture using material and energy balances. *Cytotechnology* **29**, 159-166.

11. Niknahad, H., S. Khan, C. Sood and P.J. Obrien. (1994). Prevention of Cyanide-Induced Cytotoxicity by Nutrients in Isolated Rat Hepatocytes. *Toxicol Appl Pharmacol* **128**, 271-279.

12. Sibille, B., C. Filippi, M.A. Piquet, P. Leclercq, E. Fontaine, X. Ronot, M. Rigoulet and X. Leverve. (2001). The mitochondrial consequences of uncoupling intact cells depend on the nature of the exogenous substrate. *Biochem J* **355**, 231-235.

13. Tiefenthaler, M., A. Amberger, N. Bacher, B.L. Hartmann, R. Margreiter, R. Kofler and G. Konwalinka. (2001). Increased lactate production follows loss of

mitochondrial membrane potential during apoptosis of human leukaemia cells. *Br J Haematol* **114**, 574-580.

14. Zhang, J.G., M.A. Tirmenstein, F.A. Nicholls-Grzemski and M.W. Fariss. (2001). Mitochondrial electron transport inhibitors cause lipid peroxidation-dependent and -independent cell death: Protective role of antioxidants. *Arch Biochem Biophys* **393**, 87-96.

15. Nyberg, G.B., R.R. Balcarcel, B.D. Follstad, G. Stephanopoulos and D.I.C. Wang. (1999). Metabolism of peptide amino acids by Chinese hamster ovary cells grown in a complex medium. *Biotechnol Bioeng* **62**, 324-335.

16. CRC press, c., OH. (2000/01). *In* CRC handbook of chemistry and physics. CRC Press, Cleveland, OH.

17. Yang, Y.S. and R.R. Balcarcel. (2003). 24-well plate spectrophotometric assay for preliminary screening of metabolic activity. *Assay and Drug Development Technologies* **1**, 461-468.

18. Forrester, R.L., L.J. Wataji, D.A. Silverman and K.J. Pierre. (1976). Enzymatic Method for Determination of CO_2 in Serum. *Clin Chem* **22**, 243-245.

19. Evans, S.M., A. Casartelli, E. Herreros, D.T. Minnick, C. Day, E. George and C. Westmoreland. (2001). Development of a high throughput in vitro toxicity screen predictive of high acute in vivo toxic potential. *Toxicol Vitro* **15**, 579-584.

CHAPTER IV

96-WELL PLATE ASSAY FOR SUBLETHAL METABOLIC ACTIVITY

Abstract

A 96-well plate assay has been devised for estimation of sublethal metabolic activity for compounds administered to *in vitro* cell cultures during 6 and 24 h exposures. This screen combines a resazurin reduction assay with lactate production and glucose consumption rate assays to assess effects of compounds on both culture viability and metabolic inhibition. In this paper, the assay is demonstrated by determining the extent to which five glycolysis inhibitors, namely phloretin, 2-DG, iodoacetate, fluoride, and oxamate, induce metabolic inhibition without cell death for *in vitro* fibroblast cell cultures. During 6-h exposures, iodoacetate was found to be the most potent inhibitor of glycolysis, while iodoacetate and phloretin were most cytolethal. 2-DG had the largest sublethal metabolic range, spanning just over two orders of magnitude in concentrations between its IC_{50}'s for cytolethality and metabolic inhibition. This method provides a simple and inexpensive way to determine global metabolic and cytolethal effects of compounds for *in vitro* cell culture systems. It should be of use directly for large-scale screening and ranking of compounds during drug discovery and development, in conjunction with or following some more direct measure of therapeutic efficacy of a prospective drug candidate. Moreover, first-hand determination of the concentrations over which a compound has lethal, sublethal metabolic, or no such effects should serve as

a cost-effective and time-saving first step in a given research study, preceding more expensive, lengthy, and/or detailed *in vitro* methods.

Introduction

Current cytotoxicity assays, such as MTT, alamar blue™, and neutral red, are widely used because they are cheap, easily quantified, and reproducible.[1] However, all of these assays oversimplify the events that they measure, providing a binary outcome for multi-step, kinetic processes. The measured endpoints are generally late events of cell death and the information obtained is limited.[2,3] Although tests for cytotoxicity will remain indispensable in modern drug development, there is a growing need for *in vitro* assays that assess toxicity of a compound more subtly at sublethal levels, which are recognized to be more indicative of mechanism and more predictive of toxicity.[4] Significant progress in technologies including genomics, proteomics, and metabonomics are providing the opportunity for measuring cellular responses at different levels of the biological hierarchy and regulation.[5-7] These techniques have great potential for studying the mechanism of a compound's action in a biochemical system and are certainly high-content yielding methods, yet they are very expensive, labor intensive, and not high-throughput. One major challenge for the application of these new techniques in toxicology is to determine appropriate doses at which to extract meaningful information.[7] Suitable dose selection is also required prior to the use of other more detailed *in vitro* testing for genotoxicity, induction of mutation, or programmed cell death. Cytotoxicity assays have played an important role in this regard, providing an upper bound for concentrations that induce cell death.[4] Additional simple, global, sensitive, and

quantitative assays for measuring a morbidity state are needed to provide lower bounds in defining a sublethal concentration range.

In this work, we implemented dual measurements of culture viability and metabolism in a 96-well plate assay which can bound the range of sublethal metabolic activity for a compound during an acute exposure (24 h or less) *in vitro*. In developing the assay, we tested a group of compounds that are reported to work as inhibitors of glycolysis, including phloretin, 2-DG, iodoacetate, fluoride, and oxamate. The sites of action for these inhibitors are listed in table 4.1.[8-12] These inhibitors can be used as mechanistic tools for studying glycolysis, a prominent pathway in biochemistry, but whose regulation is also attracting attention with regard to its role in cell death[13-16] and disease treatment.[17-19] Of particular interest to us for subsequent metabolic control analysis experiments was the determination of concentrations of the aforementioned inhibitors that would be sufficient for inhibiting glycolysis in our fibroblast cell line yet without causing cell death. Of more general interest to the reader at large is the creation of a combined protocol for the assessment of cytolethality and metabolic inhibition of compounds on *in vitro* mammalian cell lines. This protocol provides dual dose response curves that bound a sublethal metabolic activity range.

Materials and methods

Cell culture and media

Mouse fibroblast cells (ATCC CRL10225) used in this study were grown in "maintenance medium" consisting of DMEM (Mediatech, Herndon, VA, USA) supplemented with 10% FBS (Sigma, St. Louis, MO, USA), 10 U/mL penicillin-10

μg/mL streptomycin (Sigma), and 4 mM L-glutamine (Mediatech). The cells were maintained in 75 cm^2 T-flasks (Corning, NY, USA) in an incubator (Model 3100 series, Forma Scientific, Marietta, OH, USA) controlled at 37 °C, 95% humidity, and 10% CO_2. Every 4-6 days, cultures were trypsinized using a 0.25% solution of trypsin (Mediatech), counted by microscopy (Model BX60, Olympus, USA) using trypan blue (Mediatech) with a hemacytometer (Double Neubauer Counting Chamber Set, VWR International, Suwanee, GA, USA), and subcultured at an initial cell density of 2×10^5 cells/mL in maintenance medium. Medium used during a screen for testing compounds (test medium) is based on bicarbonate-free/glucose-free RPMI 1640 medium (Sigma), which is supplemented with 10 mM glucose, 10 mg/L insulin, 5 mg/L holotransferrin, 10 U/mL penicillin-10 μg/mL streptomycin, and 2000 mg/L sodium bicarbonate (all from Sigma). Serum is not used during a screen to avoid the need for deproteinization of samples prior to enzymatic assays.[20]

Test compounds

2-DG, sodium fluoride, sodium iodoacetate, sodium oxamate, and phloretin were all purchased from Sigma in powder form. Concentrated stocks of all chemicals were made in test medium. Stock concentrations were 1000 mM 2-DG, 100 mM sodium fluoride, 1 mM sodium iodoacetate, 500 mM sodium oxamate, and 1 mM phloretin. Prior to a screen, 5.0 mL volumes of test media with 11 different concentrations of a chemical were prepared by further dilution of concentrated stock into test medium.

Enzymatic assays for glucose and lactate

The glucose and lactate concentration in each well of a 96-well plate (NUNC™, Nalge Nunc International, Denmark) used in a screen ("screening plate") is measured by

enzymatic assays in separate 96-well plates, one for each assay ("assay plates") (Nalge Nunc International). The assay recipes used allow determination of glucose in the range of 0 to 10 mM and lactate in the range of 0 to 3 mM. Both assays are based on those developed by Bergmeyer and Lowry.[21,22] The glucose assay utilizes two reactions: in the first reaction, hexokinase catalyzes the conversion of glucose to G6P (Equation 4-1), and in the second reaction, G-6-PDH catalyzes the conversion of G6P to 6-phosphogluconate, with stoichiometric quantities of $NADP^+$ converted to NADPH (Equation 4-2). The amount of NADPH produced is directly proportional to the glucose concentration contained in the sample and can be detected by absorbance.

$$Glucose + ATP \xrightarrow{Hexokinase} G-6-Phosphate + ADP \quad (4\text{-}1)$$

$$G-6-Phosphate + NADP^+ \xrightarrow{G-6-PDH} 6-Phosphogluconate + NADPH \quad (4\text{-}2)$$

In the lactate assay, LDH catalyzes the reaction of lactate and NAD^+ into pyruvate and NADH. The NADH produced is detected by the increased absorbance (Equation 4-3).

$$Lactate + NAD^+ \xleftrightarrow{LDH} Pyruvate + NADH \quad (4\text{-}3)$$

In this protocol, a serum-free, low-protein test medium and reformulated assay reagent recipes were used to reduce measurement noise and increase protocol efficiency.[20] For the glucose assay, reagent A contains 15 mM ATP, 2.5 mM $NADP^+$, 1 mM $MgCl_2$, 0.5 mM DTT, and 0.31 U/mL G-6-PDH in 25 mM Tris buffer solution with pH adjusted to 8.0 using NaOH; and reagent B is prepared by dissolving hexokinase in deionized water at a concentration of 6.67 U/mL (all from Sigma). For the lactate assay, reagent A contains 163.64 mM hydrazine, 64.21 mM glycine, and 10.55 mM NAD^+ in

water with pH adjusted to 9.5 using NaOH, and reagent B is 1000 U/mL LDH solution (all from Sigma).

To conduct an assay, each well of an assay plate is pre-filled with either 170 μL lactate assay reagent A or 165 μL glucose assay reagent A. Then, 20 μL samples from a screening plate are transferred to each well of an assay plate. The initial OD's of each well on an assay plate are read at 340 nm using a μQuant Universal Microplate Spectrophotometer (Bio-Tek® Instruments, Winooski, Vermont, USA). Then, 10 μL of lactate assay reagent B or 15 μL of glucose assay reagent B is added to each well of an assay plate. The lactate assay is incubated for 1 h and the glucose assay is incubated for 2 h. Final OD's are determined at 340 nm for both assays. All steps were performed at a stable room temperature of 21°C, and the assay incubation time was confirmed to be conservatively long enough to reach endpoints confirmed by unchanged absorbance in longer time.

Resazurin reduction assay for relative culture viability

The relative viability of test cultures during the three hours following the conclusion of either a 6 h or 24 h exposure is determined using a resazurin reduction assay. Resazurin reduction assay reagent was prepared by dissolving resazurin (Sigma) into PBS (Mediatech) at the concentration of 0.0105% (wt/vol).[23] To conduct the assay, each well of a screening plate containing 100 μL of culture is provided with 10 μL of resazurin reduction assay reagent using a 12-channel manual pipettor (VWR International). After incubation for 3 hr in the incubator at 37°C, the fluorescence from each well is measured at a wavelength of 590 nm using an excitation wavelength of 560

nm and a sensitivity setting of 50 on a Bio-Tek FL600 plate reader (Bio-Tek Instruments).

Protocol for 96-well plate assay for sublethal metabolic activity

In preparation of an assay, five rows of a 96-well plate are seeded with 100 μL of a fibroblast cell culture using a manual single channel pipettor (VWR International) and incubated for 10 h to allow cells to attach. The other three rows are reserved as cell-free, left empty for the time being. The cell culture used to seed the plate is harvested from an 80-90% confluent culture in a 75-cm^2 T-flask, centrifuged at 200×g for 10 min (Model 5677, Forma Scientific), and resuspended in maintenance medium at a density of 1.0×10^6 cells/mL within a 50-ml centrifuge tube (Corning). This density corresponds to approximately 50% confluency in a 96-well at the time of seeding.

The screen is initiated by removing the maintenance medium and washing all wells once with 200 μL of PBS pre-warmed to 37°C, and then filling wells of each of the 12 columns with 100 μL of test media containing a specific concentration of a test compound. In this particular design, there are eleven distinct, nonzero concentrations tested plus one control, and each concentration is tested with five replicates with culture and three replicates cell-free. The well plate is next incubated for either 6 or 24 h at 37°C, 95% humidity, and 10% CO_2. At the end of the exposure period, 20 μL samples for metabolite assays are taken and immediately transferred to assay plates, which are pre-filled with reagents needed for the enzymatic assays. In the case of a 6-h exposure period, one sample is taken from each well for a lactate assay. In the case of a 24-h exposure, two samples are taken from each well for a lactate and glucose assay, diluting the lactate samples 6-fold before assaying them. Next, the remaining medium in each well is

removed, all wells are washed with 200 μL of pre-warmed PBS, 100 μL of fresh compound-free test medium is added to each well of the screening plate, 10 μL of resazurin reagent is added to each well, and fluorescence is read at the end of incubation at 37°C for 3 h. All liquid handling steps were accomplished using a manual 12-channel pipettor (VWR International).

A variation in the protocol for the resazurin assay was also tested during development to probe the effect of having compounds present during the assay and investigate possible detachment of cells during the washing step. Here, wells were re-filled to 100 μL volumes by addition of 20 μL (for 6 h exposures) or 40 μL (for 24 h exposures) of compound-containing medium. Comparison of results obtained by each procedure revealed a significant yet small difference (about 1%) in results (not shown), signifying that cell detachment during medium exchange and washing was not a problem and that the presence or absence of the compound did not affect the resazurin reduction assay. Additionally, comparison of absolute fluorescences from resazurin reduction assays for control culture wells during 6-9 hr and 24-27 hr indicated that growth rate was negligible under test conditions.

Calculation of lactate production, glucose uptake, and resazurin reduction relative to control cultures

The change in absorbance of NADH (for lactate) or NADPH (for glucose) during an enzymatic assay is linearly proportional to the concentration of the respective metabolite in a sample. The amount of lactate produced or glucose consumed by the cells during an exposure period is calculated as the difference between changes in absorbance for culture samples and cell-free samples, and normalized to the difference exhibited by the control cultures. Equation 4-4 provides an expression for lactate production relative to

the control; a similar equation is used for glucose consumption relative to the control, glucose uptake (% of control), not shown.

$$\text{Lactate Production (\% of control)} = \frac{(\Delta OD_{cell} - \Delta OD_{cell-free})_{test}}{(\Delta OD_{cell} - \Delta OD_{cell-free})_{control}} \times 100 \qquad (4\text{-}4)$$

Typical values for changes in absorbance for samples from culture wells and cell-free wells ranged from 0.04-1.00 and 0.02-0.03, respectively, for lactate during 6 h exposure, and 0.8-2.8 and 2.8-2.9, respectively, for glucose during 24 h exposure.

For the resazurin reduction assay, only final fluorescence is measured. The resazurin reduction (RR) relative to the control is calculated as shown in equation 4-5.

$$\text{RR (\% of control)} = \frac{(Fluorescence_{cell} - Fluorescence_{cell-free})_{test}}{(Fluorescence_{cell} - Fluorescence_{cell-free})_{control}} \times 100 \qquad (4\text{-}5)$$

Typical values for fluorescence for culture wells and cell-free wells ranged from 900-36,000 and 875-925, respectively.

Determination of IC50 for metabolism, IC50 for resazurin reduction, and the sublethal metabolic activity range

The median inhibitory concentration (IC_{50}) values for glucose and lactate metabolism (IC_{50GLC}, IC_{50LAC}, or IC_{50MET} in general) and for resazurin reduction (IC_{50RR}) were obtained from semi-logarithmic dose-response curves (Figure 4-1). Either a Sigmoidal function (Equation 4-6) or a dual exponential function (Equation 4-7) was used to fit each of the curves. Curve fitting was accomplished using the "curve fitting toolbox" in Matlab® (Mathworks, Inc), with choice of fit based on the goodness of regression coefficient (R^2). IC_{50} values were back calculated from the fitted functions. The sublethal metabolic activity range was calculated as the log of the ratio of IC_{50RR} over IC_{50MET} (Equation 4-8).

$$y = \frac{100}{1 + e^{-a(x-b)}} \tag{4-6}$$

$$y = ae^{bx} + ce^{dx} \tag{4-7}$$

$$\text{Sublethal metabolic activity range} = \log\left(\frac{IC_{50RR}}{IC_{50MET}}\right) \tag{4-8}$$

Statistical tests

Differences between results obtained from 6-h and 24-h exposures for IC_{50LAC}, IC_{50RR}, and sublethal metabolic activity range for individual compounds were tested for significance using two-sample t-tests. These same differences between 6-h and 24-h results were also tested for significance by taking data for all the compounds together (in conglomeration) and using paired comparison t-tests, with data paired by compound. For such conglomerate analyses, the logarithms of the ratio of paired IC_{50}'s were compared to zero, while the differences between pairs of data for sublethal metabolic activity were compared to zero. Differences between IC_{50LAC} and IC_{50GLC} for individual compounds from 24-h exposures were tested for significance also using paired comparison t-tests, with data paired by well plate (since both values were determined from same well plate). This same difference was also tested for significance taking the data in conglomeration, still using a paired comparison t-test, but comparing the logarithm of the ratio of the paired quantities to zero. Differences between resazurin reduction relative to control measured in the presence and absence of compound for all compounds at 6h and 24 hr were compared using paired comparison t-test, with data paired by each concentration.

Results

Determination of sublethal metabolic activity for fibroblast cultures treated with glycolysis inhibitors

The degree to which fibroblast glycolysis could be inhibited without causing cell death was explored using five inhibitors of glycolysis, namely phloretin, 2-DG, iodoacetate, fluoride, and oxamate. Results from a 6-h exposure provide two dose response curves for each of the five inhibitors, each curve consisting of 11 points normalized to controls (Figure 4-1). The data for lactate production correspond to the average rate of lactate production over the 6-h period. The data for resazurin reduction are taken as an indication of the average number of viable cells during the three hours following the exposure. Dose response data sets that exhibited a gradual transition over the concentration range tested (all of the lactate production data and the resazurin reduction data for iodoacetate) were fitted using dual exponential functions. Dose response data sets that exhibited a sharp transition (all the resazurin data except that for iodoacetate) were fitted using Sigmoidal functions. The data demonstrate that lactate production can be notably inhibited at concentrations lower than those affecting resazurin reduction with the discrepancy depending on the type of compound. This range in which central metabolism can be significantly inhibited yet without effect on resazurin reduction is interpreted as a range of sublethal metabolic activity for a given compound. In this study, sublethal metabolic activity was evident for concentrations that were one or more orders of magnitude lower than those causing cell death.

(A)

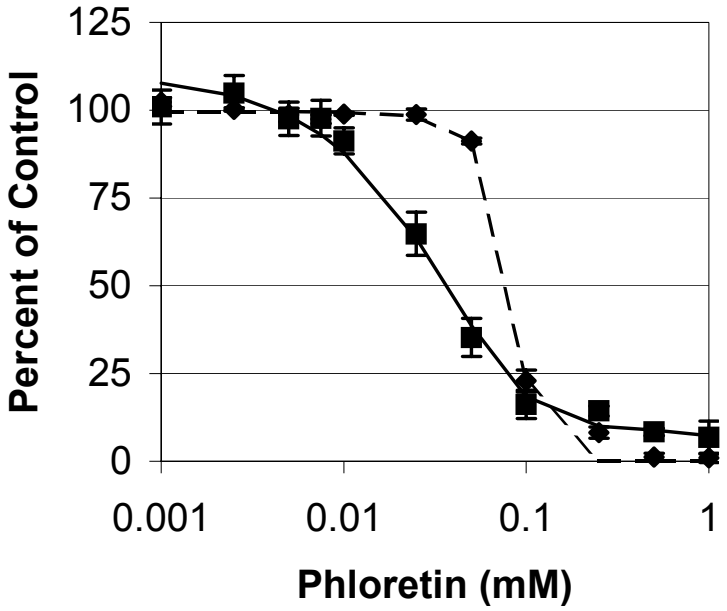
125
100
75
50
25
0
Percent of Control
0.001
0.01
0.1
1
Phloretin (mM)

(B)

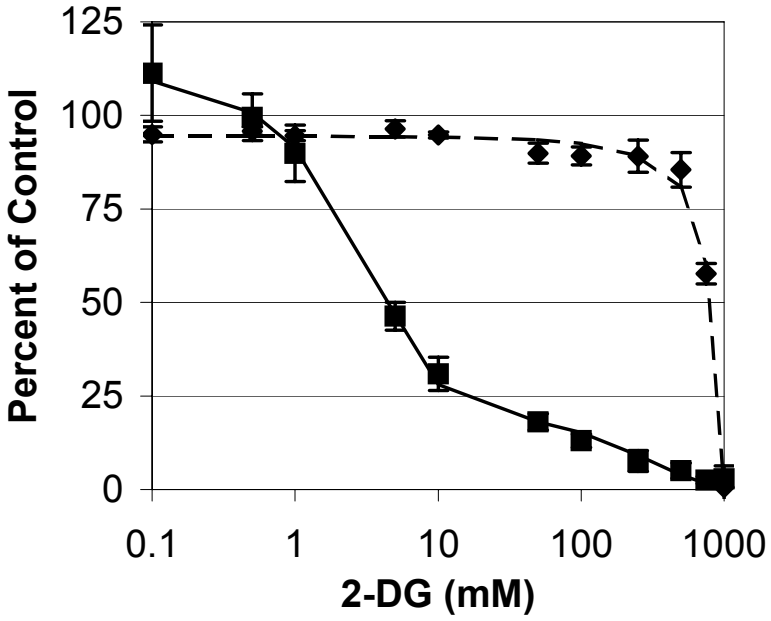
125
100
75
50
25
0
Percent of Control
0.1
1
10
100
1000
2-DG (mM)

(C)

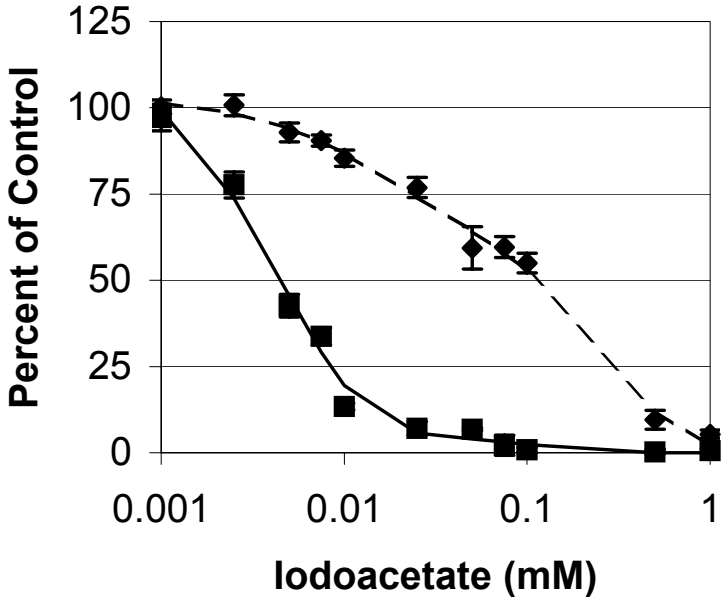
125
100
75
50
25
0
Percent of Control
0.001
0.01
0.1
1
Iodoacetate (mM)

(D)

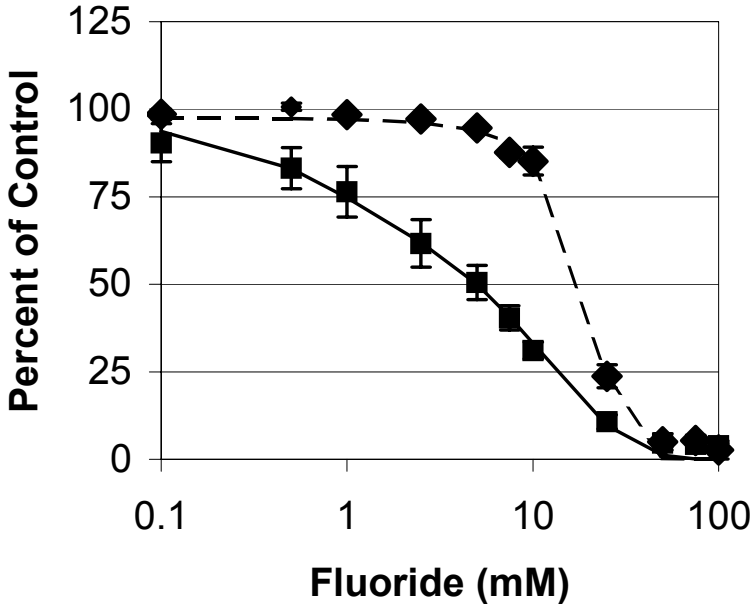
125
100
75
50
25
0
Percent of Control
0.1
1
10
100
Fluoride (mM)

(E)

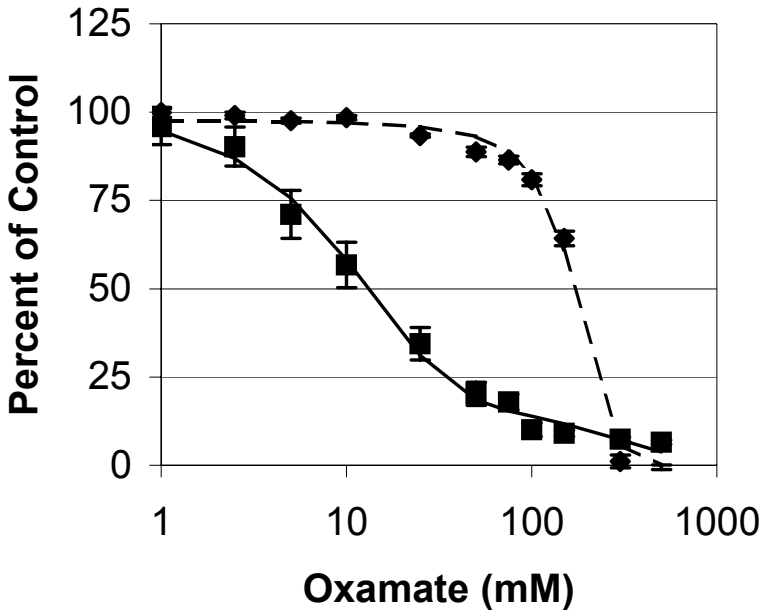

Figure 4.1. Resazurin reduction and lactate production for fibroblast cell cultures exposed for 6 h to different concentrations of phloretin (A), 2-DG (B), iodoacetate (C), fluoride (D), and oxamate (E). (■) and (♦) denote measured lactate production and resazurin reduction, respectively, each as percentages of control cultures. Measured points shown in the figure are averages and standard deviations of five wells from a single 96-well plate. Solid and dashed lines correspond to fitted functions for lactate production and resazurin reduction, respectively. Each experiment was replicated three times (Only one replicate for each compound is shown).

The cytolethal and metabolic inhibition effects of each compound during a 6-h exposure are quantitatively compared based on calculated IC50's for resazurin reduction and lactate production, respectively (Table 4-1). The data for IC_{50RR} indicates that phloretin and iodoacetate were the most cytolethal, followed by fluoride, oxamate, and 2-DG, in order of decreasing cytolethality. Meanwhile, the data for IC_{50LAC} show that iodoacetate was the most potent metabolic inhibitor, followed by phloretin, fluoride and 2-DG, and oxamate, in order of decreasing potency. The orders of rankings based on cytolethality and potency for metabolic inhibition differ. However, the IC_{50LAC}'s were

less than corresponding IC_{50RR}'s for each of the five compounds. The range to which a compound exerts sublethal metabolic activity is quantified as the logarithm of the ratio of IC_{50RR} to IC_{50LAC}. This quantity is the order of magnitude, in a base-10 system, between the IC50's. As shown in table 4-1, sublethal ranges spanned orders of magnitude as wide as 2.3 and as little as 0.3. 2-DG exhibited the greatest span, followed by iodoacetate, oxamate, fluoride, and phloretin, in order of decreasing range for sublethal metabolic activity.

Table 4-1. IC_{50} values for lactate production and resazurin reduction and sublethal metabolic activity range for five compounds tested on fibroblast cultures during 6-h exposures. The inhibitors are listed in the order of the steps of glycolysis, along with their sties of action. Data shown in the table are average and standard deviation of three independent replicates of the 96-well plate assay.

Chemical	Target	IC50 (mM)		Sublethal Metabolic Activity Range
		Lactate Production	Resazurin Reduction	
Phloretin	GLUT1	0.05 ± 0.01	0.0828 ± 0.0001	0.3 ± 0.1
2-Deoxyglucose	Hexokinase	4.1 ± 0.5	756 ± 79	2.3 ± 0.1
Sodium Iodoacetate	GAPDH	0.0049 ± 0.0003	0.12 ± 0.01	1.41 ± 0.04
Sodium Fluoride	Enolase	4.7 ± 1.4	18.2 ± 2.3	0.6 ± 0.2
Sodium Oxamate	LDH	14.2 ± 1.2	86 ± 16	1.117 ± 0.004

Comparison of sublethal metabolic activity during 6-h and 24-h exposures

The extent to which the results of a screen are dependent on exposure time was explored by comparing results obtained during 24 h versus 6 h exposures (Figure 4-2). The only substantial effect was for the cytolethality of iodoacetate, as evidenced in an IC_{50RR} that is reduced by an order of magnitude. This makes iodoacetate the most cytolethal compound based on 24-h results and places it as fourth largest in regard to its

sublethal metabolic activity range, whereas the ranking based on metabolic inhibition remained unchanged.

After exclusion of iodoacetate, analyses of data for all compounds in conglomeration revealed that IC_{50} values for resazurin reduction were barely statistically significant ($p = 0.0495$), yet with 4 of 5 compounds exhibiting statistical significance individually. That IC_{50RR}'s determined over 24 h are less than those determined over 6 h conforms with an understanding that cell death may exhibit varying kinetics and may not be complete within 6 h. Differences in IC_{50LAC} values from 6 h and 24 h assays were not statistically significant in conglomeration ($p = 0.1800$), though 2 of 5 compounds were statistically significant individually. Notably, IC_{50LAC}'s for iodoacetate were not observably different. The combined effects of changes in IC50's for lactate production and resazurin reduction yielded ranges for sublethal metabolic activity from 24-h exposure data that were generally slightly lower than those from 6-h exposure data. The differences analyzed in conglomeration were not statistically significant ($p = 0.0739$), though 2 of 5 compounds were statistically significant individually.

(A)

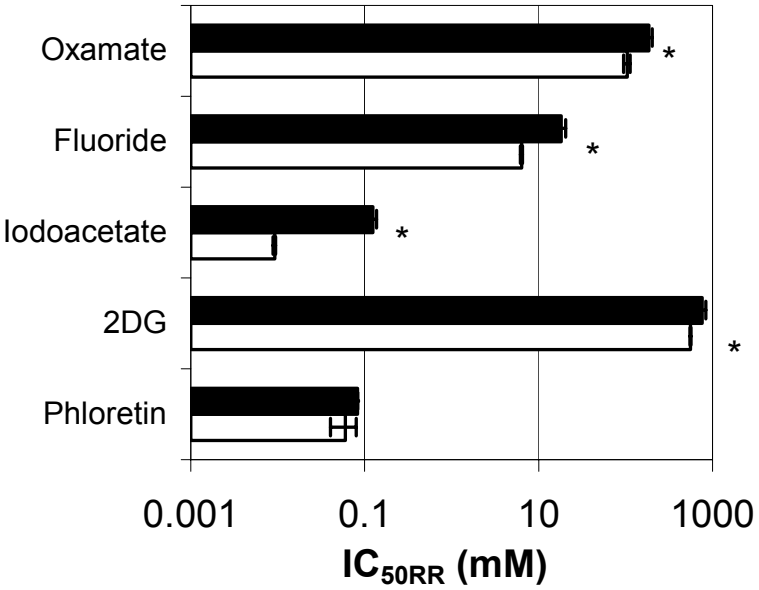
Oxamate
Fluoride
Iodoacetate
2DG
Phloretin
*
*
*
*
0.001
0.1
10
1000
IC50RR (mM)

(B)

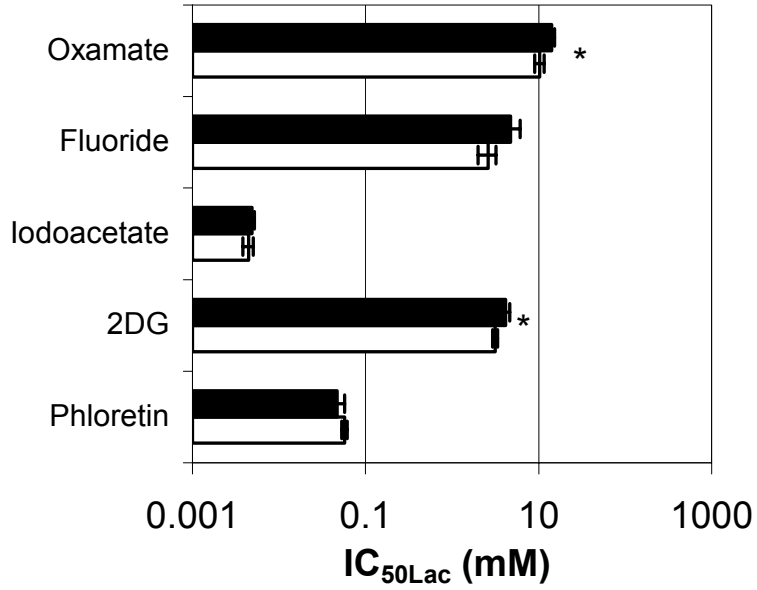
Oxamate
Fluoride
Iodoacetate
2DG
Phloretin
*
*
0.001
0.1
10
1000
IC50Lac (mM)

(C)

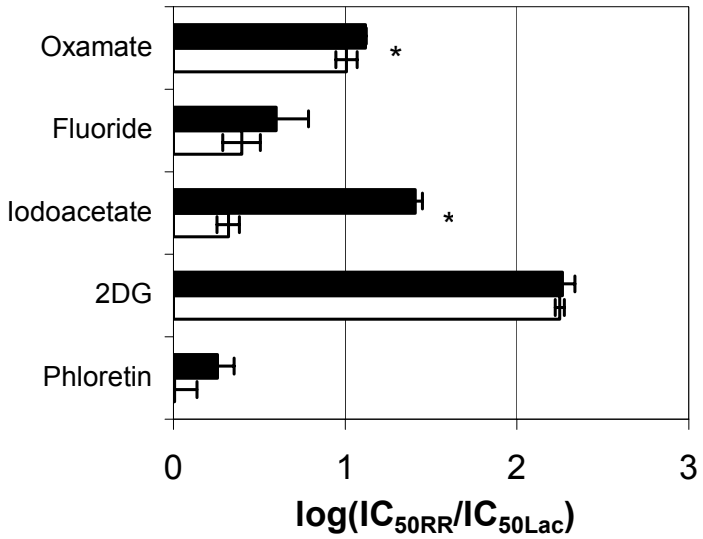

Figure 4.2. Comparison of IC_{50}'s and sublethal ranges determined during 6-h versus 24-h exposures. Black and white bar represent 6- and 24-h results, respectively, for IC_{50} for resazurin reduction (A), IC_{50} for lactate production (B), and sublethal metabolic activity range (C). Results shown are averages and standard deviations of three independently conducted replicate screens. Mean differences of data taken in conglomeration for each group, excluding iodoacetate data in A and C, were -0.24±0.15 (Fig. A: n =4, p = 0.0495), -0.09 ± 0.13 (Fig. B: n = 4, p = 0.1800), and –0.14±0.10 (Fig. C: n =5, p = 0.0739). Results for individual compounds that are statistically significant at the 95% confidence level are denoted with an asterisk.

Comparison of sublethal metabolic activity based on glucose consumption versus lactate production

During assay development, we also measured glucose consumption during 24-h exposures for all compounds except for 2-DG (Figure 4-3). Samples for glucose assay from cultures exposed to 2-DG were processed, but, as was evident from cell-free controls, 2-DG interfered with the hexokinase-based enzymatic assay (data not shown). A conglomerate analysis of paired differences reveals that IC_{50LAC} values were statistically less than those for IC_{50GLC}, but none of the results for individual compounds were statistically significant. The small differences between IC50's for metabolic inhibition

observed in this study suggest a possibility to use one or the other for estimation of sublethal metabolic activity range, as needed for a particular study.

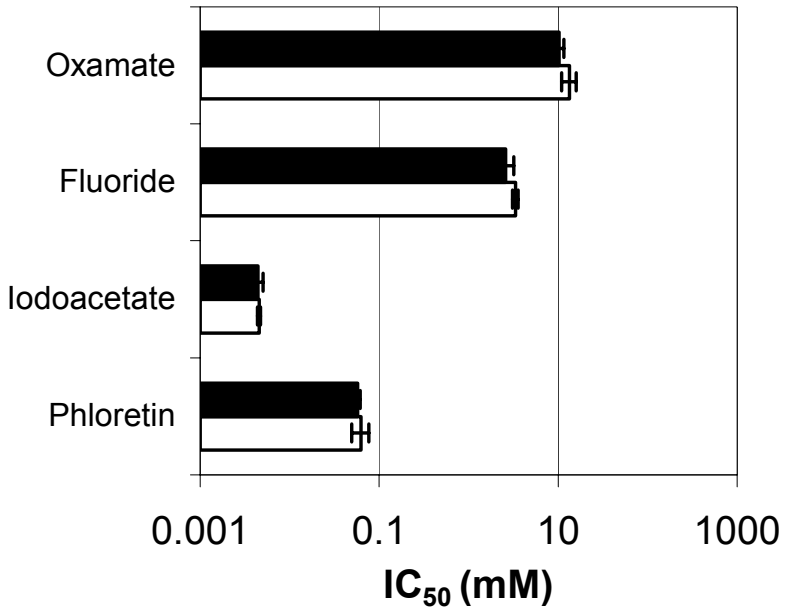

Figure 4.3. Comparison of 24-hr IC50 values based on lactate production and glucose consumption. Black and white bars represent IC50 values for lactate production and glucose consumption, respectively. Results shown are averages and standard deviations of three independently conducted replicate screens. The mean difference for data **taken** in conglomeration was –0.16±0.22 (n =12, p = 0.0314). None of the differences for individual compounds were statistically significant at the 95% confidence level.

Discussion

This work provides a proof of a concept regarding a prospective new dimension to mammalian cell-based assays, namely that of a range over which compounds can have noticeable effects on glucose and lactate metabolism, yet without causing cell death as defined by resazurin reduction during acute exposures. The interpretation of this range as a sublethal metabolic range involves an assumption that net resazurin reduction indicates

number of viable cells, which in turn depends on the assumption that viable cells have a constant cell-specific resazurin reduction rate. The mechanism of resazurin reduction is not very clear, but the use of its activity as an indicator for viability has been widely practiced due to its easy performance and low cost.[24,25] In chapter III, the assumption of using it as an indicator of viability was found to be acceptable for the fibroblast cell line during exposures with antimycin A and potassium cyanide upon comparison of viability results obtained with MTT, resazurin reduction, and trypan blue assays.[26]

Still, since the rate of resazurin reduction, like any other cellular biochemical reaction, may vary depending on substrate and product metabolite levels and as well as enzyme levels and effective activities, some degree of caution should be exercised in interpreting the results. The present results differentiate the effects of compounds on resazurin reduction activity from those on glucose and lactate metabolism. Under the assumption that reduced resazurin reduction indicates death of cells, the two dose response curves separate the entire spectrum of compound concentrations into three zones. The resazurin reduction data bounds the upper range where death occurs while the metabolic assay separates a sublethal metabolic activity range with that of the "sub-metabolic" range.

Prospective applications for this screen are conceivably numerous. More intricate experiments of *in vitro* cellular studies involving more expensive or elaborate techniques, such as 2-D gels or gene chips or using radio-labeled substrates, ought to benefit tremendously from first-hand, quantitative, relatively inexpensive dose-response data obtained in a day's time. For instance, the assay may be used to compare *in vitro* cellular environments (i.e. design of test media or serum-free formulations in general), to study

chemical toxins, to screen candidate drugs, and/or to select clones or differentiate between cell types, broadly spanning fields of biotechnology through toxicology and pharmacology to medicine. More generally, this work demonstrates the strategy for parallel measurements of a functional criterion (here, metabolism) with one for culture viability. Obtaining dose information for potency and lethality, and hence relative safety *in vitro*, both from the same screen should be of value for large-scale screening of compounds during early stages of drug discovery and development. Ideally, improvement of preliminary methods for screening compounds, medium, and cells for *in vitro* studies should help increase the efficiency and productivity of subsequent steps in a research project, lowering costs in the end.

References

1. Slaughter, M.R., P.J. Bugelski and P.J. O'Brien. (1999). Evaluation of Alamar Blue reduction for the in vitro assay of hepatocyte toxicity. *Toxicol Vitro* **13**, 567-569.

2. Freshney, R.I. (2000). Cytotoxicity, pp. 329-330. *In* Culture of Animal Cells, A Manual of Basic Techniques. John Wiley & Sons, New York.

3. Waterfield, C.J., J. Delaney, M.D.J. Kerai and J.A. Timbrell. (1997). Correlations between in vivo and in vitro effects of toxic compounds: Studies with hydrazine. *Toxicol Vitro* **11**, 217-227.

4. Eisenbrand, G., B. Pool-Zobel, V. Baker, M. Balls, B.J. Blaauboer, A. Boobis, A. Carere, S. Kevekordes, J.C. Lhuguenot, R. Pieters and J. Kleiner. (2002). Methods of in vitro toxicology. *Food Chem Toxicol* **40**, 193-236.

5. Nicholson, J.K., J. Connelly, J.C. Lindon and E. Holmes. (2002). Metabonomics: a platform for studying drug toxicity and gene function. *Nat Rev Drug Discov* **1**, 153-161.

6. Lindon, J.C., J.K. Nicholson, E. Holmes and J.R. Everett. (2000). Metabonomics: Metabolic processes studied by NMR spectroscopy of biofluids. *Concepts Magn Resonance* **12**, 289-320.

7. Hellmold, H., C.B. Nilsson, I. Schuppe-Koistinen, K. Kenne and L. Warngard. (2002). Identification of end points relevant to detection of potentially adverse drug reactions. *Toxicol Lett* **127**, 239-243.

8. Kerai, M.D.J. and J.A. Timbrell. (1997). Effect of fructose on the biochemical toxicity of hydrazine in isolated rat hepatocytes. *Toxicology* **120**, 221-230.

9. Zeng, C.M., Y.X. Zhang, L.L. Lu, E. Brekkan, A. Lundqvist and P. Lundahl. (1997). Immobilization of human red cells in gel particles for chromatographic activity studies of the glucose transporter Glut1. *Biochimica Et Biophysica Acta-Biomembranes* **1325**, 91-98.

10. Ikemoto, A., D.G. Bole and T. Ueda. (2003). Glycolysis and glutamate accumlation into synaptic vesicles - Role of glyceraldehyde phosphate dehydrogenase and 3-phosphogylcerate kinase. *J Biol Chem* **278**, 5929-5940.

11. Pagliaro, L. and D.L. Taylor. (1992). 2-Deoxyglucose and Cytochalasin-D Modulate Aldolase Mobility in Living 3t3 Cells. *Journal of Cell Biology* **118**, 859-863.

12. Hamilton, E., M. Fennell and D.M. Stafford. (1995). Modification of Tumor Glucose-Metabolism for Therapeutic Benefit. *Acta Oncol* **34**, 429-433.

13. Downward, J. (2003). Cell biology - Metabolism meets death. *Nature* **424**, 896-897.

14. Gonin-Giraud, S., A.L. Mathieu, S. Diocou, M. Tomkowiak, G. Delorme and J. Marvel. (2002). Decreased glycolytic metabolism contributes to but is not the inducer of apoptosis following IL-3-starvation. *Cell Death Differ* **9**, 1147-1157.

15. Plas, D.R. and C.B. Thompson. (2002). Cell metabolism in the regulation of programmed cell death. *Trends Endocrinol Metab* **13**, 74-78.

16. Vander Heiden, M.G., D.R. Plas, J.C. Rathmell, C.J. Fox, M.H. Harris and C.B. Thompson. (2001). Growth factors can influence cell growth and survival through effects on glucose metabolism. *Mol Cell Biol* **21**, 5899-5912.

17. Bakker, B.M., P.A.M. Michels, F.R. Opperdoes and H.V. Westerhoff. (1999). What controls glycolysis in bloodstream form Trypanosoma brucei? *J Biol Chem* **274**, 14551-14559.

18. Brazil, M. (2003). Promise for glycolysis inhibitor. *Nat Rev Drug Discov* **2**, 338-338.

19. Liu, H.P., N. Savaraj, W. Priebe and T.J. Lampidis. (2002). Hypoxia increases tumor cell sensitivity to glycolytic inhibitors: a strategy for solid tumor therapy (Model C). *Biochem Pharmacol* **64**, 1745-1751.

20. Balcarcel, R.R. and L.M. Clark. (2003). Metabolic screening of mammalian cell cultures using well- plates. *Biotechnol Prog* **19**, 98-108.

21. Bergmeyer, H.U. (1974). Methods of Enzymatic Analysis. Academic Press, New York, USA.

22. Lowry, O.H. and J.V. Passonneau**.** (1972). A flexible System of Enzymatic Analysis;. Academic Press, Orlando, USA.

23. Evans, S.M., A. Casartelli, E. Herreros, D.T. Minnick, C. Day, E. George and C. Westmoreland. (2001). Development of a high throughput in vitro toxicity screen predictive of high acute in vivo toxic potential. *Toxicol Vitro* **15**, 579-584.

24. Batchelor, R.H. and M.J. Zhou. (2004). Use of cellular glucose-6-phosphate dehydrogenase for cell quantitation: applications in cytotoxicity and apoptosis assays. *Anal Biochem* **329**, 35-42.

25. O'Brien, J., I. Wilson, T. Orton and F. Pognan. (2000). Investigation of the Alamar Blue (resazurin) fluorescent dye for the assessment of mammalian cell cytotoxicity. *Eur J Biochem* **267**, 5421-5426.

26. Yang, Y.S. and R.R. Balcarcel. (2004). Determination of carbon dioxide production rates for mammalian cells in 24-well plates. *Biotechniques* **36**, 286-+.

CHAPTER V

METHOD FOR CHARACTERIZING CHANGES IN METABOLIC STATE OF MAMMALIAN CELLS

Abstract

A 24-well plate assay for measuring metabolic rates of glucose, lactate, and CO_2 in conjunction with a carbon balance model are presented herein for characterizing changes in the metabolic state of fibroblast cells treated with chemicals at sublethal levels. The assay and method are demonstrated by testing four well characterized metabolic agents, oxamate, fluoride, antimycin A, and DNP, which act on different sites in glycolysis, the electron transport chain, and mitochondria. Depending on the sites of action, different patterns of increases and decreases of the three metabolic rates were observed. Moreover, higher sensitivity of one metabolic rate was associated with the closeness of the pathway to the action site of the compound. Furthermore, in response to four chemicals at different doses, cells responded by altering metabolic state in three different ways: uniform change of metabolic rates, metabolic shift, and metabolic switch.

Introduction

Toxicity testing with cell cultures has often focused on late, irreversible cell death events as endpoints.[1,2] These approaches appear too simplistic and the mechanistic information obtained is limited.[3,4] Demonstrating the lack of toxicity may also require more subtle analyses of molecular events and precise metabolic regulation preceding cell death.[3,5,6] The insurgence of high throughput genomics and proteomics allows

multidimensional readouts of molecular events at unprecedented levels of details.[7] The information obtained by them is mechanism indicative and toxicity predictive.[7-9] However, the methods are expensive and labor intensive. They were generally applied at only a single dose but a compound acts as a function of doses.[10] Moreover, functional information can not be inferred from gene and protein expressions without including the metabolic status of the whole organism. [6,7,9,11,12] In some cases, toxic effects for some chemicals may not involve gene and protein expressions.[12,13] Metabolic status should be included to augment and complement the information provided by measuring genetic and proteomic responses.[6,9,11,12]

Metabolic rates define the minimum information needed for describing metabolism and cell physiology.[14] Traditional methods have often used large volumes of cultivation systems (such as flasks and reactors) for measuring metabolic rates.[15] Those approaches have often been used in bioprocess and bioengineering research for studies of metabolism to improve cellular properties.[14,16,17] However, applications of these methods for screening purposes are hindered due to their low throughput, high cost, and lengthy time-consumption.[15] Development of high throughput methods for measuring metabolic rates is necessary for applications in toxicity testing and pharmaceutical research, but also to satisfy the requirement in other areas like functional genomics and metabolic engineering.[18,19] Measuring metabolic rates in micro-scaled well-plate systems offers an attractive format, which allows parallel cultivation of independent, large numbers of cultures and has the potential to be automated.[20] Reported metabolic rate assays performed in well plate systems include measurement of acidification rate, glucose, lactate, oxygen, and CO_2.[15,21-25] However, most of these assays measure only single or at

most two metabolites, whereas a multidimensional approach for simultaneous measurement of multiple metabolites would offer a more comprehensive understanding of changes in cellular metabolism in response to various stresses.[26]

In this work, I developed a high throughput, multi-parallel method for measuring metabolic rates of glucose, lactate, and CO_2 in 24-well plates to characterize the changes in central carbon metabolism of mammalian cells. In developing the method, four metabolic agents, oxamate, fluoride, antimycin A, and DNP, were tested at sublethal levels to verify the assay and obtain different metabolic statuses. The sites of action for these agents are listed in table 1.[27-31] The measured rates were used directly, as well as in conjunction with a carbon balance model to characterize the changes in metabolic state of fibroblast cells. Applications of the method include preclinical toxicity testing, screening novel drug candidate, cell line screening, and medium optimization.

Materials and methods

Cell culture and media

The cell line used is a mouse fibroblast cell line obtained from ATCC (CRL-10255). During routine maintenance, cultures are grown in a 75 cm^2 T-flask (Corning, NY) in an incubator (Model 3100 series; Forma Scientific, Marietta, OH, USA) controlled at 37 °C, 95% humidity, and 10% CO_2. The maintenance medium consists of Dulbecco's Modification of Eagle's medium (DMEM) (Mediatech, Herndon, VA, USA), which is supplemented with 10% fetal bovine serum (FBS) (Sigma, St. Louis, MO, USA), 10 U/mL penicillin-10 μg/mL streptomycin (Sigma), and 4 mM L-glutamine (Mediatech). Subculturing is conducted every 4-6 days by removing the medium,

detaching the cells with 0.25% trypsin-0.1% EDTA (Mediatech), and diluting the culture with fresh medium to a cell density of 2×10^5 cells/mL. At least 3 passages after the initial thaw are performed before using the cell culture for screening experiments.

Two different media are used during a screen, one is for attaching cells to the screen well plate, and the other is for measuring concentration changes of metabolites during chemical exposure. The media components are identical to the "pretest" medium and "test" medium for CO_2 production rate assay as described in chapter III. Medium used during cell attachment prior to the start of screen ("pretest" medium) is based on bicarbonate-free/glucose-free RPMI 1640 medium (Sigma), which is supplemented with 10% FBS, 25 mM D-glucose, 10 U/mL penicillin-10 μg/mL streptomycin (Sigma), and buffered with 50 mM HEPES (Mediatech). Medium used during the chemical exposure ("test" medium) is the same as the pretest medium, with the exceptions of substituting 10 mg/L insulin and 5 mg/L holotransferrin for serum, reducing glucose to 4.0 mM and increasing phenol red to 30.0 mg/mL (Sigma). The designs of the pretest medium and test medium are for precise measurement of metabolite concentration change in a screen.[15,25] Sodium bicarbonate is not used as buffer since it will confound the lesser amount of CO_2 produced by cells. Instead, a higher concentration of HEPES is used to minimize the pH change, which allows more liquid phase CO_2 to accumulate in a stable bicarbonate form. Serum is used in the pretest medium to deactivate the trypsin for cell attachment, but not in the test medium to avoid the need for deproteinization of samples prior to enzymatic assays. The increased phenol red concentration in the test medium is for spectroscopic pH measurement. The decreased glucose concentration in the test medium is for increasing the precision of the glucose assay.

Test chemicals

Sodium oxamate, sodium fluoride, antimycin A, and 2,4-dinitrophenol (DNP) were all purchased from Sigma. Concentrated stocks of oxamate and fluoride were made in culture water, whereas a concentrated stock of DNP was made in DMSO and a concentrated stock of antimycin A was made in ethanol, respectively. Prior to a screen, test media with five different concentrations of a chemical plus control were prepared by further dilution of concentrated stocks into test medium. The control and the five test media are then given necessary amounts of pure solvent such that the final concentration of solvent in every medium was equal at 1% (v/v). The solvent impact on culture metabolism was found to be negligible by comparing metabolic rates of control cultures added with 1% of water, ethanol, and DMSO.

Metabolic rate screening

Metabolic rate screening for measuring changes in extracellular glucose, lactate, and CO_2 of fibroblast cell cultures is carried out in 24-well plates (BD Biosciences, San Jose, CA, USA). To increase the efficiency and reduce the cost, prior to a 24-well plate screen, the sublethal concentration range for each chemical is determined in a 96-well plate screen during 6- and 24-h exposures (described in Chapter 4).[24] From such tests, concentration ranges in which there were changes in metabolism but no cell death were determined for each chemical (Table 5.1). From such a narrowed range, concentration points for a chemical are selected for further testing in this 24-well plate screen.

Table 5.1. Sublethal concentration range for each compound. Concentration points tested for each chemical in 24-well plate screening are selected from within a sublethal concentration range. The range of sublethal activity for each compound was determined by dual measurements of culture viability (using alamar blue assay) and metabolism (using glucose and lactate assay) during 6 hr and 24 hr exposure in a 96-well plate assay. The lower bound is defined by the minimum observed concentration required to elicit changes in metabolism. The upper bound is defined as the maximum concentration which does not cause significant cell death (viability greater than 85% of control confirmed by alamar blue assay).

Chemical	Target	Test Range (mM)			Sublethal Range (mM)					
					6-h			24-h		
Oxamate	LDH	6	–	50	2.5	–	75	5	–	50
Fluoride	Enolase	1	–	3	0.1	–	10	0.1	–	5
Antimycin	Complex III	$2.5e^{-6}$	–	$1e^{-4}$	$2.5e^{-6}$	–	0.01	$2.5e^{-6}$	–	0.01
DNP	Mitochondria	0.003	–	0.05	$2.5e^{-3}$	–	1.0	$2.5e^{-3}$	–	1.0

A complete 24-well plate screen consists of three major steps: attaching cells into a 24-well plate, treating cells with chemical, and analyzing concentration changes of metabolites. The procedures are similar to conducting a CO_2 production rate assay as described in chapter III.[25] In preparation of a 24-well plate screen, each well in three rows of a 24-well plate is seeded with 500 μL of a fibroblast cell culture, and the remaining one row is reserved as cell-free. The cell culture used to seed the plate is harvested from a 80-90% confluent culture in a 75 cm^2 T-flask, centrifuged at 200 g for 10 min (Model 5677, Forma Scientific) and resuspended in pretest medium at a cell density of 1.5×10^6 cells/mL in a 50-mL centrifuge tube (Corning). The cell seeding is accomplished using a manual single pipettor. Vortexing of the cell culture is done before seeding to each well to minimize the seeding variation. The well plate is then incubated in an oven (VWR International, Suwanee, GA, USA) with ambient levels of CO_2 at 37 °C for 10 hr to allow cell attachment. Next, the pretest medium is removed; all wells are washed with pre-

warmed phosphate-buffered saline (PBS) (Mediatech) at 37 °C, and 500 μL of test media containing specific compound concentrations are added to each well, including the cell-free well. Each well of the plate is then sealed by manual application of custom made plugs and incubated in the oven for 6 hr at 37 °C. At the end of the incubation period, absorbencies at 562 and 720 nm are read first for pH measurement, and each well is then unsealed and sampled immediately for an enzymatic assay of dissolved carbon dioxide and bicarbonate. Finally, samples are taken for enzymatic assays for glucose and lactate, and cell number and viability are determined for one well of each column (of each chemical concentration) by hemocytometer (Double Neubauer Counting Chamber Set; VWR International) with trypan blue staining (Mediatech). Each experiment was performed twice to provide a replicate data set.

During cell attachment and incubation, an oven with ambient CO_2 (300 ppm) instead of a CO_2 incubator is used to minimize the interference of environmental CO_2 on measurement of CO_2 produced by cells. During chemical exposure, airtight well sealing with reduced headspace by the plugs prevents release of CO_2 and allows accumulation of more dissolved carbon dioxide in equilibrium with bicarbonate in the liquid phase, from which samples will be taken for the CO_2 enzymatic assay. The sealing plugs are made of translucent polycarbonate. Their dimensions and design are described in the chapter III.[25] The translucency of the plug allows the spectrophotometric pH measurement, which is required for calculation of CO_2 in the headspace.

Metabolite assays

Determination of CO_2 production by cells consists of two measurements: medium pH and total liquid phase CO_2 (dissolved CO_2 and HCO_3^-). The principle, recipe, and

detailed procedures of the methods are described in chapter III.[25,32,33] Briefly, the pH is determined by measuring absorbance of the pH indicator, phenol red, at a wavelength of 562 nm. To correct for variations due to plug clarity, condensation, and well plate background, an absorbance at 720 nm is taken and subtracted. The total liquid phase CO_2 is determined by enzymatic assay in a separate 96-well plate. Triplicate measurements for each well of a 24-well plate were conducted.

The glucose and lactate concentrations are also measured by enzymatic assays in separate 96-well plates. Both assays are based on those developed by Bergmeyer and Lowry [34,35] and reformulated to new protocols which allow determination of glucose in the range of 0-5 mM and lactate in the range of 0-3 mM.[15] Deproteinization steps are omitted to increase the efficiency and precision of the assays. Triplicate measurements for each metabolite in each well of a 24-well plate are performed.

Absorbance readings for pH measurement are performed on a Bio-Tek FL600 plate reader (Bio-Tek Instruments, Winooski, Vermont, USA) with the temperature controlled at 37°C, and absorbance readings for all enzymatic assays are performed on a μQuant Universal Microplate Spectrophotometer (Bio-Tek Instruments) at room temperature.

Calculation of concentration differences

The carbon dioxide exists in the liquid phase and gas phase in a sealed system. With the measured pH and total liquid phase CO_2, the total CO_2 present in a well can be calculated based on dissociation equilibrium and Henry's law, and expressed in concentration form based on culture volume as

$$C_{CO_2}^{Tot} = C_A + \frac{\frac{HV_{gas}C_A}{V_{liq}RT}}{(1 + K \cdot 10^{pH})} \quad (5\text{-}1)$$

with a dissociation constant K of 7.28×10^{-7} mol/L and a Henry's law constant of 4.2×10^{6} Pa·L/mol taken from the literature.[36] The volumes of cell culture and headspace are 0.5 and 1.1 mL, respectively. The value of ideal gas constant R used is 8.31 $x10^{3}$ Pa·L/mol/K. With the measured metabolite concentrations at the final time point, concentration change of a metabolite during a 6-hr incubation for each well containing cell cultures can be calculated as the difference between the culture samples and cell-free samples (Equation 5-2).

$$\Delta C_{met} = C_{met,cult}(t_f) - C_{met,cell-free}(t_f) \quad (5\text{-}2)$$

Metabolic network model and consistency with sets of measured rates

To characterize the metabolic state of fibroblast cells under chemical treatment, a simplified, 6-flux metabolic network (Figure 1 and Table 2) is devised and its consistency checked with the three measured metabolic rates at different conditions. The network represents two major central carbon metabolic pathways for energy production: glycolysis and the TCA cycle; and consists of three components: the conversion of glucose to pyruvate, the anaerobic conversion of pyruvate into lactate, and aerobic conversion of pyruvate to CO_2. The creation of the network follows the principle that only feasible and observable biochemical reactions should be included in an assumed network for valuable information.[14] Amino acids and other biosynthesis pathways are excluded. The unobservable sequence of reactions between critical metabolites in glycolysis and the TCA cycle are lumped as overall fluxes: v_1, v_{11}, and v_{20}.

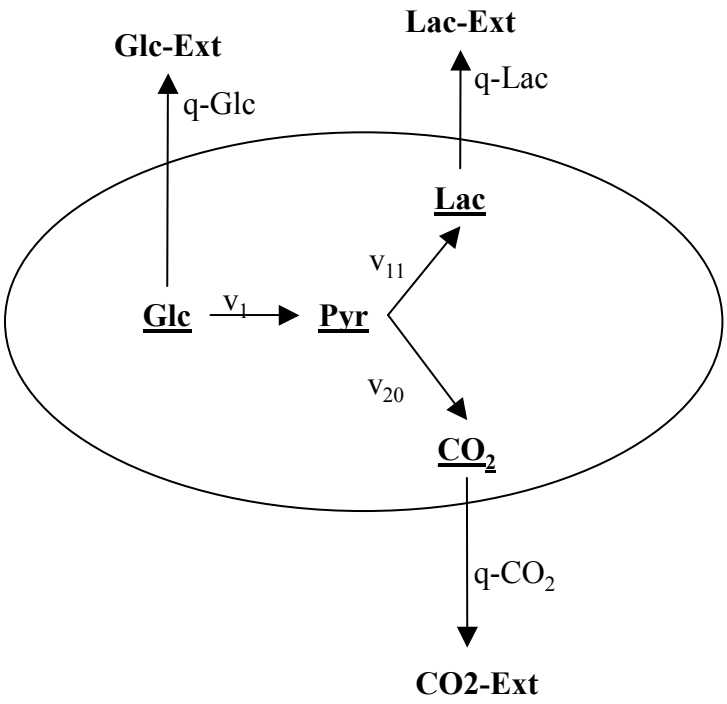

Figure 5.1. Metabolic networks. The network represents glycolysis and TCA cycle. The intracellular fluxes are denoted by v_i, and the measured metabolic rates are denoted with q_i. The species used in material balance equations to derive the constraint equation are underlined.

Table 2. Reactions used for the metabolic networks.

1	$Glc+2NAD^{+}+2ADP+2Pi$	$\rightarrow$	$2\ Pyr + 2\ NADH^{+} + 2\ ATP + 2\ H_20 + 2\ H^{+}$
11	$Pyr+NADH+H^{+}$	$\rightarrow$	$Lac+NAD^{+}$
20	$Pyr+4NAD^{+}+FAD+ADP+3H_2O+Pi$	$\rightarrow$	$3CO_2+4NADH+FADH_2+ATP+4H^{+}$

The method for checking consistency between the simplified network and the three measured rates is developed based on the method described by Stephanopoulos [37], but modified for statistical comparison of the changes in metabolic state of cells. The generation of constraint equations for consistency testing starts with the pseudo-inverse solution method, which assumes that the pathway intermediates are at a pseudo-steady

state. Under this assumption, the three measured rates (q_{glc}, q_{lac} and q_{CO_2}) and the three intracellular fluxes (v_1, v_{11}, and v_{20}) are related by 4 material balances around the intermediates (glucose, lactate, CO_2 and pyruvate), as shown in matrix form:

$$\begin{bmatrix} -1 & 0 & 0 & -1 & 0 & 0 \\ 0 & -1 & 0 & 0 & 1 & 0 \\ 0 & 0 & -1 & 0 & 0 & 3 \\ 0 & 0 & 0 & 2 & -1 & -1 \end{bmatrix} \cdot \begin{bmatrix} q_{glc} \\ q_{lac} \\ q_{CO_2} \\ v_1 \\ v_{11} \\ v_{20} \end{bmatrix} = \begin{bmatrix} 0 \\ 0 \\ 0 \\ 0 \end{bmatrix}$$

The numbers in the matrix are stoichiometric coefficients for the 4 intermediates in the transport and reaction equations (Table 2, transport equations not listed), which are placed into the matrix with rows for each metabolite balanced and columns for each rate/flux. As 6 fluxes are related by 4 balances, measuring three metabolic rates yields an overdetermined system of equations, with one redundant measurement. The redundant information can be used to check the consistency between the metabolic reaction network and the measured rate data set. To describe the various steps for derivation of the redundant equation, the system of linear equations in matrix form is simply expressed as

$$G^T v = 0 \tag{5-3}$$

where G^T represents the transposed stoichiometric matrix (as shown above), and v is the vector which collects the measured rates and intracellular fluxes. By collecting the measured rates in a new vector, v_m, and the intracellular fluxes in another vector, v_c, G^T can be partitioned and equation 5-3 can be rewritten as:

$$G^T v = G_m^T v_m + G_c^T v_c = 0 \tag{5-4}$$

From equation 5-4, v_c can be calculated as

$$v_c = -(G_c^T)^{\#} G_m^T v_m \tag{5-5}$$

where

$$(G_c^T)^{\#} = (G_c G_c^T)^{-1} G_c \tag{5-6}$$

By inserting v_c back to equation 5-4, the redundant matrix R can be obtained:

$$Rv_m = (G_m^T - G_c^T (G_c^T)^{\#} G_m^T) v_m = 0 \tag{5-7}$$

If R is not of full rank, it can be reduced down to just the number of rows that equal its rank, R_r, and the equation 5-7 is written as:

$$R_r v_m = 0 \tag{5-8}$$

in which, the rows contained in the matrix R_r represent independent relationships that should be satisfied by the measurements. In fact, the product of $R_r v_m$ is rarely equal to 0 due to errors on measurements and/or errors in the model. As a consequence of such errors, it is better to express equation as

$$\varepsilon = R_r v_m \tag{5-9}$$

where ε is the vector of residuals. For the simplified network of this work, the $R_r v_m$ yields one redundant equation:

$$\varepsilon = q_{glc} + \frac{1}{2} q_{lac} + \frac{1}{6} q_{CO_2} \tag{5-10}$$

which describes the carbon material balance (carbons entering a cell as glucose should be equal to the carbons exiting a cell as lactate and CO_2).

The measured data from a 24-well plate screen are concentration changes of glucose, lactate, and CO_2 (Table 5.3). Average metabolic rates for a culture in a single

well can be calculated as the concentration difference for a metabolite divided by an estimate of the average viable cell density during the incubation and the time.

$$q = \frac{\Delta C}{n_v t} \tag{5-11}$$

However, since the cell number and incubation time in the denominator are the same for all three rates in one well, it is more convenient to do the consistency test on the metabolite concentration differences directly. The numbers of cells and the incubation time can still affect the value of ε by altering the magnitude of the observed changes. Thus, the variations due to cell number differences between wells are minimized by normalizing ε to q_{glc} for each well. The normalized ε is calculated as

$$\varepsilon_{norm} = \frac{\varepsilon}{q_{glc}} = 1 + \frac{1}{2}\frac{\Delta C_{lac}}{\Delta C_{glc}} + \frac{1}{6}\frac{\Delta C_{CO_2}}{\Delta C_{glc}} \tag{5-12}$$

The magnitude of ε_{norm} indicates the extent of deviation of one measured data set from the simplified network. If the simplified network matches the measured data sets perfectly, ε_{norm} is equal to 0, while a positive value of ε_{norm} corresponds to carbons from glucose being in excess of those captured in lactate and CO_2, and vice versa for negative ε_{norm}.

With a data set from only a single replicate, it is not possible to know if the inconsistency between the network and the measured rates is due to measurement errors or the incorrect network when ε_{norm} is nonzero. However, with multiple replicates provided by 24-well plate experiments, reliable judgment can be made by statistical tests. The measurement errors of the metabolites are confirmed to be random and normally distributed. The normalized residuals, ε_{norm}, the sum of measured concentration

differences, is therefore also normally distributed, which allows statistical comparisons using a t-test. The judgment whether the difference between an average of normalized residuals for a given condition and 0 is significant or not is based on a one-sample t-test:

$$t_1 = \frac{\bar{\varepsilon}_{norm} - 0}{Std\ Error} \tag{5-13}$$

The judgment whether the difference between the averages of normalized residuals at different conditions is significant or not is based on a two-sample t-test:

$$t_2 = \frac{\bar{\varepsilon}_{norm1} - \bar{\varepsilon}_{norm2}}{Std\ Error} \tag{5-14}$$

Comparison of averages of 6 replicates at one condition to zero has the degree of freedom equal to 5, while comparison of average of 6 replicates at one condition to the other condition has the degree of freedom equal to 10. From the t distribution table, t value greater than 2.571 for t_1 and 2.228 for t_2 indicate the differences are significant at a 95%confidence level. Significant differences between an average of the normalized residuals and zero mean the network is not consistent with the measured data sets for a given condition. Significant differences between different conditions mean a metabolic switch has occurred, meaning the carbon balance is no longer upheld to the same extent as a control culture.

Statistical tests

Differences between control and test cultures for concentration differences of metabolites, ratio of metabolic rates are compared using two-sample t-tests. During comparison of concentration differences of metabolites, concentration differences of a metabolite of all wells in a well plate are normalized to the first well to minimize the

effect of cell number variation between well plates. All statistical treatments are accomplished in Microsoft Excel.

Results

Determination of concentration changes of glucose, lactate, and CO_2

The assay was demonstrated by measuring metabolite concentration changes of fibroblast cells treated over a 6-hr incubation period with oxamate, fluoride, antimycin A, and DNP at different levels. The concentrations tested for each chemical were selected from a sublethal concentration range determined by a 96-well plate screen for 6- and 24-hr exposure levels. No occurrence of cell death at the concentrations tested was further confirmed using trypan blue exclusion method immediately at the end of the 6-hr incubation period for each screening experiment. Applying the newly developed 24-well plate assay, 18 data sets of concentration differences for glucose, lactate, and CO_2 over a 6-hr period were obtained in parallel from each well (Table 5.3, 6 wells for cell-free). In one well plate, a chemical can be tested at 5 distinct, nonzero concentrations with three replicates using our design, this being one possible layout. The measurement errors for glucose, lactate, and CO_2 assays are less than 0.12, 0.05, and 0.05 mM, respectively. Small variations are present between wells at a specific condition, which might be due to cell seeding variation.

Table 5.3. Change in metabolite concentration, ratio, and residual. Concentration differences of glucose, lactate, and CO_2 are measured values. Negative values indicate metabolite consumption, whereas positive values indicate metabolite production. The measured data sets are used to calculate the ratio and the normalized residual for each well.

Oxamate (mM)	ΔGlc (mM)	ΔLac (mM)	ΔCO_2 (mM)	ΔLac/ΔGlc	$\Delta CO_2/\Delta Glc$	ε_{norm}
0	-1.57	2.33	1.14	1.49	0.73	0.136
	-1.53	2.25	1.11	1.47	0.72	0.144
	-1.49	2.35	1.30	1.57	0.87	0.070
6	-1.62	2.67	1.15	1.64	0.71	0.060
	-1.26	2.25	0.83	1.79	0.66	-0.005
	-1.66	2.58	0.76	1.55	0.46	0.149
9	-1.14	1.88	0.97	1.65	0.85	0.035
	-1.19	2.09	0.52	1.76	0.43	0.049
	-1.29	2.08	0.64	1.61	0.49	0.113
15	-0.94	1.18	0.75	1.25	0.79	0.241
	-1.21	1.56	0.74	1.28	0.61	0.256
	-1.06	1.36	0.76	1.28	0.72	0.241
30	-0.78	0.68	0.48	0.87	0.61	0.465
	-0.92	0.91	0.55	1.00	0.60	0.401
	-0.77	0.70	0.55	0.91	0.71	0.429
50	-0.67	0.53	0.42	0.79	0.63	0.499
	-0.84	0.48	0.54	0.57	0.65	0.606
	-0.78	0.59	0.55	0.76	0.71	0.501

Fibroblast cells metabolism responded to four chemicals differently as indicated by changes in concentration differences of glucose, lactate, and CO_2 (Figure 5.2). Monotonic decreases for all three metabolites were observed with increasing concentrations of oxamate. The differences from control were significant at 9 mM and greater. Similar responses of the three metabolites were observed with fluoride. The difference from control is significant at 1 and 3 mM. In contrast, antimycin A induced increased concentration differences of glucose and lactate while decreased concentration differences of CO_2. Significant changes were observed at 2.5×10^{-6} mM and the impact

reached saturation at 1×10^{-5} mM. Contrary to the effect of oxamate and fluoride, DNP caused simultaneous increases for all three metabolites with increasing concentrations.

Comparison of sensitivities of responses of the three metabolic rates to each chemical

The extents to which the responses of the three metabolic rates (changes in concentration difference) to each given chemical were compared based on response coefficients (Figure 5.3). The response coefficient indicates the sensitivity of the response of one metabolic rate to the concentration changes of a given chemical, which is calculated as

$$\frac{\partial \ln \Delta Met}{\partial \ln C} = \frac{\ln \Delta Met_{\max} - \ln \Delta Met_{\min}}{\ln C_{\max} - \ln C_{\min}} \tag{5-15}$$

in which $\Delta Met_{\max}$ and $\Delta Met_{\min}$ are observed maximum and minimum changes of concentration differences for a metabolite, and $C_{\max}$ and $C_{\min}$ are corresponding tested concentration points. For oxamate, the response of lactate is most sensitive, whose response coefficient is about three times greater than those for glucose and CO_2. For antimycin A, the CO_2 response is most sensitive with a response coefficient about three times greater than those for glucose and lactate. For fluoride and DNP, no metabolite is significantly more sensitive than others at a 95% confidence level.

(A)

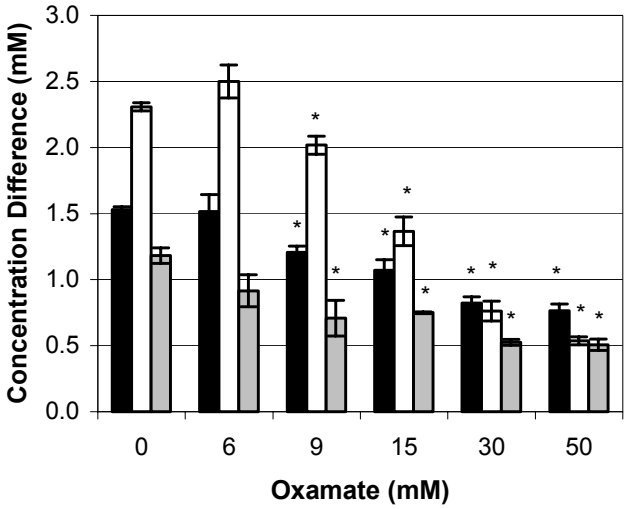
Concentration Difference (mM)
3.0
2.5
2.0
1.5
1.0
0.5
0.0
0
6
9
15
30
50
Oxamate (mM)

(B)

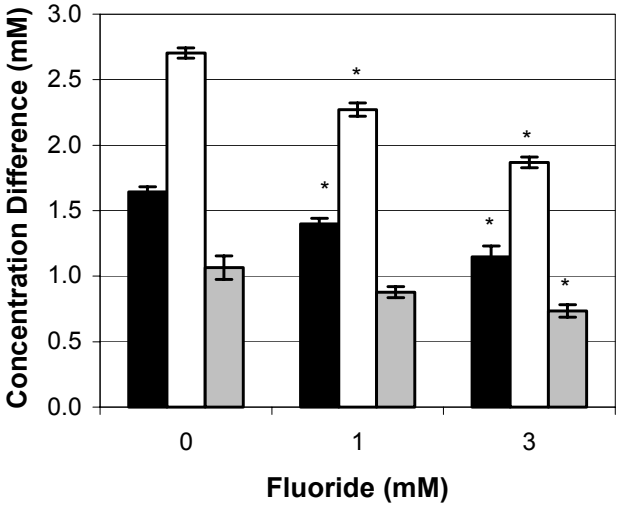
Concentration Difference (mM)
3.0
2.5
2.0
1.5
1.0
0.5
0.0
0
1
3
Fluoride (mM)

(C)

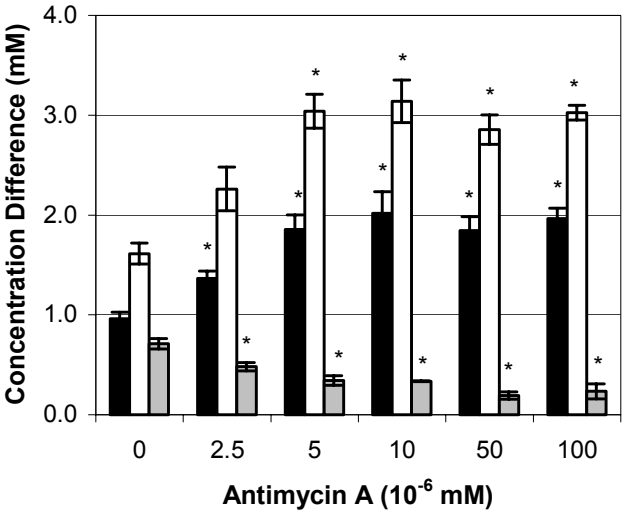

(D)

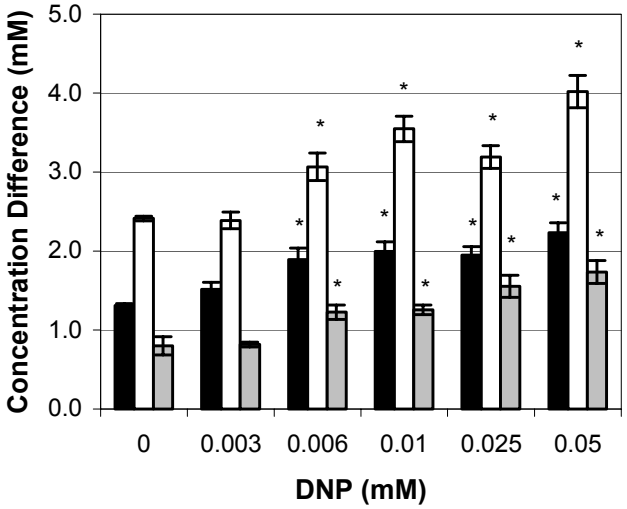

Figure 5.2. Changes in concentration differences of glucose, lactate, and CO_2 of fibroblast cell cultures exposed for 6 h to different concentrations of oxamate (A), fluoride (B), antimycin A (C), and DNP (D). Black bars represent glucose, white bars represent lactate, and gray bars represent CO_2. Measured points shown in the figure are averages and standard error of the mean of three replicates from a single 24-well plate. "*" represents changes in metabolite concentrations significantly different from the control at a 95% confidence level. Each experiment was replicated twice (Only one replicate for each compound is shown).

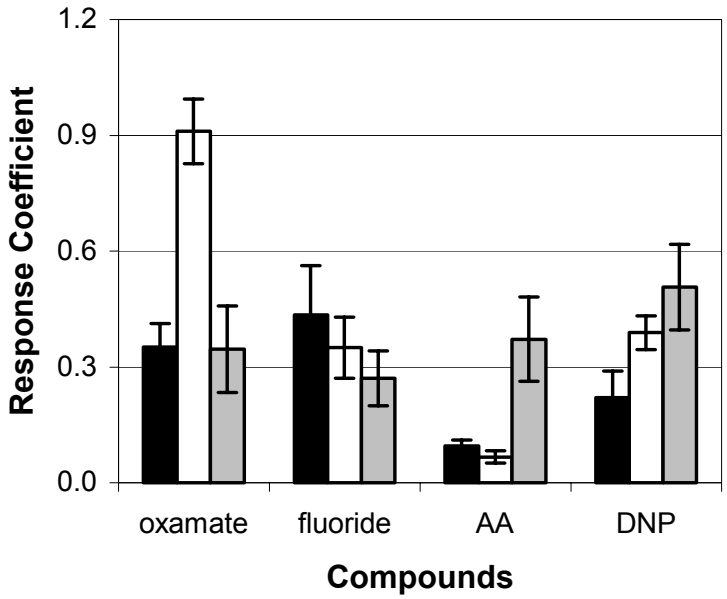

Figure 5.3. Comparison of responses of metabolic rates of glucose, lactate, and CO_2 to each chemical. Black, while, and gray bars represent the response coefficients of glucose, lactate, and CO_2 respectively. Results in the figure are the average and standard error of the mean of 6 replicates measured from two separate 24-well plate experiments.

Metabolic shift indicated by changes in ratios of metabolic rates

The co-measurement of multiple metabolites allows metabolic rate to be analyzed. The data collected from each well yield ratios of $\Delta C_{lac} / \Delta C_{glc}$ and $\Delta C_{CO_2} / \Delta C_{glc}$ (Table 5.3). The averages of 6 replicates for each condition from two repeated well plate experiments were then calculated and plotted as a function of doses (Figure 5.4.). Oxamate caused significant, continuous decreases in ratios of $\Delta C_{lac} / \Delta C_{glc}$ with increasing concentrations from 15 mM, while changes in $\Delta C_{CO_2} / \Delta C_{glc}$ are not significant for all tested concentrations. Contrary to oxamate, antimycin A caused significant decreases in ratios of $\Delta C_{CO_2} / \Delta C_{glc}$ at 2.5×10^{-6} mM and

greater, while ratios of $\Delta C_{lac}/\Delta C_{glc}$ were constant at all concentrations. For fluoride and DNP, changes in $\Delta C_{lac}/\Delta C_{glc}$ and $\Delta C_{CO_2}/\Delta C_{glc}$ were not observed at all concentrations tested.

(A)

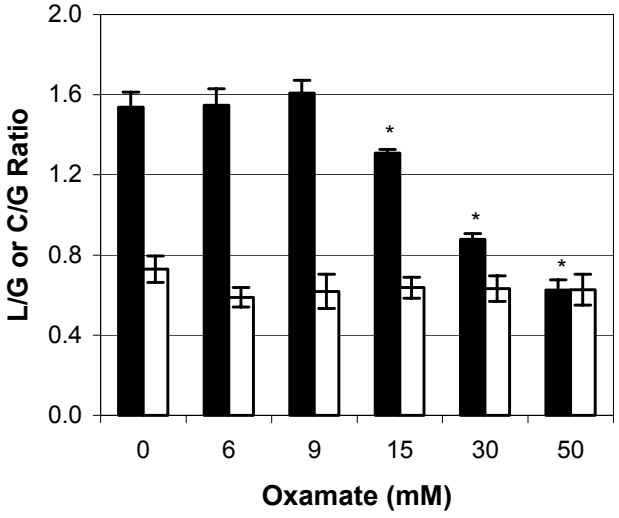

(B)

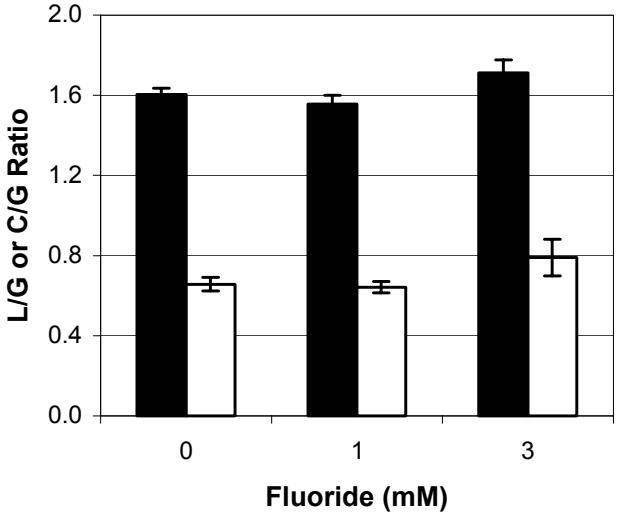

(C)

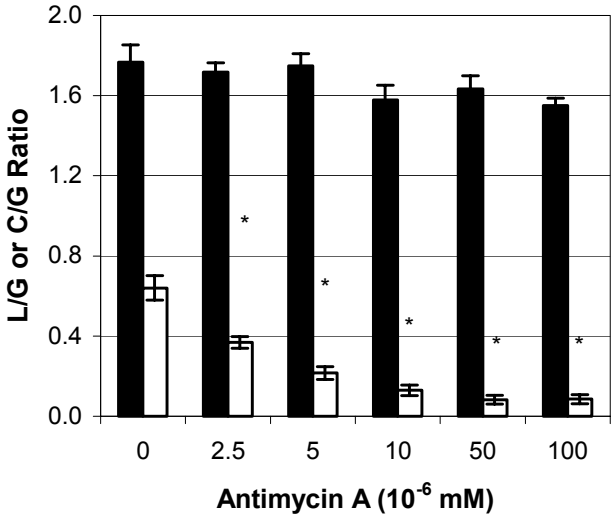

(D)

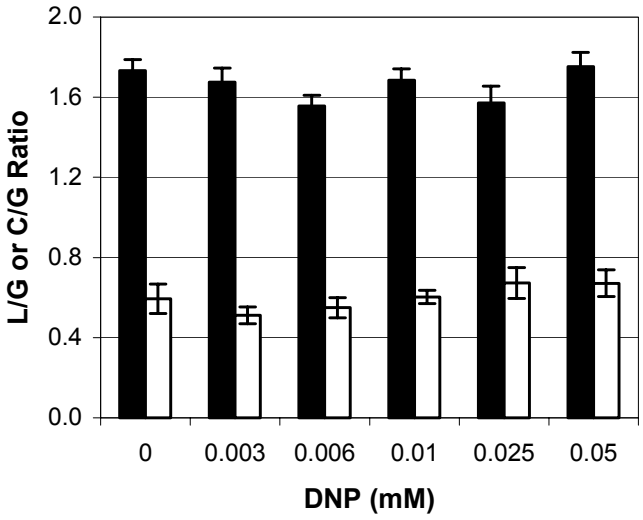

Figure 5.4. Changes in ratios of concentration differences of metabolites of fibroblast cell cultures exposed to four chemicals. Black bars represent ratios of $\Delta C_{lac} / \Delta C_{glc}$, and white bars represent ratio of $\Delta C_{CO_2} / \Delta C_{glc}$. Each point shown in the figure is the average and standard error of the mean of 6 replicates measured from two separate 24-well plates, each plate with three replicates. "∗" represents that differences from the control are significant at a 95% confidence level.

Changes in consistency between the carbon balance and the measured metabolic rates

The co-measurement of three metabolites allows further analysis of consistencies between the data sets and an assumed simple network. A normalized residual was calculated for every well (Table 5.3). Multiple replicates allow statistical analysis. The consistency was first checked for control cultures. The average of normalized residuals from 30 wells that served as control over 10 different experiments is 0.067, which is only slightly greater than 0.000, but the difference is significant at a 95% confidence level. Thus, the measured data sets for control cultures are not consistent with the assumed metabolic network. Moreover, more carbon is entering cells as glucose than can be accounted for by the carbon leaving as lactate and CO_2. As expected, the 30 normalized residuals from control cultures follow a normal distribution (Figure 5.5), which confirms our ability to compare averages of residuals between different test conditions using t-tests.

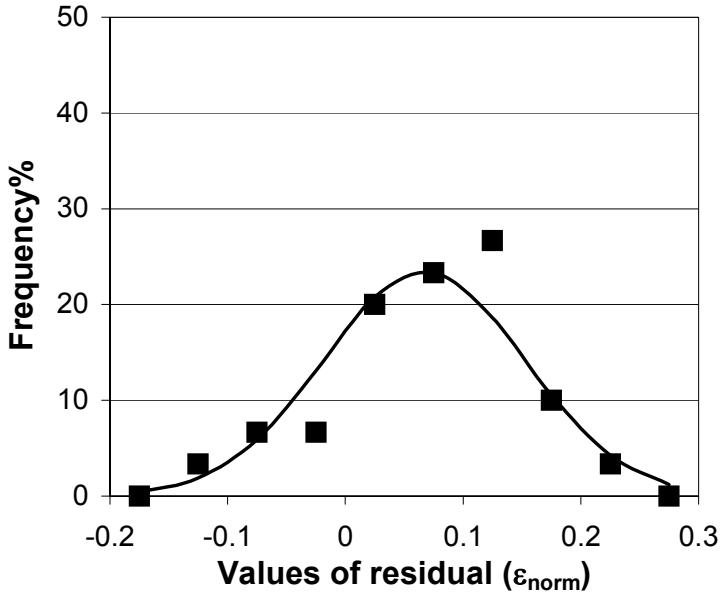

Figure 5.5. Frequency distributions of ε_{norm} calculated from 30 control cultures. "■" denotes the percentage of frequency of normalized residuals falling within the range interval. The Solid line is simulated using the normal distribution function, $Z = \frac{ni}{s\sqrt{2\pi}} e^{-\frac{1}{2}\left[\left(Y-\bar{Y}\right)/s\right]^2}$. n is the sample size, 30; i is the interval of the frequency distribution, 0.05; $\bar{Y}$ is the average of the samples, -0.067; and s is the standard deviation of samples, 0.085.

Even though the data sets are not consistent with the network, changes in consistencies as functions of doses for a given chemical can be quantified and compared statistically (Figure 5-6). Oxamate caused increases in the normalized residuals in a monotonic manner up to 0.6 at 50 mM. Their differences from control were significant at 15 mM and greater. Antimycin A also induced significant increases in normalized residuals at 1×10^{-5} mM and greater. The increases did not exceed 4.21. For cultures treated with fluoride or DNP, the differences from control are not consistent at all tested concentrations.

(A)

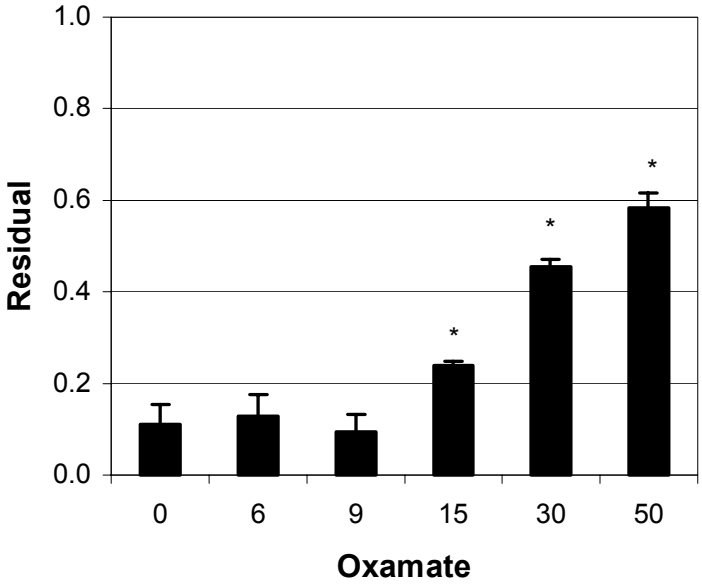
1.0
0.8
0.6
0.4
0.2
0.0
Residual
*
*
*
0
6
9
15
30
50
Oxamate

(B)

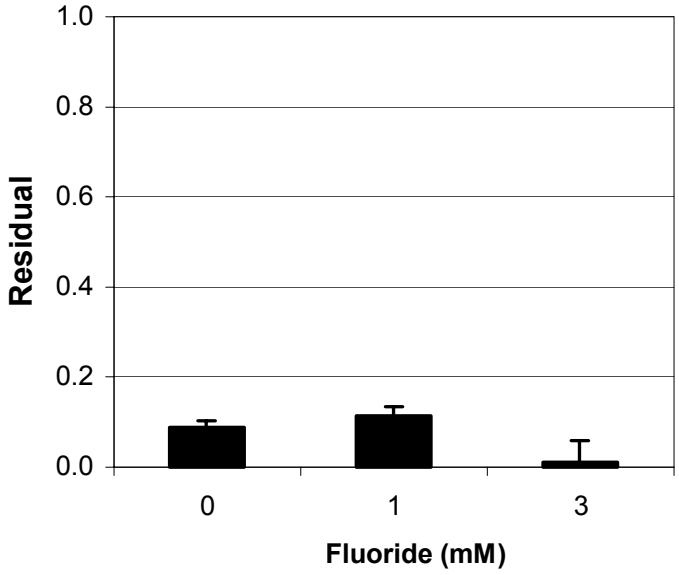
1.0
0.8
0.6
0.4
0.2
0.0
Residual
0
1
3
Fluoride (mM)

(C)

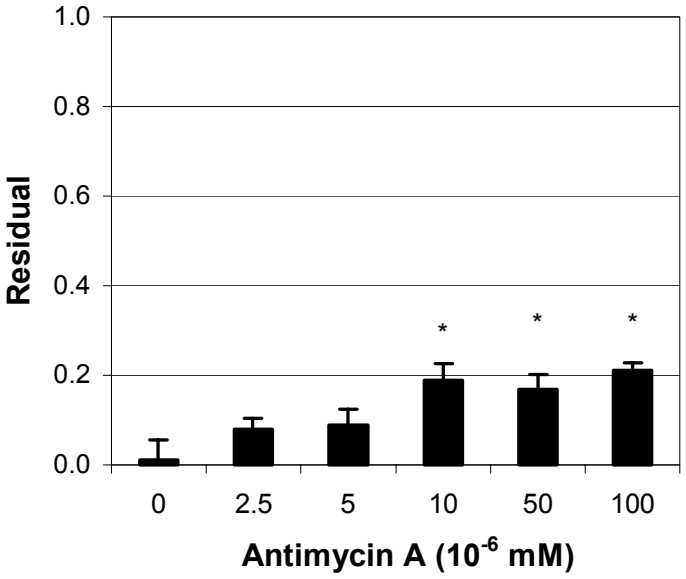

(D)

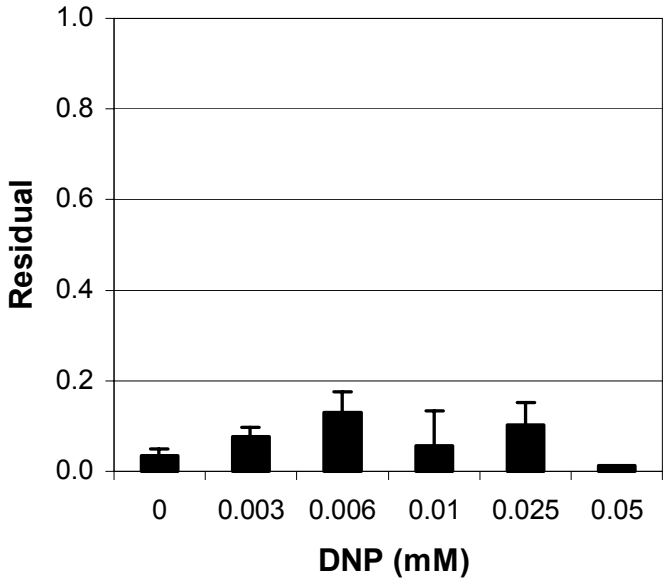

Figure 5.6. Normalized residuals for fibroblast cells exposed to four chemicals. Each point shown is the average and standard error of the mean of 6 normalized residuals for a given condition. "*" represents changes in average ε_{norm} significantly different from the control at 95% C.D.

As summarized in figure 5-7, the metabolic state of fibroblast cells changed in three different ways in response to four chemicals at different levels: (1) changes in metabolic rates without changing relative ratios and consistencies, (2) metabolic shift indicated by changes in relative ratios of metabolic rates but without changing consistencies, and (3) metabolic switch indicated by changes in consistencies. One, two or three types of changes may be observed for a chemical at different doses. Changes in metabolic rates of the three metabolites induced by DNP and fluoride at all tested concentrations were proportional, compared to control, with ratios and consistencies remaining constant. For oxamate, changes in metabolic rates were observed at 9 mM without causing changes in ratios and consistencies, and changes in ratios and consistencies were observed at 15 mM and greater. For antimycin A, changes in metabolic rates and ratio were both observed at 2.5×10^{-6} mM and 5×10^{-6} mM, and all three types of changes were observed at 1×10^{-5} mM and greater. Based on the concentration range where the type of change is located, change in ratios is a subset of change in metabolic rates, and change in consistencies is a subset of change in ratios.

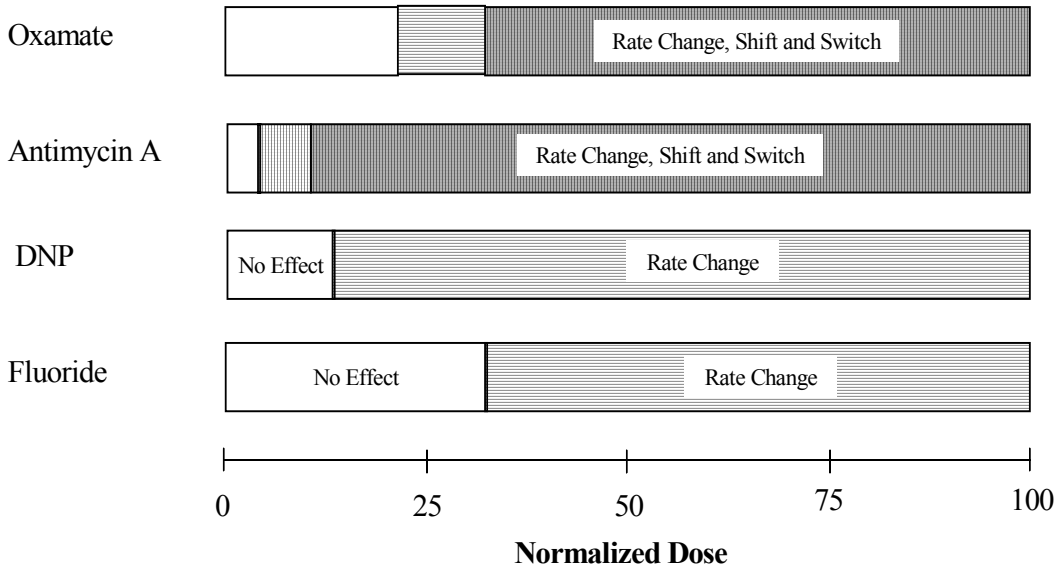

Figure 5.7. Changes in metabolic state of fibroblast cells exposed to four chemicals. White bars indicate the zone where no any effects occur, white bars with horizontal lines inside indicate the zone where rates change, white bars with vertical lines inside indicate the zone where pathway shift occurs, and grey bars indicate the zone where pathway switch occur. The mixed symbols means types of changes are overlapped. Doses of each chemical are normalized to their maximum tested sublethal concentration, oxamate at 50 mM, fluoride at 3 mM, antimycin A at 1×10^{-4} mM, and DNP at 0.01 mM.

Discussion

In this work, a new 24-well plate assay was developed for measuring average metabolic rates (changes in concentrations) of glucose, lactate, and CO_2 of mammalian cells. The rates were measured during a short, 6-hr incubation period so that changes in metabolite concentrations are sufficient to detect a difference, but not so much as to affect cell physiology and metabolic states. The metabolites were analyzed using enzymatic methods, which have been reformulated to a minimized scale and allows for multiplexed detection using spectrophotometric microplate readers. The assay in conjunction with a carbon balance based network provides a simple way for metabolic flux analysis with reduced cost, increased throughput, and reproducibility. It allows for

getting metabolic rates with adequate replication and doing consistency for adherent, non-growing cells that cannot be analyzed in a continuous culture. Achievement of rates with multiple replicates enhanced statistical analysis of the data sets and made consistency testing more rigorous.

The new assay was first applied for charactering the abilities of chemicals to alter metabolic state of fibroblast cells. The four tested model chemicals are well known metabolic agents with well-characterized mechanisms of action and have often been used for metabolic studies. Oxamate acts on LDH to inhibit conversion of pyruvate to lactate. Inhibition of this reaction reduces NAD^+ and causes a build up of glyceraldyhyde-3-phosphate, which in turn raises the levels of fructose-1,6-bisphosphate and inhibits phosphofructokinase, thereby halting glycolysis.[38] Inhibition of conversion of glucose to pyruvate, which is also the substrate for the TCA cycle, will decrease CO_2 production. Fluoride inhibits glycolysis by blocking substrate binding to enolase, thereby both the aerobic and anaerobic reactions are decreased.[27,39] Antimycin A blocks complex III in the electron transport chain and inhibits respiration.[30,40] DNP uncouples electron transport from ATP synthesis and stimulate respiration.[31,41-43] Both agents decrease the efficiency of energy production and the consequent increase in energy demand is contested by increasing glucose to produce ATP via glycolysis. Inhibition of glucose consumption and lactate production by oxamate and fluoride has been reported.[26,44] Alternatively, stimulation of glucose consumption and lactate production by antimycin A and DNP has also been reported.[26,42,43,45-47] The observed increased and decreased concentration differences of glucose, lactate, and CO_2 witnessed in our results agreed with the mechanisms of action and results reported previous.

Further data analysis by ratios and consistency checking indicated three types of changes in metabolic states of fibroblast cells in response to four chemicals at different levels. In such a short 6 hr incubation period, the chance to regulate the metabolic pathway through the genetic mutation and the gene expression is very small. The regulation of the enzyme activity is the most possible reason. Relating the targeted enzyme to the response sensitivity of metabolites uncovered an interesting phenomenon: the most sensitive metabolite to a chemical is the closest one to the action site. If this is a general phenomenon, the method could be used to generate clues for pinpointing action sites of chemicals.

Combination of the assay and certain cell lines could provide a way to characterize the chemicals with more detailed information. In turn, combination of the assay and chemicals with well-characterized effects may also provide a way to characterize cell lines. The action sites of the four agents tested are in or closely related to glycolysis, reduction of pyruvate to lactate, and TCA cycle, which are connected by a branch point of pyruvate. When one pathway was blocked, flux distribution into the other two pathways did not change as indicated by the constant relative ratios of metabolic rates as the function of doses. This suggests that pyruvate is a very rigid branch point, around which one flux perturbation will not have an appreciable effect on the distribution of the other two fluxes.

Consistency testing indicated another interesting phenomenon. The network matched the data sets fairly well for control cultures. However, carbon balance was severely broken for antimycin A and oxamate at some levels as indicated by the normalized residuals. The maximum normalized residual is up to 0.58 at 50 mM of

oxamate, which suggests that 58% percent of carbon being produced by glucose did not end as lactate and CO2. It has been reported that a larger fraction of the carbon from glucose was directed to biomass at the low $\Delta C_{lac} / \Delta C_{glc}$.[48] The lost carbon also could be ended as other extracellular metabolites (such as alanine), pile up in certain intracellular intermediate (s), or go to RNA and DNA through the pentose phosphate pathway, saved in glycogen, or synthesized to lipids. Answering where the lost carbon go needs second tier investigations of total cell mass analysis, lipid analysis, protein analysis, etc.

Development of the method was intended for screening impacts of chemicals on cellular metabolism. The method allows parallel tests of chemicals at many doses. The information obtained is high content and mechanism indicative. Many improvements and extensions of this work are necessary, such as automation of the procedures, measurement of more metabolic parameters, and screening broader sets of chemicals. It should be beneficial as a complement to genomics and proteomics for more systemic information. Other applications of the method include functional characterization of metabolic state for drug action on desired target and other targets for pharmaceutical research, cell line selection, medium design, and optimization of additives for enhanced pharmaceutical production, identification of the suitable target for genetic modification in metabolic engineering.

References

1. Flint, O.P. (1998). Predicting in vivo toxicity. *Toxicol Vitro* **12**, 591-595.

2. Zucco, F. and A.L. Vignoli. (1998). In vitro toxicology in Europe 1986-1997 - Final report to the European Commission DGXI Financial Contribution no. B4-3040/96/424/DEB/E2. *Toxicol Vitro* **12**, 739-+.

3. Freshney, R.I. (2000). Introduction, pp. 4-5. *In* Culture of animal cells, a manual of basic techniques. A John Wiley & Sons, New York, USA.

4. Waterfield, C.J., J. Delaney, M.D.J. Kerai and J.A. Timbrell. (1997). Correlations between in vivo and in vitro effects of toxic compounds: Studies with hydrazine. *Toxicol Vitro* **11**, 217-227.

5. Eisenbrand, G., B. Pool-Zobel, V. Baker, M. Balls, B.J. Blaauboer, A. Boobis, A. Carere, S. Kevekordes, J.C. Lhuguenot, R. Pieters and J. Kleiner. (2002). Methods of in vitro toxicology. *Food Chem Toxicol* **40**, 193-236.

6. Zucco, F., I. De Angelis, E. Testai and A. Stammati. (2004). Toxicology investigations with cell culture systems: 20 years after. *Toxicol Vitro* **18**, 153-163.

7. Orphanides, G. (2003). Toxicogenomics: challenges and opportunities. *Toxicol Lett* **140**, 145-148.

8. Lord, P.G. (2004). Progress in applying genomics in drug development. *Toxicol Lett* **149**, 371-375.

9. Hellmold, H., C.B. Nilsson, I. Schuppe-Koistinen, K. Kenne and L. Warngard. (2002). Identification of end points relevant to detection of potentially adverse drug reactions. *Toxicol Lett* **127**, 239-243.

10. Perlman, Z.E., M.D. Slack, Y. Feng, T.J. Mitchison, L.F. Wu and S.J. Altschuler. (2004). Multidimensional Drug Profiling By Automated Microscopy. *Science* **306**, 1194-1198.

11. Nicholson, J.K., J. Connelly, J.C. Lindon and E. Holmes. (2002). Metabonomics: a platform for studying drug toxicity and gene function. *Nat Rev Drug Discov* **1**, 153-161.

12. Lindon, J.C., J.K. Nicholson, E. Holmes and J.R. Everett. (2000). Metabonomics: Metabolic processes studied by NMR spectroscopy of biofluids. *Concepts Magn Resonance* **12**, 289-320.

13. Korke, R., A. Rink, T.K. Seow, M.C.M. Chung, C.W. Beattie and W.S. Hu. (2002). Genomic and proteomic perspectives in cell culture engineering. *J Biotechnol* **94**, 73-92.

14. Stephanopoulos G. (1999). Metabolic fluxes and metabolic engineering. *Metab Eng* **1**, 1-11.

15. Balcarcel, R.R. and L.M. Clark. (2003). Metabolic screening of mammalian cell cultures using well- plates. *Biotechnol Prog* **19**, 98-108.

16. Lee, K., F. Berthiaume, G.N. Stephanopoulos and M.L. Yarmush. (1999). Metabolic flux analysis: A powerful tool for monitoring tissue function. *Tissue Eng* **5**, 347-368.

17. Shimizu, K. (2000). An overview on metabolic systems engineering approach and its future perspectives for efficient microbial fermentation. *J Chin Inst Chem Eng* **31**, 429-442.

18. Fischer, E., N. Zamboni and U. Sauer. (2004). High-throughput metabolic flux analysis based on gas chromatography-mass spectrometry derived C-13 constraints. *Anal Biochem* **325**, 308-316.

19. Sauer, U. (2004). High-throughput phenomics: experimental methods for mapping fluxomes. *Current Opinion in Biotechnology* **15**, 58-63.

20. Kumar, S., C. Wittmann and E. Heinzle. (2004). Minibioreactors. *Biotechnology Letters* **26**, 1-10.

21. John, G.T., I. Klimant, C. Wittmann and E. Heinzle. (2003). Integrated optical sensing of dissolved oxygen in microtiter plates: A novel tool for microbial cultivation. *Biotechnol Bioeng* **81**, 829-836.

22. Wodnicka, M., R.D. Guarino, J.J. Hemperly, M.R. Timmins, D. Stitt and J.B. Pitner. (2000). Novel fluorescent technology platform for high throughput cytotoxicity and proliferation assays. *J Biomol Screen* **5**, 141-152.

23. Yang, Y. and R.R. Balcarcel. (2003). 24-well plate spectrophotometric assay for preliminary screening of metabolic activity. *Assay and drug development technologies* **1**, 461-468.

24. Yang, Y.S. and R.R. Balcarcel. (2004). 96-Well Plate Assay for Sublethal Metabolic Activity. *Assay and drug development technologies* **2**, 353-361.

25. Yang, Y.S. and R.R. Balcarcel. (2004). Determination of carbon dioxide production rates for mammalian cells in 24-well plates. *Biotechniques* **36**, 286-+.

26. Eklund, S.E., D. Taylor, E. Kozlov, A. Prokop and D.E. Cliffel. (2004). A microphysiometer for simultaneous measurement of changes in extracellular glucose, lactate, oxygen, and acidification rate. *Anal Chem* **76**, 519-527.

27. Niknahad, H., S. Khan, C. Sood and P.J. Obrien. (1994). Prevention of Cyanide-Induced Cytotoxicity by Nutrients in Isolated Rat Hepatocytes. *Toxicol Appl Pharmacol* **128**, 271-279.

28. Kerai, M.D.J. and J.A. Timbrell. (1997). Effect of fructose on the biochemical toxicity of hydrazine in isolated rat hepatocytes. *Toxicology* **120**, 221-230.

29. Hamilton, E., M. Fennell and D.M. Stafford. (1995). Modification of Tumor Glucose-Metabolism for Therapeutic Benefit. *Acta Oncologica* **34**, 429-433.

30. Zhang, J.G., M.A. Tirmenstein, F.A. Nicholls-Grzemski and M.W. Fariss. (2001). Mitochondrial electron transport inhibitors cause lipid peroxidation-dependent and -independent cell death: Protective role of antioxidants. *Arch Biochem Biophys* **393**, 87-96.

31. Linsinger, G., S. Wilhelm, H. Wagner and G. Hacker. (1999). Uncouplers of oxidative phosphorylation can enhance a Fas death signal. *Mol Cell Biol* **19**, 3299-3311.

32. Yang, Y.S. and R.R. Balcarcel. (2003). 24-well plate spectrophotometric assay for preliminary screening of metabolic activity. *Assay and Drug Development Technologies* **1**, 461-468.

33. Forrester, R.L., L.J. Wataji, D.A. Silverman and K.J. Pierre. (1976). Enzymatic Method for Determination of CO_2 in Serum. *Clin Chem* **22**, 243-245.

34. Bergmeyer, H.U. (1974). Methods of Enzymatic Analysis. Academic Press, New York, USA.

35. Lowry, O.H. and J.V. Passonneau**.** (1972). A flexible System of Enzymatic Analysis;. Academic Press, Orlando, USA.

36. Nyberg, G.B., R.R. Balcarcel, B.D. Follstad, G. Stephanopoulos and D.I.C. Wang. (1999). Metabolism of peptide amino acids by Chinese hamster ovary cells grown in a complex medium. *Biotechnol Bioeng* **62**, 324-335.

37. Stephanopoulos G., A.A.A., Nielsen Jens. (1998). Metabolic Engineering: Principles and Methodologies. 22.

38. Goldberg, E.B. and S.P. Colowick. (1965). The role of glycolysis in the growth of tumor cells, III. Lactic dehydrogenase as the site of action of oxamate on the growth of cultured cells. *J Biol Chem* **240**, 2786-2790.

39. Voet, D., J.G. Voet and C.W. Pratt**.** (1999). Fundamentals of Biochemistry. John Wiley & Sons, New York.

40. Gniadecki, R., T. Thorn and J. Vicanova. (2000). Role of Mitochondria in Ultraviolet-Induced Oxidative Stress. *Journal of Cellular Biochemistry* **80**, 216-222.

41. Khayat, Z.A., T. Tsakiridis, A. Ueyama, R. Somwar, Y. Ebina and A. Klip. (1998). Rapid stimulation of glucose transport by mitochondrial uncoupling

depends in part on cytosolic Ca2+ and cPKC. *American Journal of Physiology-Cell Physiology* **44**, C1487-C1497.

42. Sibille, B., C. Filippi, M.A. Piquet, P. Leclercq, E. Fontaine, X. Ronot, M. Rigoulet and X. Leverve. (2001). The mitochondrial consequences of uncoupling intact cells depend on the nature of the exogenous substrate. *Biochem J* **355**, 231-235.

43. Sibille, B., X. Ronot, C. Filippi, V. Nogueira, C. Keriel and X. Leverve. (1998). 2,4 dinitrophenol-uncoupling effect on Delta Psi in living hepatocytes depends on reducing-equivalent supply. *Cytometry* **32**, 102-108.

44. Sanfeliu, A., C. Paredes, J.J. Cairo and F. Godia. (1997). Identification of key patterns in the metabolism of hybridoma cells in culture. *Enzyme Microb Technol* **21**, 421-428.

45. Tiefenthaler, M., A. Amberger, N. Bacher, B.L. Hartmann, R. Margreiter, R. Kofler and G. Konwalinka. (2001). Increased lactate production follows loss of mitochondrial membrane potential during apoptosis of human leukaemia cells. *Br J Haematol* **114**, 574-580.

46. Pilatus, U., E. Aboagye, D. Artemov, N. Mori, E. Ackerstaff and Z.M. Bhujwalla. (2001). Real-time measurements of cellular oxygen consumption, pH, and energy metabolism using nuclear magnetic resonance spectroscopy. *Magnetic Resonance in Medicine* **45**, 749-755.

47. Patel, N., Z.A. Khayat, N.B. Ruderman and A. Klip. (2001). Dissociation of 5' AMP-activated Protein Kinase Activation and Glucose Uptake Stimulation by Mitochondrial Uncoupling and Hyperosmolar Stress: Differential Sensitivities to Intracellular Ca^{2+} and Protein Kinase C Inhibition. *Biochem Biophys Res Commun* **285**, 1066-1070.

48. Gambhir, A.K., R.; Lee, J.; Fu, P. C.; Europa, A. F.; Hu, W. S. (2003). Analysis of Cellular Metabolism of Hybridoma Cells at Distinct Physiological States. *J Biosci Bioeng* **95**, 317-327.

CHAPTER VI

CONCLUSIONS AND RECOMMENDATIONS

Conclusions

The overall aim described in the introduction of this thesis was to develop high throughput metabolic rate assays for screening purposes. At the start of my work, established approaches for measuring metabolic rates were primarily for large-scale cultivation systems. Such methods are expensive, time consuming, low throughput, all which are obstacles for applications of metabolic flux analysis method in areas that require large numbers of test, such as screening of drugs and toxicants in drug discovery and development and screening of mutants in functional genomics. Now at the end of my work, a series of metabolic rate assays performed in 24- and 96-well plates are developed and demonstrated for use in screening chemicals (Table 6.1).[1-3] The assays were demonstrated to be more sensitive for toxicity testing than those based on cell death events, and have comparable sensitivity with cell growth inhibition. A sublethal screen provides a simple solution to overcome the challenge of dose selection faced by users of many intricate approaches. Measurement of multiple metabolic rates in well plates enables characterization of compounds for their abilities to alter metabolic state as a function of doses and the information obtained is mechanism indicative.

The assays developed in this work help strengthen the field of metabolic flux analysis by providing an easy way to obtain sets of fluxes with adequate replicates. Achievement of fluxes with multiple replicates, collected from multi-parallel cultures in

well plates, resulted in the ability to not only increase the precision of the fluxes measured but also enhance the statistical analysis of data sets for more rigorous consistency testing. The statistical analysis of central carbon balance enabled quantitative comparison of deviations of flux data sets from a network at different metabolic states, though inability of closing the carbon balance by measuring glucose, lactate, and CO_2 suggested that more metabolic parameter be measured.

Table 6.1. Summary of metabolic rate assays developed in this work.

Assay Name	Well plate	Time	Application
Acidification rate	24	90 minutes	Rapid screening for a preliminary dose response curve of effects on global metabolism
CO_2 production	24	6 hours	Screening for a dose response curve of effects on respiration
Sublethal activity	96	6 and 24 hours	Screening for two dose response curves of effects on metabolism and viability to determine sub-lethal concentration range
Glc/Lac/CO_2	24	6 hours	Screening for effects on several pathways to characterize changes in metabolic state

Recommendations

The assays were designed to meet different purposes. To test a chemical, they can be used in a sequence; the easier ones should be used first to pave the way for the use of relatively complicated ones, which can increase the overall efficiency and reduce the total cost of a testing process. They also can be used in parallel with other assays in a complex testing strategy. Certainly, many improvements and extensions of my work are necessary. These include but are not limited to adapting of the assays for automation, measurement

of more metabolic rates, validation for toxicity prediction, and extension to wider research areas.

(1) Improvements

Currently, all procedures of the assays that I have developed, such as cell seeding, culture incubation, and metabolite assays, were operated manually in 24- and 96-well plates. Automation of the assay requires further improvements with respect to procedures and assay reagents. In my work, cell seeding is the most tedious step, which might be overcome by using automatic liquid handling systems. The protocols should be further simplified and avoid those which are not suitable for automatic operations, such as washing steps. Minimization is the trend for high throughput screening. The enzymatic assays for metabolite measurements should be further minimized and optimized. Higher densities well plates, such as 384-well plates, are necessary to further increase the throughput. Moreover, more metabolites, such as amino acids, should be measured and added into current systems for a more detailed metabolic map. Methods that allow multiplexed detections, such as those light-based, are preferred for metabolite measurements. Other techniques, such as HPLC, GC, NMR, and Mass spectroscopy also can be considered.

(2) Test broader chemicals and cell lines

My work has demonstrated the feasibility of measuring metabolic rates in high throughput well plates using a regular, continuous cell line (mouse fibroblast) and a few well-known metabolic agents. Their uses for toxicity prediction have not been validated yet. Broader species/cell types and chemical reference sets should be tested. Genomics and proteomics have been tested for toxicity prediction purposes with some

biological system models and chemicals. Testing same biological systems and chemicals for metabolic effects and relating the results to those measured by genomics and proteomics as well as to results measured by classical toxicity endpoints would be a good starting point.

(3) Biopharmaceutical process development

Optimization of culture environment and development of highly productive cell lines are important for the design of high-yield processes in biopharmaceutical process development. The process of medium optimization is a slow, grueling, and tedious process due to a large number of components contained in the medium and their complicated interactions. The components of current medium used for industrial cell lines are far being fully optimized and require much further improvements. Increasing specific productivity of monoclonal antibody production, maximization of cell density, elongation of culture period, and minimization of toxic byproducts (such as lactate and ammonia), are major aims for optimization of medium.[4,5] The well plate-based metabolic rate assays that I have developed provide measurements of several endpoints concerned by medium optimization, including cell growth, glucose consumption, and lactate production. When they are complemented with more necessary endpoints, such as monoclonal antibody and ammonia production, a powerful platform will be created for medium optimization process. Moreover, the assay can be used for screening and identification of new chemical enhancers as medium additives.

Another possible application of well plate-based metabolic rate assays is to investigate cellular metabolism and signaling pathways that influence proliferation and productivity. Activation of membrane-bound receptor and signal transduction pathways

will alter cellular metabolic state. By employing cell signaling and metabolic inhibitors and modulators and the metabolic rate assays, much information can be revealed regarding the nature of signal transduction and metabolic pathways. Achievement of relation between these pathways and cell physiology will open new areas for further improvement of cellular properties.

(4) Measure flux control coefficients

Metabolic control analysis (MCA) provides a methodology to describe how cells regulate metabolism in response to changes in system parameters of complex enzyme systems.[6] In MCA, the control exerted by each enzyme in a metabolic network over metabolic fluxes is described quantitatively as a control coefficient. Determination of control coefficients of enzymes in pathways can help identify the target for genetic modifications in metabolic engineering and for disease treatment in drug discovery and pharmaceutical research.[7] The flux control coefficient is defined as the fractional change in the logarithm of flux against the fractional change in logarithm of enzyme activity.

$$C_{xase}^{J} = \frac{\partial \ln J}{\partial \ln E_{xase}} \tag{6-1}$$

where C_{xase}^{J} represents flux control coefficient, J represents flux, $xase$ represents a certain enzyme, and E_{xase} represents enzyme activity. The flux control coefficient of the enzyme can be obtained from the response of the metabolic flux to an inhibitor relative to the effect of the inhibitor on the isolated enzyme:[8]

$$C_{xase}^{J} = \frac{R_I^J}{\varepsilon_I^{xase}} = \lim_{I \to 0}\left(\frac{\partial \ln J}{\partial \ln I} \Big/ \frac{\partial \ln E_{xase}}{\partial \ln I}\right) \tag{6-2}$$

where I represents inhibitor, R_I^J represents response coefficient (defined as fractional changes in fluxes over fractional changes in concentrations of the inhibitor), and ε_I^{xase} represents elasticity (defined as fractional changes in enzyme activity over fractional changes in concentrations of the inhibitor). My work has demonstrated the feasibility for determining response coefficients in well plates in chapter V. The measurement of enzyme activity has previously often been performed in well plates. Thus, in the future, they may be combined and further optimized, yielding an easy, inexpensive method for determination of flux coefficients.

References

1. Yang, Y. and R.R. Balcarcel. (2003). 24-well plate spectrophotometric assay for preliminary screening of metabolic activity. *Assay and drug development technologies* **1**, 461-468.

2. Yang, Y.S. and R.R. Balcarcel. (2004). 96-Well Plate Assay for Sublethal Metabolic Activity. *Assay and drug development technologies* **2**, 353-361.

3. Yang, Y.S. and R.R. Balcarcel. (2004). Determination of carbon dioxide production rates for mammalian cells in 24-well plates. *Biotechniques* **36**, 286-+.

4. Bibila, T.A. and D.K. Robinson. (1995). In Pursuit of the Optimal Fed-Batch Process for Monoclonal-Antibody Production. *Biotechnol Prog* **11**, 1-13.

5. Xie, L.Z. and D.I.C. Wang. (1997). Integrated approaches to the design of media and feeding strategies for fed-batch cultures of animal cells. *Trends Biotechnol* **15**, 109-113.

6. Cascante, M., L.G. Boros, B. Comin-Anduix, P. de Atauri, J.J. Centelles and P.W.N. Lee. (2002). Metabolic control analysis in drug discovery and disease. *Nat Biotechnol* **20**, 243-249.

7. Stephanopoulos G., A.A.A., Nielsen Jens. (1998). Metabolic Engineering: Principles and Methodologies. 22.

8. Fell, D.A. (1997). Understanding the control of metabolism. Portland Press Ltd, London.